

AN ASSESSMENT OF ATMOSPHERIC RIVERS AS FLOOD PRODUCERS
IN ARIZONA

by

Saeahm Kim

A Thesis Submitted to the Faculty of the

DEPARTMENT OF HYDROLOGY AND WATER RESOURCES

In Partial Fulfillment of the Requirements

For the Degree of

MASTER OF SCIENCE

In the Graduate College

THE UNIVERSITY OF ARIZONA

2015

STATEMENT BY AUTHOR

This thesis has been submitted in partial fulfillment of requirements for an advanced degree at the University of Arizona and is deposited in the University Library to be made available to borrowers under rules of the Library.

Brief quotations from this thesis are allowable without special permission, provided that an accurate acknowledgement of the source is made. Requests for permission for extended quotation from or reproduction of this manuscript in whole or in part may be granted by the head of the major department or the Dean of the Graduate College when in his or her judgment the proposed use of the material is in the interests of scholarship. In all other instances, however, permission must be obtained from the author.

SIGNED: Saeahm Kim

APPROVAL BY THESIS DIRECTOR

This thesis has been approved on the date shown below:

Date

ACKNOWLEDGEMENTS

I would like to thank my advisor, Dr. Katherine Hirschboeck, for her guidance and support throughout the years of research. I would also like to thank my committee members, Dr. Victor Baker and Dr. Larry Winter, for their interest in my work and their suggestions on improvement. Elzbieta Czyzowska, Kyle Hartfield, and Martin Munro provided valuable assistance with the watershed maps used in this study, for which I am grateful.

The SSM/I data used in this study are produced by Remote Sensing Systems and sponsored by the NASA Earth Sciences MEaSUREs DISCOVER Project. The data are available at www.remss.com. The IVT grid point data were generously provided by Jonathan Rutz and James Steenburgh, to whom I am grateful. I would also like to thank The Climate Assessment for the Southwest (CLIMAS) for sponsoring parts of this research and the Laboratory of Tree-Ring Research for graduate assistantship support.

Finally, I would like to thank the Department of Hydrology and Water Resources for giving me this opportunity, and my friends and family for supporting me.

TABLE OF CONTENTS

LIST OF FIGURES	6
LIST OF TABLES	8
ABSTRACT	9
1. INTRODUCTION	11
2. BACKGROUND AND MOTIVATION	12
2.1 ATMOSPHERIC RIVERS AND FLOODING	15
2.2 INLAND PENETRATION INTO ARIZONA	17
2.3 PURPOSE	20
3. DATA AND PHYSIOGRAPHIC SETTING	22
3.1 ARIZONA FLOOD PEAK DATA	22
3.2 ATMOSPHERIC RIVER DATA	25
3.2.1 INTEGRATED WATER VAPOR (IWV) DATA FROM SSM/I	27
3.2.2 VERTICALLY INTEGRATED IVT GRID POINT MEASUREMENTS	29
3.3 ARIZONA AR DAYS	30
3.4 PHYSIOLOGICAL AND CLIMATIC SETTING	33
4. THE IMPORTANCE OF ARS AS FLOOD PRODUCERS	35
4.1 INTERANNUAL VARIABILITY AND SEASONALITY OF ARS	35
4.2 AR FRACTION	41
4.3 MAGNITUDE OF ARS AND NON-AR FLOOD PEAKS	43
4.3.1 AR INFLUENCE OF RANK AND PEAK FLOW EVENTS	44
4.3.2 DIFFERENCE IN MEANS OF AR AND NON-AR PEAKS	47

4.3.3 AR AND NON-AR ANNUAL PEAK COMPARISON	51
4.3.4 AR VS. NON-AR WINTER STORMS	58
5. EXPLORATION OF FACTORS THAT MAY INFLUENCE THE SPATIAL VARIABILITY OF AR FLOODING	59
5.1 BASIN CHARACTERISTICS	59
5.2 AR TRAJECTORIES	64
6. DISCUSSION	66
7. CONCLUSION	71
8. REFERENCES	74
APPENDIX	
APPENDIX A	80
APPENDIX B	122
APPENDIX C	126
APPENDIX D	131

LIST OF FIGURES

1.	Generalized Physiography of Arizona	18
2.	Map of Arizona showing major watershed boundaries, elevation, and the location of the flood peak gauging stations used in this study	25
3.	Satellite-derived Integrated Water Vapor (IWV) Composite Image	29
4.	Illustration of the procedure used to identify Arizona flood peaks associated with atmospheric rivers originating in the eastern North Pacific Ocean	33
5.	Monthly distribution of AR-related peaks in Arizona grouped by physiographic region for the cool season months during the WY 1988 – 2011 study period	37
6.	Interannual variation of the total number of cool-season AR Days affecting Arizona	38
7.	AR fractions at selected gauging stations by watershed during WYs 1988 – 2011	42
8.	Comparison of annual peaks for Northern Arizona stations	52
9.	Comparison of annual peaks for Southeastern Arizona stations	54
10.	Comparison of annual peaks for Eastern Arizona Transition Zone 1 stations	55
11.	Comparison of annual peaks for East Central AZ Transition Zone 2 stations	55
12.	Comparison of annual peaks for North Central Transition Zone 3 stations	56
13.	Drainage basin area and AR fraction	60
14.	Maximum elevation and AR fraction	60
15.	Outlet elevation and AR fraction	61
16.	Percentage of slope > 30 and AR fraction	62
17.	Mean basin slope and AR fraction	62

18.	Percentage of forest cover and AR fraction	63
19.	Soil permeability and AR fraction	64

LIST OF TABLES

1.	Research Design for Assessing the Role of Atmospheric Rivers as Flood Producers in Arizona	21
2.	Site information for the selected gauging stations shown on Figure 3	24
3.	Definitions of atmospheric rivers from various sources in chronological order	32
4.	Arizona flood-related atmospheric river dates by month (WY 1988 – 2011)	36
5.	Contingency table for evaluating the importance of AR vs. non-AR mechanisms on Flood Peak Rank	44
6.	Chi Square Test results for the selected watersheds (based on actual discharge)	46
7.	The t-statistic values for difference in means of AR and non-AR peaks	50
8.	Mean discharge of annual peaks by mechanism for Northern AZ / Colorado Plateau	53
9.	Mean discharge of annual peaks by mechanism for Southeastern AZ	54
10.	Mean discharge of annual peaks by mechanism for Mogollon Rim / Transition Zone	57
11.	Contingency table for evaluating the difference between ranking of AR and non-AR winter peak flow events	58
12.	Contingency table for evaluating the importance of trajectory and entry on the number of peak flow events	65
13.	Contingency table for evaluating the importance of point of entry on the number of peak flow events	65

ABSTRACT

Atmospheric rivers (ARs) are long, narrow plumes of concentrated water vapor that are a critical factor in the transport of moisture from oceans to continents in the mid-latitudes. Much of the existing research on the impact of ARs on the United States focuses on the Pacific Coastal states and their importance as contributors to precipitation, their impact on water resources, and their role as flood producers.

The objective of this study is to determine the importance of Pacific Ocean ARs penetrating further inland and affecting flooding in the state of Arizona. The following questions were addressed: (1) Are certain regions in Arizona more susceptible to AR-related flooding? (2) Do ARs produce flooding events of greater magnitude in Arizona than floods produced by other mechanisms? (3) Are there identifiable variables or conditions that influence the frequency, magnitude, and location of AR-related flooding in the state?

Based on a study of selected watersheds throughout Arizona, results showed that the most active region of AR-related flooding in Arizona is associated with the abrupt increase of elevation along the Mogollon Rim of the state's Central Highlands Transition Zone physiographic region. The percentage of AR-related flooding events in this region can reach over 50% for some watersheds, such as the Verde and the Salt. The influence of ARs on flooding is weaker to the north, in the Colorado Plateau region, and to the south, where summer convective storm activity in the "Sky Islands" of the Basin and Range physiographic region is a more common flood producer, and where the most extreme floods are associated with late-summer tropical cyclones. When ARs did affect

northern or southern Arizona, they did not have the same degree of influence on flood magnitude and frequency as in the Mogollon Rim / Central Highlands watersheds, which implies that watersheds in the Mogollon Rim / Central Highlands have characteristics that are favorable for AR-related flooding. Lastly, in addition to the importance of the Central Highlands' orography on AR flooding, another finding of this study points to the importance of the trajectory of the inland-penetrating AR as a factor. The corridor along which the AR enters the region can strongly affect which ARs will produce floods and which ARs will not, with a south/southwesterly trajectory across Baja California producing the largest percentage of AR floods in Arizona in this study.

1. Introduction

Atmospheric rivers (ARs) are long, narrow plumes of concentrated water vapor in the lower troposphere that are responsible for much of the horizontal moisture transport in the mid-latitudes (Zhu and Newell 1998). They produce extreme precipitation and major flooding events in the Pacific Coast states of the United States due, in part, to the orographic forcing of ARs over coastal topography (Smith et al. 2010; Ralph and Dettinger 2012). In certain regions – such as California – ARs dominate the flood record, are responsible for the largest winter storms, and contribute greatly to the water resources of that area (Dettinger et al. 2011).

Atmospheric rivers can also penetrate inland and have been linked to precipitation and flooding in the interior of the United States, demonstrating that the influence of AR storms is not limited to west coastal regions (Moore et al. 2012; Rutz and Steenburgh 2012; Rutz et al. 2014, 2015). Arizona, as California's neighbor to the east, has also been affected by precipitation and flooding associated with AR events in specific areas and watersheds (see Neiman et al. 2013; Rivera et al. 2014), but a large-scale regional assessment of the importance of ARs as flood producers in Arizona has not yet been done. Unlike the Pacific Coastal states, where the cause of flooding is dominated by precipitation from synoptic-scale winter storms, Arizona's flood hydroclimatology is far less homogeneous (Hirschboeck 2000). The flood record of Arizona includes events produced by (1) non-AR and AR-associated winter synoptic storms, (2) localized or widespread summer convective storms, and (3) precipitation enhanced by the influx of moisture from Eastern Pacific tropical cyclones (see Hirschboeck 1987, 1988).

The goals of this study are to assess the importance of atmospheric river events as flood producers in Arizona watersheds, and to explore how flood events produced by ARs compare to those produced by other mechanisms in terms region of influence, magnitude, and frequency. Specifically, this study will address the following questions:

1. Are certain regions in Arizona more susceptible to AR-related flooding than others?
2. Do ARs produce flooding events of greater magnitude than floods produced by other mechanisms?
3. Are there identifiable variables or conditions that influence the frequency, magnitude, and location of AR-related flooding in the state?

2. Background and Motivation

Features now commonly referred to as “atmospheric rivers” were documented more than 50 years ago by Weaver (1962) as one of three different storm types that he identified as producing precipitation and flooding in California. Weaver’s types were based upon the latitude at which the storms had initially formed. His “Low-latitude” type storms developed near Hawaii and moved towards the Pacific West Coast. These events were a prototype for what became known as a “pineapple express” (PE) storms and today are understood to be a specific type of atmospheric river. Pineapple express atmospheric river events draw moisture from the tropics (e.g., near Hawaii), affect the North American West Coast, and have been associated with heavy rainfall and flooding events in California (see Dettinger 2004; Monteverdi 1995; Estes 1998). Prior to the advent of satellite observations, compilations of historically observed PEs provided the most

consistent records of atmospheric river events influencing the North American West Coast (see Dettinger 2004; Dettinger et al. 2011).

Satellites opened up a new way to observe these plumes of water vapor. Newell et al. (1992) produced a pilot study on the presence of filamentary structures in the atmosphere, which they called “tropospheric rivers,” and found that they persisted for a period of approximately ten days and displayed an eastward movement. Four or five of these rivers were present in the Northern and Southern hemispheres at any given time, moving into the mid-latitudes. Zhu and Newell (1998) studied water vapor fluxes in the troposphere and proposed a new algorithm and term to describe and identify these features, now referred to as “atmospheric rivers”. They found that atmospheric rivers (ARs) cover less than 10% of the globe at any given time, but are responsible for much of the water vapor transport into the mid-latitudes. This study was one of the earliest to quantify the importance of ARs in the transport of water vapor across latitudes globally.

Regional studies have provided more specific information on the impacts of ARs including their ability to produce extreme precipitation and flooding. For example, Viale and Nuñez (2011) studied winter orographic precipitation in the Andes during the period 1970 – 1976, and found that ARs were associated with 80% of the heaviest orographic precipitation events and AR storms produced twice as much precipitation as non-AR winter storms. Lavers et al. (2011) demonstrated that the ten largest winter flooding events in the United Kingdom since 1970 were associated with AR events. Such works suggest that ARs may pose a flooding hazard in every region they affect.

Many studies in the last decade have focused on the impacts that ARs have on precipitation and flooding in the Pacific Coast states of North America. Ralph et al. (2004) evaluated the characteristics and structure of an AR associated with a precipitation event in northern California and concluded that this case study was representative of composites of many other AR events detected using Special Sensor Microwave Imager (SSM/I) and geostationary (GEOS) satellite data. Their study also set a baseline value of integrated water vapor ($IWV \geq 2$ cm) for identifying ARs, a value that has held up in subsequent studies.

Neiman et al. (2008a) provided the first long-term characterization of the properties of ARs and their impacts in western North America, including the seasonality of ARs and the precipitation events associated with ARs from British Columbia to California. They looked at SSM/I composites for the period 1 October 1997 – 30 September 2005 and made observations of AR activity for the northwest coast (British Columbia, Washington, and Oregon) and the southwest coast (California). Their study found that the southwest coast experienced half as many days as the northwest coast on which an AR was present, and that ARs primarily occurred during the warm season in the northwest and the cool season in the southwest.

Dettinger et al. (2011) examined the AR days from Neiman et al. (2008a) and PE days going as far back as WY 1948, and they assessed the precipitation and streamflow during and following these events with a focus on California. These events were found to contribute 20 – 50% of the state's total precipitation and to strongly influence both the water supply and flooding in California. This study also showed how important AR

events are for California's water resources and the dominance they have in California's precipitation and flood records.

Although these findings provide valuable insight into the behavior of AR events affecting California, the Neiman et al. (2008a) and Dettinger et al. (2011) studies only considered ARs making landfall within the latitude band $32.5^{\circ}\text{N} - 52.5^{\circ}\text{N}$. Because this range does not account for ARs crossing the west coast of the Baja Peninsula, Rutz and Steenburgh (2012) expanded on the findings of Dettinger et al. (2011) by including ARs as far south as 24°N , which significantly increased the AR fraction over the southwestern U.S. Their analysis indicated that ARs have a greater impact on precipitation in non-coastal western states, such as Arizona, than earlier studies had suggested. A later section will expand on the importance of this inland penetration.

2.1 Atmospheric Rivers and Flooding

Atmospheric rivers have been linked to many precipitation and flooding events in the Pacific coast states of North America. Ralph et al. (2006) found that all flooding events that had occurred in the Russian River between October 1997 and February 2006 were associated with ARs, thereby showing how ARs can dominate in some watersheds as the sole major flood producing mechanism.

Smith et al. (2010) modeled the behavior of an AR as it moves over terrain, comparing changes in water vapor flux, amount of precipitation, and location in which precipitation develops in three simulations where the terrain was variable. They found that there was a significant reduction in total precipitation when the terrain was completely removed, and that precipitation seems to be driven primarily by orographic

forcing and is limited to areas of sharp elevation changes. These results suggest that a key factor in why ARs can produce extreme precipitation and flooding is the orographic lifting of AR-related moisture over the coastal topography. Extreme precipitation and flooding may therefore be more likely to occur in watersheds that are affected by orographic precipitation.

Neiman et al. (2011) examined stream flow data collected from four major watersheds in western Washington with varying topographic characteristics. Their results showed that the surrounding topography of the watershed and the orientation at which the AR made landfall were influential on flooding behavior. The watershed with the greatest direct exposure to the Pacific Ocean received the most consistent year-to-year peak flows, while the watershed that had a limited window of unobstructed terrain between it and the Pacific showed the most variability. The orientation at which the greatest peak flows occurred varied, depending on which orientation optimized the orographic control of precipitation.

Moore et al. (2012) presented a case study of an extreme precipitation event that produced flooding in Tennessee and Kentucky. This event was associated with an AR that developed in the eastern tropical Pacific and was transported into the Mississippi Valley, which supported the production of two quasi-stationary mesoscale convective systems (MCS) and heavy precipitation over a fixed region. This study was one of the earliest on AR events that penetrated the interior of the U.S. and demonstrated that ARs could produce extreme flooding in areas far from the west coast.

2.2 Inland Penetration into Arizona

Neiman et al. (2013) presented a detailed case study of the inland penetration of an AR from the Pacific Ocean into Arizona in January 2010. Their study demonstrated that ARs are capable of producing precipitation and flooding in Arizona, comparable to AR effects along the west coast of North America. This study also highlighted the importance of the AR's orthogonal orientation with respect to the Mogollon Rim, an escarpment associated with the abrupt increase in elevation that runs diagonally across Arizona in the Central Highlands physiographic region (Figure 1). A companion paper by Hughes et al. (2014) used modeled precipitation to assess the role of terrain height and AR orientation on precipitation and flooding in Arizona and found that both were important factors in determining mean precipitation amounts during inland penetration of an AR.

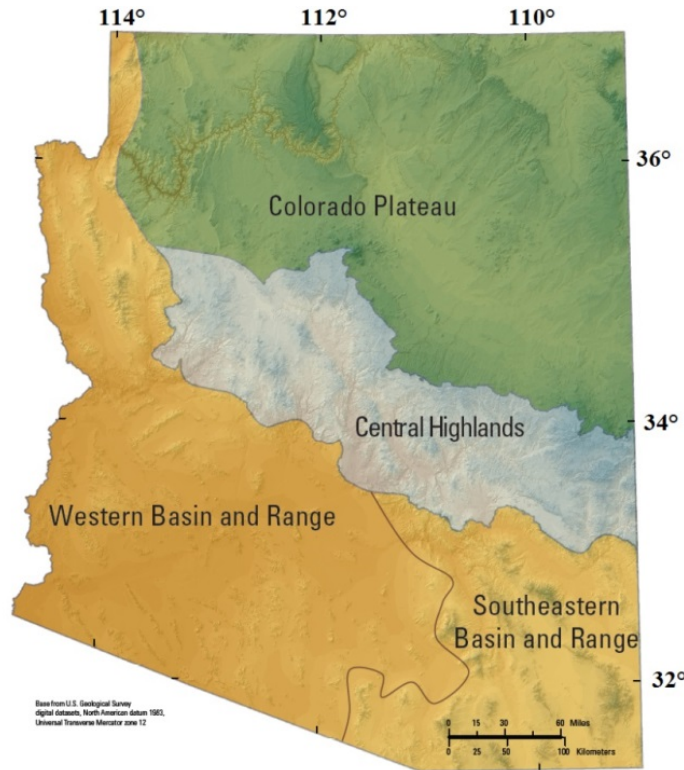


Figure 1. Generalized Physiography of Arizona. Flat Colorado Plateau to the North, complex topography in Central Highlands (Mogollon Rim) and Basin and Range to the South

Rivera et al. (2014) investigated AR-related activity in the Central Highlands regions of Arizona by analyzing the moisture transport patterns associated with extreme precipitation events in the Verde River watershed over a thirty-year period. They identified two AR types based on moisture transport and trajectory. Their Type 1 AR obtained its moisture from the tropics near Hawaii with maximum moisture transport in the lower levels of the troposphere. Their Type 2 AR had a more direct tropical origin and a meridional orientation with maximum transport in the middle troposphere. Some AR events demonstrated a mixture of both Type 1 and Type 2 features. While focused on a single watershed, this study documented that inland-penetrating ARs with different

types of trajectories are an important cause of heavy precipitation events in Arizona that also lead to flooding.

Rutz et al. (2015) summarized the most important AR trajectories affecting western North America in their comprehensive analysis of inland-penetrating ARs. They named three types of ARs (coastal-decaying, inland- or interior-penetrating), based on whether or not they maintain their AR characteristics as they move over North America. Coastal-decaying ARs were characterized by a rapid decrease in water vapor flux over the Pacific Ranges. Inland-penetrating ARs were those that maintained their trajectory eastward of the Pacific Ranges, while interior-penetrating ARs were those that maintained trajectory upon reaching the northern Rocky Mountains and the Mogollon Rim. They found that most inland- or interior-penetrating ARs made landfall north of Cape Mendocino at low elevation corridors and passed to the north or the south of the high Sierras. ARs making landfall through the Baja Peninsula were more likely to penetrate the interior, but the occurrence of these AR trajectories was relatively infrequent. Other factors that were associated with trajectories of ARs were the magnitude of the integrated vapor transport (IVT) value and increases in wind speed along the AR trajectory path. As will be shown, the Baja Peninsula trajectory defined by Rutz et al., and the likelihood of an AR penetrating into the interior along this route, has great relevance for the ability of atmospheric rivers to produce flooding in Arizona.

Although research on AR events have shown that they impact regions beyond the eastern Pacific Coast and are linked to extreme precipitation and flooding events in Arizona, no prior study has directly compared AR-related flood events in Arizona to

flooding events not associated with an AR. In addition, most of the AR-related flooding and precipitation events that have been studied in Arizona are of extreme events, and there has been relatively little research on AR-related flooding or precipitation events that may not be extreme but which are nevertheless important for water resources.

2.3 Purpose

The purpose of this study is to assess the role of atmospheric rivers as flood producers in Arizona. The research addresses both extreme and non-extreme AR-related flood events, and it assesses how AR flood events compare to other flood-producing mechanisms in Arizona – not only with respect to extreme flooding, but also in terms of the importance of ARs as dominant or frequently occurring flood-producers. This assessment has the following objectives:

- (1) To identify Arizona flood peaks that are associated with atmospheric rivers penetrating inland from the eastern North Pacific Ocean,
- (2) To assess differences in the discharge magnitude and frequency of AR flood peaks vs. non-AR related flood peaks in Arizona, and
- (3) To analyze the spatial variability of AR flood influence in Arizona.

Table 1 outlines these steps, along with the procedures for accomplishing each objective.

Table 1. Research Design for Assessing the Role of Atmospheric Rivers as Flood Producers in Arizona

OBJECTIVE	PROCEDURE
<p>(1) Identify Arizona flood peaks associated with Atmospheric Rivers (ARs) <i>(see Section 3)</i></p>	<p>Select representative Arizona gauging station flood peak records to be assessed:</p> <ul style="list-style-type: none"> • Annual peaks • Peaks-above base (partial duration series)
	<p>Compile AR records for comparison with Arizona flood peaks based on a cross-referencing of data from multiple sources:</p> <ul style="list-style-type: none"> • Compilations of ARs in published research • SSM/I satellite-based images of Integrated Water Vapor (IWV) • Gridded Integrated Water Vapor Transport (IVT) dataset
	<p>Define criteria for:</p> <ul style="list-style-type: none"> • AR-Associated Flood Peaks • AR Flood Days
	<p>Compile master list of Arizona ARs:</p> <ul style="list-style-type: none"> • ARs associated with floods • ARs not associated with floods
	<p>Compile Arizona AR image gallery:</p> <ul style="list-style-type: none"> • Snapshots of SSM/I AR water vapor imagery
<p>(2) Assess differences in AR peaks vs. non-AR peaks <i>(see Section 4)</i></p>	<p>Comparison of:</p> <ul style="list-style-type: none"> • Numbers of AR flood peaks vs. non-AR peaks • Magnitudes of AR flood peaks vs. non-AR peaks
<p>(3) Analyze spatial variability of AR flood influence in Arizona <i>(see Section 5)</i></p>	<p>Compile AR Flood Map gallery:</p> <ul style="list-style-type: none"> • Map spatial distribution of stations and watersheds flooding on each AR Flood Day • Compare with Arizona AR image gallery
	<p>Investigate factors associated with spatial variability</p> <ul style="list-style-type: none"> • Flood hydroclimatology • Physiographic regions • Other basin characteristics

This thesis is organized as follows. Section 3 describes the Arizona flood peak data and the sources of AR information that were used to compile a chronology of atmospheric rivers that affected Arizona. Section 4 explains a series of analyses used to evaluate the importance of ARs as flood producers in Arizona, Section 5 explores factors that may explain the spatial variability of AR-associated flooding in Arizona, Section 6 discusses the results, and Section 7 summarizes the research conclusions.

3. Data and Physiographic Setting

In order to assess the importance of atmospheric rivers as flood producers in Arizona, a compilation of atmospheric rivers penetrating into Arizona was compared with a database of Arizona flood peaks to identify those peaks that may have been influenced by the ARs. The following sections describe the datasets used and the physiographic setting of the watersheds examined.

3.1 Arizona Flood Peak Data

The flood peaks used in this study were based on thirty-three gauging stations in Arizona (Figure 2, Table 2). The stations selected represent different physiographic and climatic regions of the state and are a subset of the stations included in the Arizona Flood Project Database (<http://www.arizonafloodproject.org/>). This database is an expansion and update of the original database of classified flood peaks developed by Hirschboeck (1987, 1988) in her study of flood hydroclimatology in Arizona. It lists peaks-above-base streamflow discharge data (annual and partial duration peaks) observed at selected U.S. Geological gauging stations in Arizona. The peak flow data were obtained from published online data sources (<http://waterdata.usgs.gov/az/nwis/nwis>), from published

annual USGS Water-Data Reports for Arizona, and directly from the Arizona Water Science Center, as needed. Each peak-above-base included in the Arizona Flood Project Database has been classified in terms of the flood-producing storm type or circulation pattern that generated the event (e.g. winter synoptic-scale precipitation, summer convective precipitation, tropical storm-enhanced synoptic-scale or convective precipitation). Atmospheric rivers affecting Arizona occur primarily in the cool season and are associated with synoptic-scale events, hence this study focuses mainly on flooding during the cool season months of November through April. In order to use a continuous record of satellite-based information to identify ARs (see following section), this study focuses on flood peaks observed at selected Arizona gauging stations having a complete period of record from 1 October 1987 – 30 September 2011. Stations with incomplete peak flow data during this time frame were not used; hence areas of the state with un-gauged watersheds or incomplete records are not well represented in this study.

Table 2. Site information for selected gauging stations shown on Figure 3

Map #	USGS Site #	Site Name	Project Code	Drainage Area		AR Fraction *	
				(mi ²)	(km ²)	Annual peaks only	All Peaks above base
Northern Arizona / Colorado Plateau Stations							
1	9379200	Chinle Creek nr Mexican Water	CHN-Nmw	3611.8	9354.56	0.083	0.112
2	9382000	Paria R at Lees Ferry	PAR-Lee	1362.1	3527.84	0.167	0.122
3	9384000	Little Colorado nr St. Johns	LCO-Stj	711.1	1841.75	0.042	0.056
4	9401260	Moenkopi Wash at Moenkopi	MKW-Mnk	1.8	4.66	0.083	0.087
5	9402000	Little Colorado nr Cameron	LCO-Cam	23491.7	60843.5	0.083	0.162
Mogollon Rim and Central Highlands / Transition Zone Stations							
6	9424450	Big Sandy nr Wikieup ⁺	BSN-Wku	2562.3	6636.36	0.458	0.464
7	9432000	Gila blw Blue Ck, nr Virden NM	GIL-Blu	1988.2	5149.44	0.292	0.257
8	9444500	San Francisco at Clifton	SFR-Clf	2764.9	7161.09	0.375	0.436
9	9447000	Eagle Ck nr Morenci	EAG-Mor	621	1608.39	0.375	0.407
10	9447800	Bonita Ck nr Morenci	BON-Mor	302.3	782.96	0.292	0.306
11	9448500	Gila nr Solomon	GIL-Sol	0.77	1.99	0.375	0.377
12	9466500	Gila at Calva	GIL-Cal	11543.2	29896.9	0.375	0.339
13	9468500	San Carlos nr Peridot	SCL-Per	1025.8	2656.82	0.458	0.442
14	9490500	Black nr Fort Apache	BLK-Fta	1223.7	3169.38	0.458	0.525
15	9492400	East Fork White nr Fort Apache	EFK-Fta	21.7	56.2	0.333	0.333
16	9497800	Cibecue Ck nr Chrysolite	CIB-Chr	290	751.1	0.292	0.309
17	9497980	Cherry Ck nr Globe	CHE-Glo	199.8	517.48	0.417	0.56
18	9498500	Salt nr Roosevelt	SLT-Roo	4289.4	11109.5	0.542	0.485
19	9499000	Tonto Ck nr Roosevelt	TON-Roo	672.2	1741	0.458	0.57
20	9504000	Verde nr Clarkdale	VRD-Crk	3507.2	9083.65	0.458	0.52
21	9504500	Oak Ck nr Cornville	OAK-Crn	355.1	919.71	0.458	0.54
22	9505350	Dry Beaver Ck nr Rimrock	DBV-Rim	142.1	368.04	0.417	0.47
23	9505800	West Clear Ck nr Camp Verde	WCL-Cmp	241.4	625.23	0.542	0.5
24	9508500	Verde abv Horseshoe Dam	VRD-Hsd	5870	15203.3	0.542	0.5
25	9510200	Sycamore Ck nr Fort McDowell	SYC-Med	164	424.76	0.458	0.493
26	9512500	Agua Fria nr Mayer	AFR-May	585.2	1515.67	0.292	0.319
27	9513780	New nr Rock Springs	NEW-Rck	68.4	177.16	0.5	0.466
Southern Arizona / Basin and Range Stations							
28	9470500	San Pedro at Palominas	SPD-Pal	738.3	1912.2	0.083	0.065
29	9471000	San Pedro nr Charleston	SPD-Cha	1216.2	3149.96	0.083	0.121
30	9473000	Aravaipa Ck nr Mammoth	ARV-Mth	537.6	1392.38	0.167	0.286
31	9480000	Santa Cruz nr Lochiel	SCR-Loc	82	212.38	0.042	0.03
32	9480500	Santa Cruz nr Nogales	SCR-Nog	531.7	1377.1	0.125	0.156
33	9486000	Santa Cruz at Tucson	SCR-Tuc	2191.9	5677.02	0.042	0.075

* AR fraction for each station = (total AR peaks / total observed peaks) see Section 4

+ The Big Sandy watershed heads in the far western area of the Central Highlands Transition Zone and has Basin and Range characteristics in its lower reaches

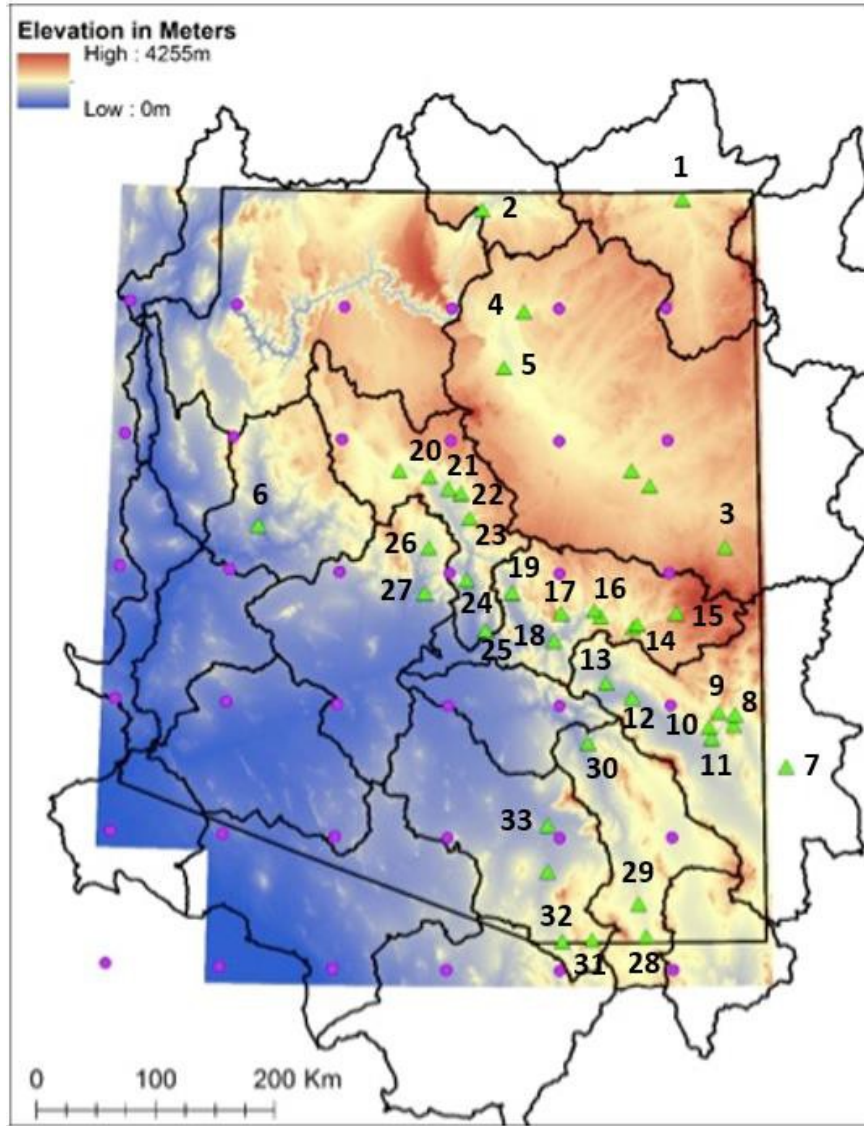


Figure 2. Map of Arizona showing major watershed boundaries, elevation, and the location of the flood peak gauging stations used in this study (green triangles)

Also shown are gridpoint locations of interpolated Integrated Water Vapor Transport (IVT) (purple circles) (see Section 3.2.2)

3.2 Atmospheric River Data

The dataset of atmospheric river events used in this study was assembled by cross-referencing AR information from multiple sources (see Table 1). Several published

studies of ARs that affected western North America provided an initial chronology of events to examine. The ARs in these studies were identified by applying specific criteria to areas of concentrated water vapor in the atmosphere, based on measurements of either Integrated Water Vapor (IWV) or Vertically Integrated Horizontal Water Vapor Transport (IVT). IWV values represent the total amount of water vapor present in a vertical column of air, expressed as depths (e.g. centimeters) and can be estimated from SSM/I satellite data¹, from atmospheric reanalyses, or from models. (IWV can also be presented as Total Precipitable Water (TPW) in millimeters of liquid water). IVT values represent the overhead transport of water vapor at a gridpoint, expressed as fluxes in $\text{kg m}^{-1} \text{s}^{-1}$, and are calculated from atmospheric reanalyses or from models by integrating the horizontal moisture flux through a series of atmospheric layers (e.g., surface to 500 mb). Following is an overview of the published sources examined to develop this study's chronology of ARs affecting Arizona.

Neiman et al. (2008a) developed a chronology of landfalling ARs affecting the North American coast. They used SSM/I to identify narrow integrated water vapor (IWV) plumes with values > 2 cm that were $> 2,000$ km in length and $< 1,000$ km in width intersecting the western North American coastline between $32.5^\circ - 52.5^\circ\text{N}$ for the period 1 October 1997 – 30 September 2005. Dettinger et al. (2011) expanded upon this work, adding AR dates for 1 October 2005 – 30 September 2008 to Neiman et al.'s record and compiling a chronology of pineapple express events (PEs) affecting the western coast North America for the period 1 October 1948 – 30 September 2008. Rivera et al. (2014)

¹ Special Sensor Microwave Imager (SSM/I) and Special Sensor Microwave Imager Sounder (SSM/IS) instruments onboard the Defense Meteorological Satellite Program (DMSP) satellites

² SSM/I data provided by Remote Sensing Systems ~~26~~ sponsored by the NASA Earth Science MEaSUREs

focused specifically on Arizona and looked at extreme precipitation events in the Verde River basin during the cool season (November – March) for the period 1 October 1979 – 30 September 2011. They determined which of these precipitation events were associated with atmospheric rivers by defining an AR as an event satisfying the AR flux algorithm by Zhu and Newell (1988) with integrated vapor transport (IVT) $> 250 \text{ kg m}^{-1} \text{ s}^{-1}$ and length $> 2,000 \text{ km}$. Using these criteria, they put together a record of extreme precipitation events in the Verde River basin that indicated whether or not each event was associated with an AR.

The AR events recorded in the above studies were then cross-referenced with an independent compilation of ARs developed for this project based on composite images of Integrated Water Vapor (IWV) and Total Precipitable Water Vapor (TPW) from satellite imagery (SSM/I data) and a gridpoint dataset of Vertically Integrated Water Vapor Transport (IVT) associated with ARs over Arizona that was kindly provided by Jonathan Rutz and James Steenburgh (personal communication, 2013). Details on these IWV and IVT datasets follow.

3.2.1 Integrated Water Vapor (IWV) Data from SSM/I

Daily Integrated Water Vapor (IWV) composite images derived from Special Sensor Microwave Imager (SSM/I) and Special Sensor Microwave Imager Sounder (SSM/IS) instruments onboard the Defense Meteorological Satellite Program (DMSP) satellites were used to identify ARs with trajectories aimed toward Arizona and likely to

penetrate inland. The images were obtained online from Remote Sensing Systems² (www.remss.com) and were examined to determine the presence or non-presence of AR patterns prior to or during each of the flood peaks at the study gauge in the Arizona Flood Project Database. The composites, available at http://images.remss.com/ssmi/ssmi_data_daily.html, are produced every twelve hours, when satellites complete one pass. SSM/I data were available on this site beginning in late 1987. This determined the starting hydrologic year or water year (WY), which begins in October and ends in September of the following year, for the study period. Figure 3 shows an example of one of the composite images used. Appendix A contains all composites evaluated for the study period of 1 October 1987 – 30 September 2011.

² SSM/I data provided by Remote Sensing Systems are sponsored by the NASA Earth Science MEaSUREs DISCOVER Project

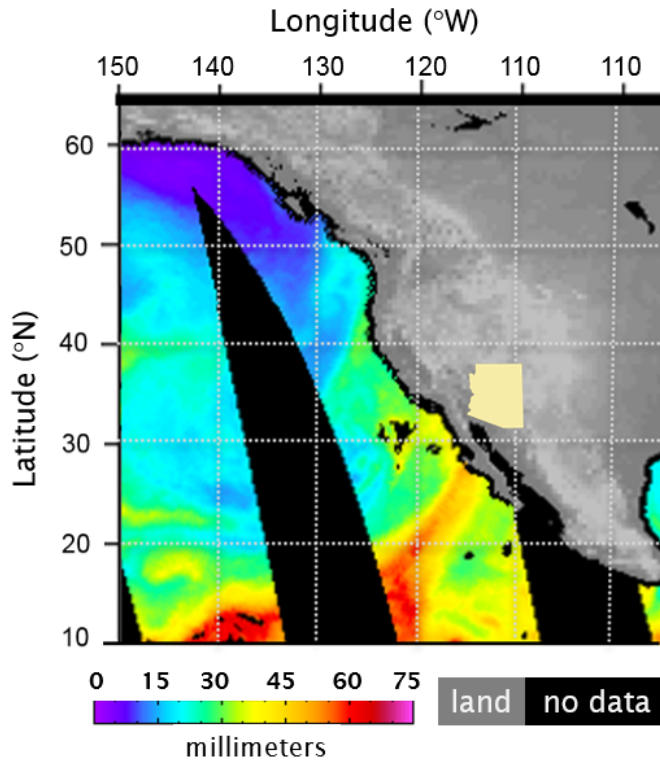


Figure 3. Satellite-derived Integrated Water Vapor (IWV) Composite Image

This 12-hour UTC PM composite shows column IWV (aka “Total Precipitable Water Vapor”) on October 31, 1987. An inset map of Arizona is superimposed. In the image, a plume of concentrated water vapor can be seen with a south-southwesterly trajectory that is targeted to cross Baja and enter Arizona. This AR event was associated with 10 flood peaks in the Arizona Flood Project Database (see Appendix A).

3.2.2 Vertically Integrated IVT Grid Point Measurements

Rutz and Steenburgh (personal communication, 2013) identified ARs that occurred in the cool season months (November – April) for the period 1 October 1988 – 30 September 2011 with the Interim European Centre for Medium-Range Weather Forecasts (ECMWF) Re-Analysis (ERA-Interim; Dee et al. 2011). They classified precipitation as AR-related if an AR had been identified at the closest ERA-Interim grid

point at any of the reanalysis times. With a spatial resolution of 1.58 latitude x 1.58 longitude and a temporal resolution of 6 hours, the Rutz and Steenburgh IVT gridpoint dataset made available to us provided a way to connect AR influence with the occurrence of peak flows in Arizona watersheds throughout the state, representing different hydroclimatic and physiographic regions. Rutz and Steenburgh identified ARs objectively as either (1) a region >2,000 km long with IWV > 20 mm, or (2) a region >2,000 km long with integrated vapor transport value (IVT) > 250 kg m⁻¹ s⁻¹.

3.3 Arizona AR Days

An initial examination of eastern North Pacific ARs in SSM/I imagery approaching California and northwest Mexico during the period 1 October 1987 – 30 September 2011 indicated that ARs associated with peak flows in the Arizona Flood Hydroclimatology Database preceded the actual peak flow by no more than two days. Prior to a peak flow occurrence, AR plumes intersected the North American continental boundary within an area bounded by 25°N – 35°N and 110°W – 130°W. On this basis, an Arizona AR Day, as defined in this study, is a day on which an AR pattern in the SSM/I with IVT > 2 cm, length > 2,000 km, and width < 1,000 km was observed in the eastern North Pacific Ocean during at least one twelve-hour satellite passing period in the region specified above. This definition is based on a review of the most common AR definitions found in the literature (Table 3). All SSM/I composites available for the study period were reviewed to identify the days that met the Arizona AR Day criteria. Cross checking the AR Days with flood information in the Database allowed the determination of which flood events, if any, appeared to be associated with ARs.

As an independent check, the Arizona AR Days were then compared with AR dates already compiled in the works of Neiman et al. (2008a), Dettinger et al. (2011), Rivera et al. (2014), and Rutz and Steenburgh (personal communication). All dates from each source were combined into a master chronology of AR events and integrated in the Arizona Flood Project Database to distinguish the ARs associated with Arizona flooding from those not associated. Lastly, watershed maps were produced to show which gauging stations recorded flood peaks in response to the flood-associated AR events. Figure 4 illustrates this procedure, and Appendix A contains an annotated AR image gallery for the chronology of AR Days compiled in this study and associated watershed maps that indicate where ARs produced flooding during the study period.

Table 3. Definitions of atmospheric rivers from various sources in chronological order.

AR Definition	Reference
“characterized by strong gradients in a southwest flow of moist stable air from a rather distant low-latitude source, with a minimum of interruption by intrusion of air from a more northerly source”	Weaver 1962 (p. 207)
“water vapor transport in the troposphere is characterized by a filamentary structure”; “the fraction of the globe they cover is 10% or less”	Zhu and Newell 1998, based on Newell and Zhu 1992
“quite narrow (<1000 km wide) relative to both their length scale (>~2000 km) and to the width scale of the sensible component of heat transport”	Neiman et al. 2008a
[Pineapple express] “steer warm, moist air from the tropics near Hawaii northeastward into California”	Dettinger 2011, based on Weaver 1962; Dettinger 2004
“as they approach the west coast of North America, ARs are typically 2,000 or more kilometers long but only a few hundred kilometers wide”	Dettinger 2011, based on Ralph et al. 2006
“areas of strong winds (greater than 12.5 ms ⁻¹ wind speed [...]) with an Integrated Water Vapour (IWV) in the atmospheric column of more than 2 cm”	Lavers et al. 2011, based on Ralph and Dettinger 2011 and Ralph et al. 2004
“concentrate those fluxes into long (>~2000 km), narrow (<~1000 km) plumes”	Neiman et al. 2011, based on Bao et al. 2006; Stohl et al. 2008; Ralph et al. 2011
“narrow plumes of SSM/I vapor with values >2 cm that were >2,000 km long and <1,000 km wide”	Dettinger et al. 2011
“thousands of kilometers long and, on average, only 400 km wide”	Ralph and Dettinger 2012
“a contiguous region ≥2000 km in length and ≤1000 km in width containing IWV values ≥20 mm”	Rutz and Steenburgh 2012
“long (>2000 km), narrow (<1000 km), low-level (below ~600 hPa) plumes of enhanced water vapor flux”	Neiman et al. 2013, based on Zhu and Newell 1998; Ralph et al. 2004, 2005, 2011; Neiman et al. 2008a, b; Smith et al. 2010
“long (about 2000 km), narrow (about 300-500 km wide) bands of enhanced water vapor flux”	Gimeno et al. 2014 (p.1), based on Newell et al. 1992
A plume of water vapor >2000 km long, <1000 km wide, and IWV value of >2 cm.	This study, based on Dettinger et al. 2011 and Rutz and Steenburgh 2012

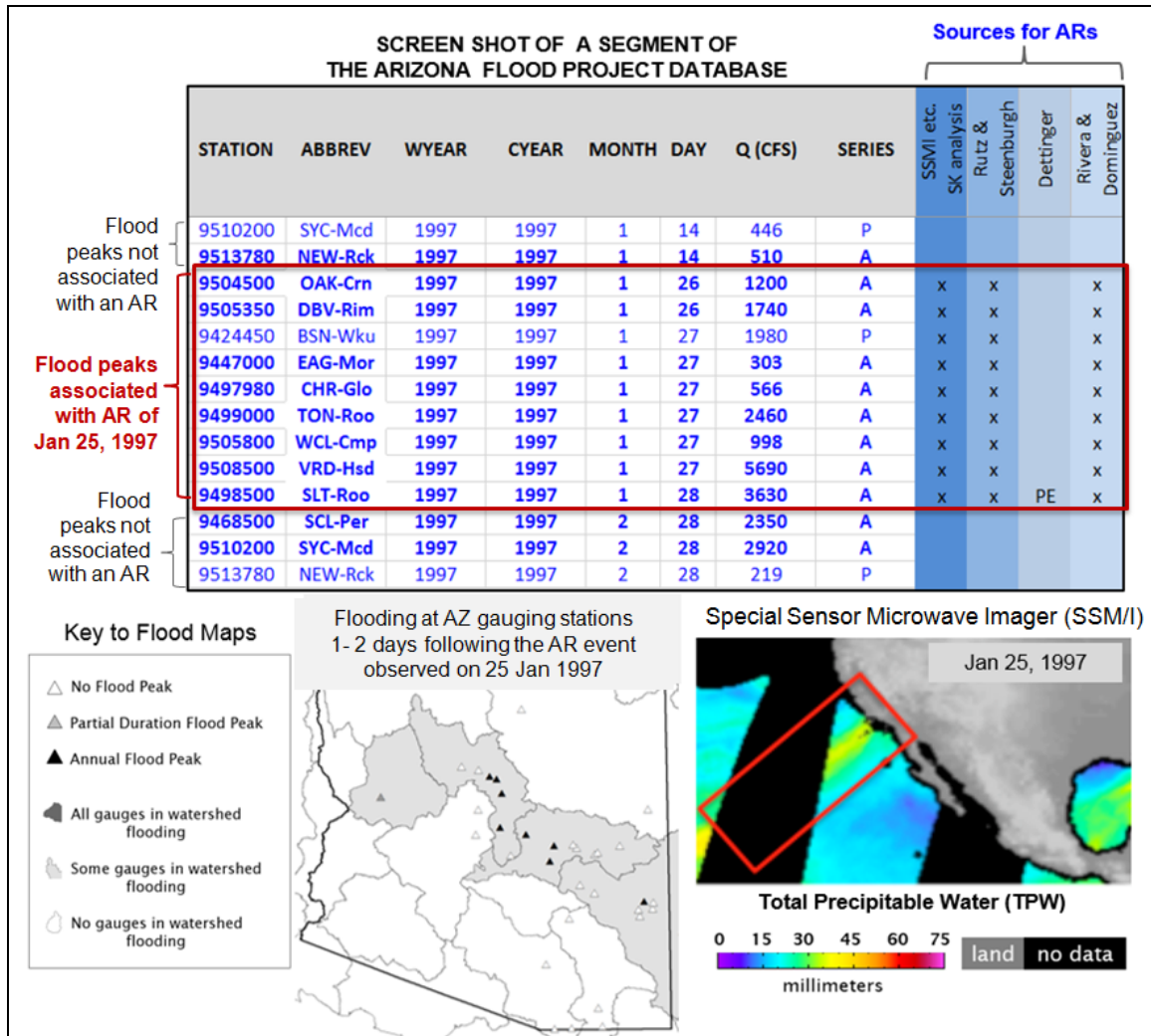


Figure 4. Illustration of the procedure used to identify Arizona flood peaks associated with atmospheric rivers originating in the eastern North Pacific Ocean.

The AR seen in SSM/I imagery on Jan 25, 1997 (red box) was also noted in each of the other AR published sources investigated for the January 26-28 flood peaks.

3.4 Physiological and Climatic Setting

Previous work has pointed to the importance of orography as a factor in the precipitation and flooding associated with atmospheric rivers (e.g., Smith et al. 2010; Neiman et al. 2011). To assess the role of orography on atmospheric rivers and flooding

in Arizona, an understanding of the physiographic setting of the state as it interacts with different types of seasonal precipitation-delivery systems is needed. Arizona can be divided into three main physiographic regions: the Colorado Plateau in the north, the Basin and Range region in the south and west, and the Central Highlands Transition Zone between these two areas, which includes the Mogollon Rim's abrupt rise in elevation (Figure 1). The Colorado Plateau region is a relatively flat, high-elevation semiarid region in northern and northeastern Arizona. It receives much of its precipitation during the summer from convective storms and in the winter from synoptic storms. Few AR-related flooding events have been observed in this region. The Basin and Range region makes up most of southern and western Arizona and consists of alternating regions of steep linear mountain ranges and relatively flat desert basins. The semiarid southeastern portion of the region is considerably more mountainous than the extremely arid southwestern portion. The region receives both AR and non-AR winter synoptic precipitation and flooding, but the most common flood-producing mechanism in this region is summer convective rainfall and the largest floods are associated with infrequent tropical storms (Hirschboeck 1987, 1988). The Central Highlands Transition Zone is comprised of mountainous terrain and valleys of varying elevations. The Mogollon Rim, an escarpment that runs from the northwest to the southeast across the region, is a prominent orographic feature associated with an abrupt increase in elevation. Precipitation and flooding in the Central Highlands is dominated by AR and non-AR winter synoptic storms, although summer convective and tropical storms also produce

some flooding. Precipitation and flooding events in the Central Highlands Transition Zone can be especially extreme due to the great orographic effect observed in this area.

4. The Importance of ARs as Flood Producers

To analyze the role and importance of atmospheric rivers as flood producers in Arizona, it is necessary to determine the yearly distribution and flooding behavior of AR events throughout the state.

4.1 Interannual Variability and Seasonality of ARs

Table 4 displays the number of Arizona AR Days occurring during the cool season months during 1 October 1987 – 30 September 2011, and indicates dates when an AR was associated with a flood peak in the Arizona Flood Project Database. Figure 5 shows the monthly distribution of AR-related peaks, and Figure 6 shows the interannual variability of AR events. The chronology of AR events during the period of record shows no significant trends over time in the number of peak-producing events, non-peak events, or the total number of events. What it does reveal is that AR activity was present during every year in the study period (Table 4, Figure 6). Even in years where there was minimal or no AR-related flooding, a nonzero number of non-flooding AR events occurred.

Table 4. Arizona flood-related atmospheric river dates by month (WY 1988 – 2011)

WY ⁺	Seasonality of AR Flood Events in each Cool-Season Month <i>numbers in each column below indicate the date, e.g., Oct 31</i>								Annual Totals		
	Oct	Nov	Dec	Jan	Feb	Mar	Apr	May	AR-flood days	AR non-flood days	Total AR-days
1988	31			17			20*, 28*		4	N/A	4
1989	14*			4		7, 11			4	7	11
1990									0	4	4
1991				4		1, 5, 26	6*, 10*		6	5	11
1992				5	13	5	13*		4	1	5
1993			5, 28	6, 16	7, 19, 24*, 26*	17			9	1	10
1994		22			7	20			3	3	6
1995			6	4, 12, 25	14	4, 10			7	3	10
1996					21				1	6	7
1997				3, 25					2	3	5
1998	2				8, 14, 17, 23	25, 28			7	3	10
1999	25*								1	6	7
2000									0	3	3
2001	10, 29*	6			13			1	5	2	7
2002			14*						1	6	7
2003		9			13, 25	15	14		5	1	6
2004		12							1	2	3
2005	20, 27		28	4, 10	11, 15, 19, 21	19*			10	2	12
2006									0	7	7
2007				5*					1	2	3
2008		30	7	5, 27	4, 22	29*			7	0	7
2009			17, 25		16, 23	3			5	2	7
2010				20, 22	6*	20*			4	4	8
2011			21, 29		19	2*			4	2	6
Total	8	5	10	18	25	18	6	1	91	75	166

* indicates that an AR was observed in SSM/I imagery only on this date

+ indicates El Niño WYs: . strong: 1998 , moderate: 2003 , weak: 2005 source: gweather.com/enso/oni.htm

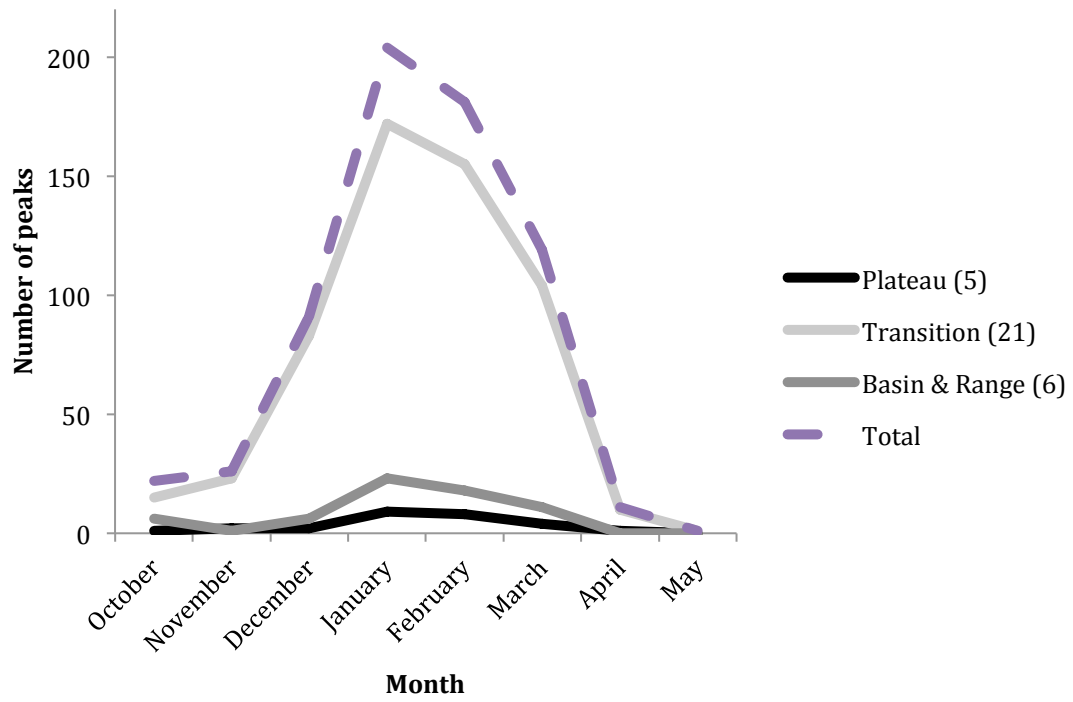


Figure 5. Monthly distribution of AR-related peaks in Arizona grouped by physiographic region for the cool season months during the WY 1988-2011 study period.

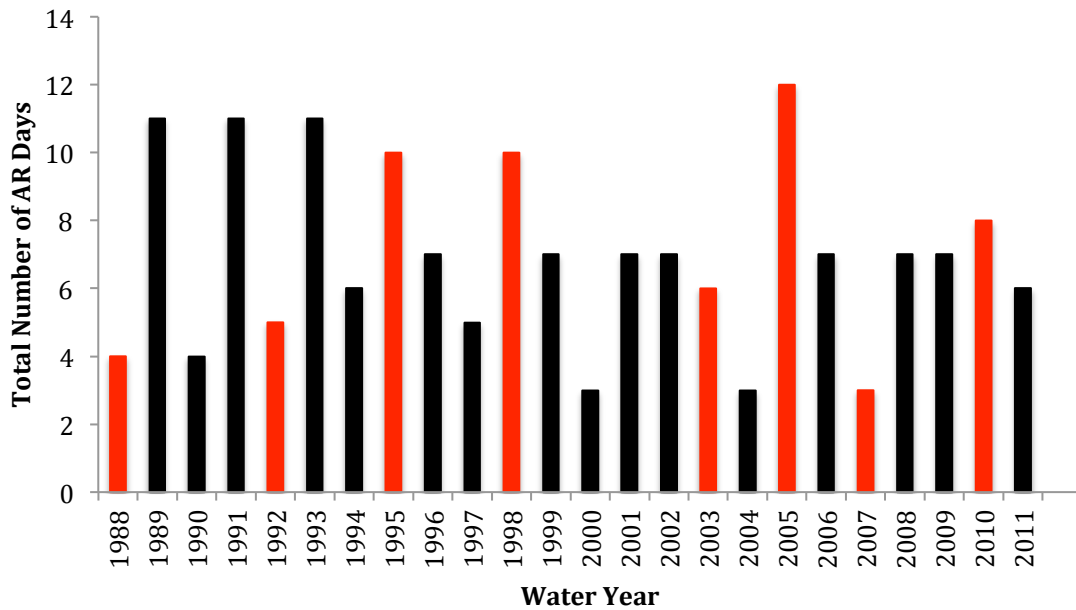


Figure 6. Interannual variation of the total number of cool-season AR Days affecting Arizona. (Red bars indicate an El Niño year. See Table 4 for associated AR flood days.)

Flood-producing AR events are linked predominantly to the cool season months. These findings support the work of Neiman et al. (2008a), which stated that ARs had occurred primarily during the warm season in the northern west Pacific coast and during the cool season in California. During the summer months ARs primarily affect regions at higher latitudes, whereas wintertime ARs can extend to lower latitudes than would be possible for summer ARs. No AR-related peak flows were present in the summer for this study because all summertime ARs during the period of record were shown to have occurred at latitudes too high to affect Arizona in the SSM/I.

Peak flow dates associated with ARs occurred throughout the period October – May, with the highest number of flood-producing events observed in the three-month

period of January – March. The sole AR event in May occurred near the end of April and was the latest AR observed during the period of study, which suggests that peak AR activity in Arizona is during October – April and that the May event was anomalous.

A comparison of the monthly distributions of all AR-related peak flows observed during the study period shows that the pattern of monthly AR flooding is similar for the three physiographic regions of Arizona (Figure 5). As the cool season progresses, the number of peak flows increases until January for all regions and then declines in the last months of AR activity.

The interannual variation of AR-related peak flows that occur in Arizona is dependent on the number of inland-penetrating ARs that influenced Arizona. Figure 6 shows the total number of cool-season AR Days that affected Arizona during the study period of 1 October 1987 – 30 September 2011. At least one AR flood occurred every hydrologic year, but not every AR was associated with flooding. There were some years in which no AR-related peak flows were observed. No clear pattern appears to be present as to which years had greater AR activity, although El Niño may play some role (Table 4, Figure 6). During an El Niño, the southwestern U.S. and northwest Mexico tend to experience increased precipitation and wetter winters. AR events that occurred during warm El Niño periods³ had a tendency to produce more AR flood days than non-El Niño ARs, but this observation is not decisive enough to say that El Niños consistently result in AR-related flooding in Arizona.

³ El Niño dates are based on compilations at: <http://ggweather.com/enso/oni.htm> and http://www.cpc.noaa.gov/products/analysis_monitoring/ensostuff/ensoyears.shtml

One observation that can be made with respect to the interannual variation of AR Days is that years with a high frequency of occurrence of AR events penetrating into Arizona also tend to be years in which many ARs actually produce floods, instead of being “non-flooding AR events.” This suggests that antecedent conditions in the watershed play an important role in flooding, and that, if AR events occur in clusters or in succession to one another, it is more likely for flooding to occur as a result of later AR storms. The widespread extreme flooding throughout Arizona in winter 1992 – 1993 was associated with multiple ARs impacting the state over a 4-month period (see discussion of these record-breaking floods in House and Hirschboeck, 1997). Other high-frequency AR years that produced a high frequency of AR flooding occurred in 1991, 1995, 1998, and 2005. Most – but not all – of these were associated with a weak, moderate or strong El Niño event (see Table 4).

There are some years on record in which there was very little or no AR-related flooding but high AR activity. Some possible factors as to why certain ARs may produce flooding and others do not will be discussed in Section 5. The lack of flooding events associated with certain ARs is notable, as it shows that not all AR events will produce flooding.

These results show that flooding associated with ARs is a seasonal occurrence in Arizona to the point of exclusion for the warm-season months (June – September). For these months, ARs are all but absent in Arizona as a flood-producing mechanism.

4.2 AR Fraction

To measure the importance of AR-related flooding within specific watersheds in Arizona, an “AR fraction” approach was used. Rutz and Steenburgh (2012) and earlier researchers have used the concept of an AR fraction to assess the amount of cool season precipitation associated with an AR compared to all cool season precipitation. Here, the AR fraction is based not on the *amount* of AR-related precipitation, but on the *number* of AR-related peak flow events. It is computed as the proportion of peak flow events associated with AR events compared to all peaks observed at a given gauging station during the study period. The following equation was used to compute AR fraction for selected Arizona gauging stations:

$$AR\ fraction = \frac{total\ \# \ AR\ peaks}{total\ \# \ observed\ peaks} \quad (1)$$

The AR fraction was calculated for each station based on: (1) annual peaks, and (2) all partial duration series “peaks-above-base” observed at that station and are listed in Table 2. High AR fraction values indicate that the watershed above the station was AR-sensitive, while lower AR fractions indicate that AR-related floods were infrequent in that watershed.

The annual and all peaks-above-base AR fractions are grouped geographically and by physiological region in Figure 7. The five stations in the Little Colorado, Upper Colorado, and San Juan watersheds were combined to represent the Colorado Plateau region. Stations located in the Gila, Verde, Salt, and Agua Fria watersheds showed higher

AR fractions compared to AR fractions for stations in the Santa Cruz, the San Pedro, and the Colorado Plateau. The Gila, Verde, Salt, and Agua Fria watersheds are all located in the Central Highlands Transition Zone; the Santa Cruz and San Pedro are in the southeastern Basin and Range Province. The implications of the AR Fraction results suggest that the mere presence of an AR does not produce flooding in a watershed, nor do ARs affect all watersheds equally. It also suggests the watersheds in the Mogollon Rim / Central Highlands region have characteristics that make them more favorable to AR-related flooding.

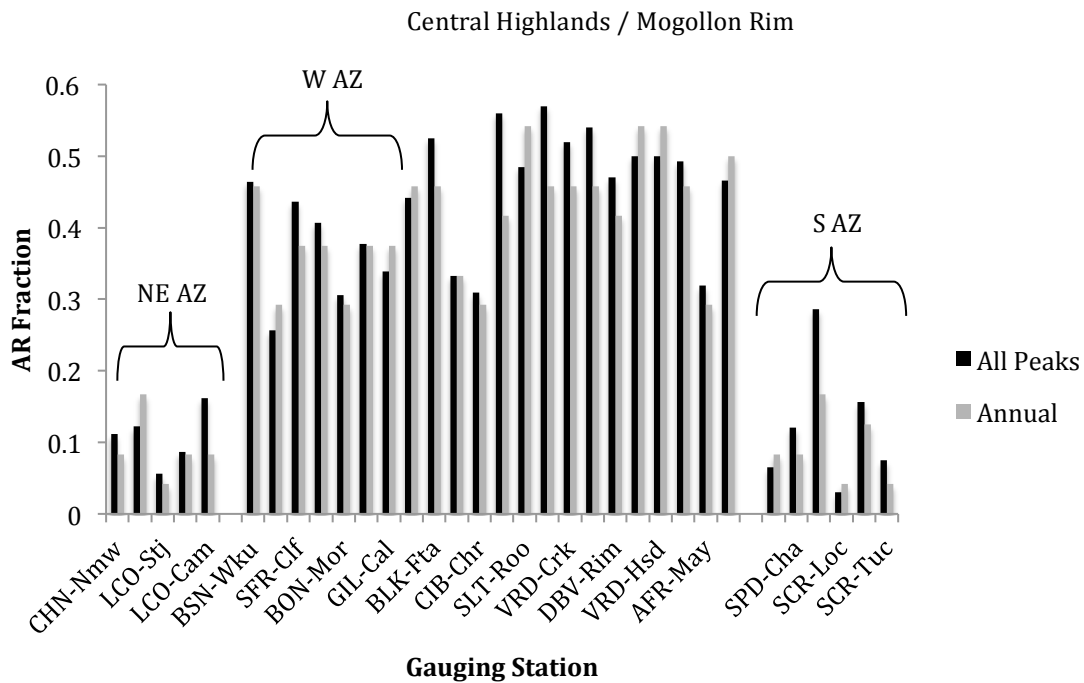


Figure 7. AR fractions at selected gauging stations by watershed during WYs 1988 – 2011

4.3 Magnitude of AR and non-AR Flood Peaks

To compare the discharge magnitudes of peak flows associated with ARs to those produced by non-AR events the peak discharges were transformed to dimensionless z-scores to facilitate station-to-station comparisons for drainage areas of varying sizes. The z-score of a peak flow at a given station was obtained using:

$$z = \frac{x - \mu}{\sigma} \quad (2)$$

where x is the \log_{10} value of the discharge of that peak, μ is the mean of that station, and σ is the standard deviation of that station.

There were regional patterns in the average z-score values calculated for AR-related floods vs. non-AR-related floods, as well as for floods occurring at other times of the year due to convective storms (see Appendix B). All stations located in the Central Highlands Transition Zone show positive average AR z-score values for both annual peaks and all peaks-above-base. For all but one station, (#15 East Fork White near Fort Apache), the AR peaks have a higher z-score value than floods produced by any other mechanism. Because most of the stations with records suitable for this study are located in the Central Highlands, the AR influence in this region is well documented and robust.

The stations in the Colorado Plateau and southern Basin and Range Province observed fewer AR-related peaks, and in many cases fewer winter peaks in general. Because of the lack of data, there is far less consistency in the z-scores calculated for these regions, so any region-wide conclusions about the magnitude of AR floods vs. non-AR floods are less reliable in these areas.

4.3.1 AR Influence on Rank of Peak Flow Events

In order to evaluate whether the largest peak events observed at a station were more likely to be associated with ARs than other flood-producing mechanisms, a Pearson's chi-square test was performed on a subset of watersheds. The test evaluated whether or not there was a statistically significant relationship between the ranking of a peak and the mechanism that produced it. The test was done as follows.

All the peak flows observed at selected gauging stations in the Gila, Verde, Santa Cruz, Little Colorado, and Salt watersheds were organized into contingency tables. The peaks were separated by the mechanism that produced them and by their ranking (top, middle, or bottom) in a given watershed. A contingency table was then used to categorize each peak by mechanism and whether it ranked in the top third, middle third, or bottom third for that watershed. Table 5 shows an example for Stations #7, 11, and 12 in the Gila River watershed.

Table 5. Contingency table for evaluating the importance of AR vs. non AR mechanisms on Flood Peak Rank. Shown are the number of events in each category

Stations analyzed: # 7, the Gila River below Blue Creek near Virden, #11 the Gila River near Solomon, and #12 the Gila River at Calva

	AR-Related	Non-AR Winter	Convective	Tropical	Total
Top Third	17	15	4	0	36
Medium Third	5	18	9	3	35
Bottom Third	6	8	19	2	36
Total	28	42	32	5	107

The chi-square test statistic was calculated as follows:

$$\chi^2 = \sum_{i=1}^n \frac{(O_i - E_i)^2}{E_i} \quad (3)$$

where O_i is the observed frequency, E_i is the expected frequency, and n is the number of cells. The expected frequency of a cell was found using the following equation:

$$E_i = \frac{r_i c_j}{n} \quad (4)$$

where r_i is the total observations for row i , c_j is the total observations for column j , and n is the total number of observations. The number of degrees of freedom was found using:

$$df = (r - 1)(c - 1) \quad (4)$$

where df is the degrees of freedom, c is the total number of columns, and r is the total number of rows.

This test was performed twice – once using the actual discharge value (in cubic feet per second) to rank the peak flows in a watershed, and again using the z-score values of discharge to rank them. The ranking by actual discharge and z-score was used to check on whether changing the way discharge was measured affected the chi-square test statistic. Comparing the actual discharge of the peaks in a watershed reveals how large the flooding produced from a storm was, but it does not indicate whether or not the peak flow produced was large with respect to the gauging station mean.

The value of the chi-square test statistic was calculated from the contingency tables for each of the five watersheds using both the direct discharge magnitudes and the z-scores of discharge (Table 6 shows an example for actual discharge; see Appendix C for all results). The chi-square test statistic indicates that there is sufficient evidence to

reject the null hypothesis that peak ranking and mechanism of peaks are independent. These results show that there is some difference in the ranking of peak flows by mechanism in the Verde and Gila watersheds, but it does not indicate whether the AR peaks are greater in magnitude than peaks produced by other means.

Table 6. Chi Square Test results for the selected watersheds (based on actual discharge)

Station	χ^2 (Discharge)	χ^2 (z-score)
#7, 11-12 Gila	26.1*	17.63*
#20, 24 Verde	23.4*	30.24*
#31-33 Santa Cruz	1.97	3.58
#3, 5 Little Colorado	9.87	18.15*
#18 Salt	19.15*	16.15

** indicates significance (at the .01 level with six degrees of freedom, the chi-square test statistic must exceed 16.81 to be significant)*

The Santa Cruz watershed shows that at a 0.010 significance level there is not sufficient evidence to reject the null hypothesis that the magnitude of the peaks and the mechanism of the peaks are independent for either the direct discharge or the z-score of discharge. The results show that in the Santa Cruz watershed the rankings of peak flow events by the type of storm that produced them are consistent. There is no evidence to suggest that a certain mechanism is more likely to produce peaks of greater magnitude than other flood-producing mechanisms.

Results for the Salt and Little Colorado watersheds show that the significance of the chi-square test statistic values for these watersheds is dependent on which method was used to determine ranking. For the Salt watershed, at the 0.010 significance level there was sufficient evidence to say that the direct discharge and the mechanism of the storm that produced the peaks were not independent, but the test statistic comparing the z-score of discharge and the storm type did not indicate that the factors were dependent.

Likewise, in the Little Colorado watershed, at the 0.010 significance level the direct discharge and the flood mechanism were independent. But the z-score of discharge and storm type were shown to not be independent of one another.

These results suggest that in the Verde and Gila basins the ranking of the magnitude of peak flows within those watersheds is dependent on the storm that produced them, and that different flood mechanisms may produce larger or smaller peaks compared to one another. For the Santa Cruz watershed, there is no indication in this analysis that storm type affects the magnitude of peak flows produced in that watershed, although companion studies to this analysis using other statistical approaches have demonstrated the significance of warm-season tropical storm-enhanced convective events for this watershed (K. Hirschboeck and D. Zamora-Reyes, personal communication, 2015). The results for the Little Colorado and Salt watersheds are mixed, suggesting that further study requiring more information needs to be done for these watersheds.

Both the Verde and the Gila watersheds are located in the Transition Zone, which suggest that the magnitude of flood events in this region may be tied to the flood mechanism that produced them. If this hypothesis holds true, it would allow for better understanding of the flooding behavior in this region and better preparation for large storm and flooding events.

4.3.2 Difference in Means of AR and Non-AR Peaks

To determine the difference in means of AR-related peak flows to non-AR winter and convective peaks, a two-sample t-test was performed at select gauging stations

comparing the means of peaks produced by AR events to non-AR winter storm peaks, and the means of AR-related peak flows to those produced by summer convective storms.

The means of the lognormal values of discharge at selected gauging stations for events produced by each of the flood-producing mechanisms were computed and the test statistic was calculated using the following equations:

$$t = \frac{x_1 - x_2}{s_{x_1x_2} \cdot \sqrt{\frac{1}{n_1} + \frac{1}{n_2}}} \quad (6)$$

$$t = \frac{x_1 - x_2}{s_{x_1-x_2}} \quad (7)$$

where x_1 and x_2 are the means of the peaks produced by different mechanisms, n is the sample size, and s is the standard deviation, found using:

$$s_{x_1x_2} = \sqrt{\frac{(n_1 - 1)s_{x_1}^2 + (n_2 - 1)s_{x_2}^2}{n_1 + n_2 - 2}} \quad (8)$$

$$s_{x_1-x_2} = \sqrt{\frac{s_1^2}{n_1} + \frac{s_2^2}{n_2}} \quad (9)$$

Eq. (6) and Eq. (8) were used to calculate the value of the t-statistic when the variances of the two sample populations were similar. If the variances were not similar, then Eq. (7) and Eq. (9) were used to find the t-statistic. To test whether the variances of the two populations were similar or not similar, the following f-test was used:

$$\frac{\text{Larger } s^2}{\text{Smaller } s^2} > 3 \quad (10)$$

where the variances are considered to be similar if the ratio is not greater than 3, and not similar if the ratio exceeds 3.

The two-sample t-test determines whether there is sufficient evidence to say that a difference in the means of AR-related peak flows and non-AR peak flows exists. If none of the stations show a difference in the means of AR and non-AR peaks, it cannot be concluded that ARs produce storm and flooding events of greater magnitude than non-AR flood-producing mechanisms. If there are stations that show a difference for one or both comparisons of the means, it suggests that the mechanism that produced a storm or flood event and the magnitude of flooding produced by that event may not be independent.

To find the difference in the means of AR-related peak flows and non-AR peak flows at select gauging stations, the mean and standard deviation for the lognormal discharge at each station were used to calculate the t-statistic for the means of AR-related peaks versus non-AR winter and convective peaks at the selected stations (Table 6). The t-statistic values were compared at a 0.010 significance level. Because both types of comparisons (AR vs. non-AR winter, AR vs. convective) throughout all gauging stations vary in degrees of freedom, there was no one consistent rejection region. The value of the rejection region for each of the stations and the degrees of freedom were found in order to test the significance of the t-statistic values (Appendix D).

The results are shown in Table 7 for the difference in means of AR vs. Non-AR winter synoptic peaks and for AR vs. summer convective peaks. In all cases, the AR-related peaks were of greater magnitude than the non-AR winter peaks and the summer convective peaks. All of the stations that showed a significant difference in the means of AR versus non-AR winter or convective peaks were located in the Central Highland Transition Zone.

Table 7. The t-statistic values for difference in means of AR and non-AR peaks

Station	AR vs. Non-AR Winter	AR vs. Convective
#6 Big Sandy nr Wikieup	3.447*	2.356
#1 CHN-Nmw	-0.411	0.058
#11 GIL-Sol	1.77	3.918*
#5 LCO-Cam	2.156	1.101
#27 NEW-Rck	3.361*	1.91
#21 OAK-Crn	5.25*	3.766*
#32 SCR-Nog	1.624	1.813
#8 SFR-Clf	1.756	3.613*
#18 SLT-Roo	3.362*	3.22*
#24 VRD-Hsd	5.692*	4.09*
<i>* indicates significance at the .01 level; see Appendix D for individual results</i>		

The gauging stations analyzed that were located in the northern Colorado Plateau or the southeastern Basin and Range regions did not show a significant difference in means between AR vs. Non-AR floods. The results for these gauging stations are in agreement with the chi-square test statistic, in which the Santa Cruz watershed showed no significant relationship between magnitude of peak flow and the flood-producing mechanism and the Little Colorado result was inconclusive.

All of the statistical analysis results indicate that, although ARs may not be universally the largest flood-producing mechanism at every gauging station in every watershed, they dominate the flood peak record in the Central Highlands Transition Zone and are responsible for some of the largest winter storms that have occurred there. The watersheds in this region are the most sensitive to AR activity and most likely to observe large AR-related flood events. The stations in the northern Colorado Plateau and the southern Basin and Range regions recorded very few AR-related floods throughout the period of record. The AR-related peaks that did occur were not significantly larger than flooding produced by other mechanisms. Therefore, these regions appear to be far less sensitive to ARs and are the least likely to experience major AR flood events.

Because there were few gauging stations with sufficiently long records in the far western and southwestern parts of Arizona to analyze for this study, the likely flooding and AR behavior in those areas can only be inferred from the results of this study. Further research into the influence of atmospheric rivers on flooding behavior of western Arizona is needed.

4.3.3 AR and non-AR Annual Peak Comparison

The previous comparisons of AR vs. non-AR peak flows were based on peaks-above-base values recorded at each gauging station. This section presents a similar comparison using annual peaks only. Annual peaks were sorted by the mechanism that produced them (AR, non-AR winter, convective, and tropical) and the mean discharge for each type of mechanism was computed. A comparison of the different flood-type discharge means revealed which mechanism produced the largest peaks at each gauging

station. Results for the annual peak comparisons are shown in Figures 8 – 12 and Tables 8 – 10. Following is a summary of the results by region.

In the Colorado Plateau, only at Stations #1 (Chinle Creek) and #5 (Little Colorado) did ARs produce the largest mean annual discharge. Observations at the other stations in this region show that the annual discharge produced by ARs is smaller than the annual discharge produced by other mechanisms. These results suggest that ARs do not produce the largest annual flooding events in the Colorado Plateau as a whole (Figure 8, Table 8).

Annual Peaks (Northern AZ / Colorado Plateau)

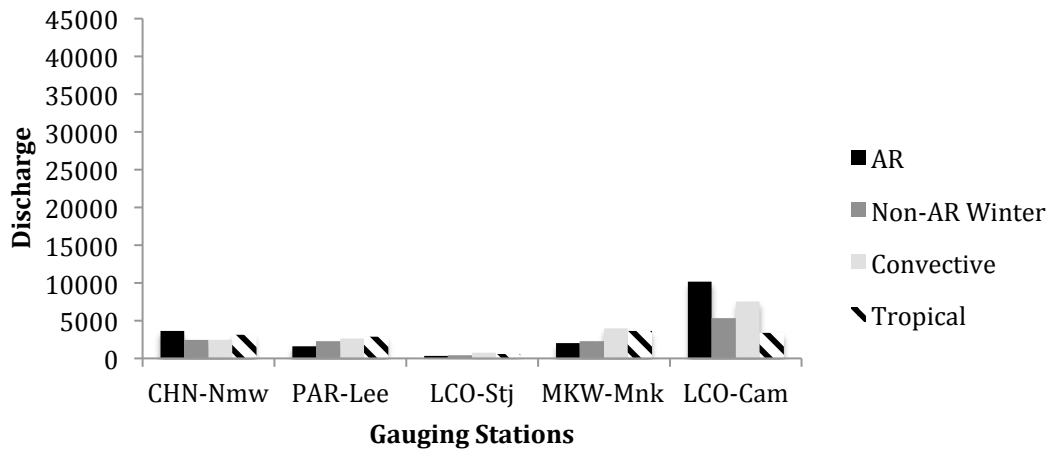


Figure 8. Comparison of annual peaks for Northern Arizona stations (Figure 2 Map #'s 1-5 in Figure 2)

Table 8. Mean discharge of annual peaks by mechanism for Northern AZ / Colorado Plateau

	AR	Non-AR Winter	Convective	Tropical
CHN-Nmw	3636.5	2456.7	2454.3	3090
PAR-Lee	1619.5	2242.3	2659.9	2854.7
LCO-Stj	289	451.2	719.9	555
MKW-Mnk	2060.5	2314.6	3973.6	3672.3
LCO-Cam	10150	5347.2	7523.3	3340

Results for the Southeastern Arizona Basin and Range region showed that at Stations #29 (San Pedro), 31, 32, and 33 (Santa Cruz) the mean annual peaks produced by ARs were greater than those produced by other mechanisms. At the two remaining stations in this region, peaks produced by non-AR winter storms had the greatest mean discharge and AR-related annual peaks had the second largest mean discharge. This suggests that in Southeastern Arizona winter storms produce the largest winter annual peak flow events, but ARs are not necessarily responsible for the largest annual peaks (Figure 9, Table 9).

Annual Peaks (Southeastern AZ /Basin and Range)

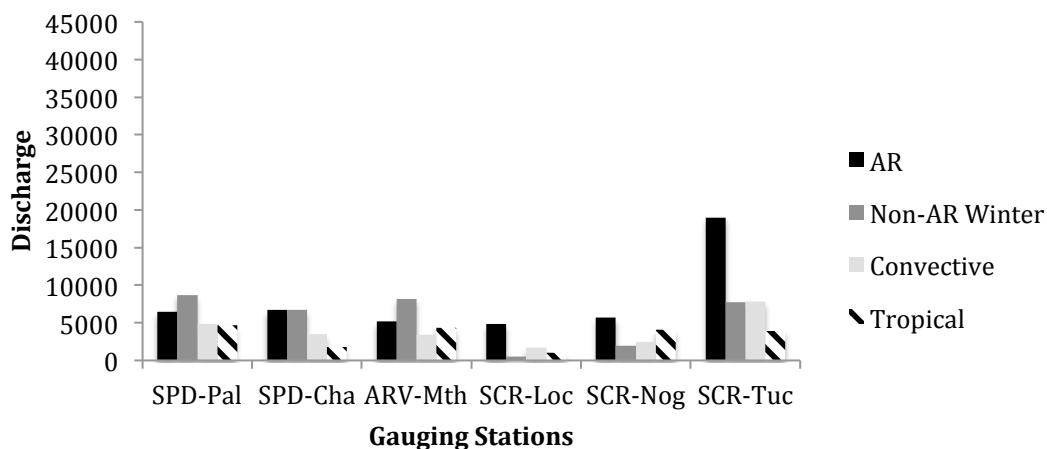


Figure 9. Comparison of annual peaks for Southeastern Arizona stations (Figure 2 Map #'s 28-33 in Figure 2)

Table 9. Mean discharge of annual peaks by mechanism for Southeastern AZ

	AR	Non-AR Winter	Convective	Tropical
SPD-Pal	6440	8677.1	4826.8	4695
SPD-Cha	6725	6689	3455.1	1815.2
ARV-Mth	5155	8182.9	3438.4	4365
SCR-Loc	4880	540.8	1670	1025.5
SCR-Nog	5713.3	1953.5	2438.2	4065
SCR-Tuc	18988	7735	7824.7	3915

The Central Highlands Transition Zone is dominated by AR-related peak flows, and with the exception of Station #15 (East Fork White) the mean annual discharge for AR peak events is greater than the mean annual discharge of any other flood-producing mechanism in this region. From these results it can be concluded that in the Central

Highlands, ARs not only dominate the flood record but also produce the overall largest annual peak flooding events (Figures 10 – 12, Table 10).

Annual Peaks (Eastern AZ / Transition Zone 1)

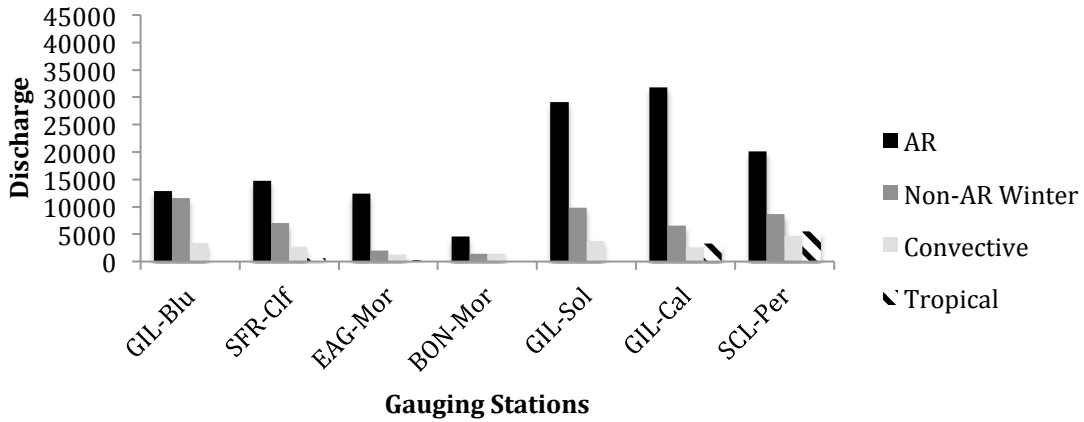


Figure 10. Comparison of annual peaks for Eastern Arizona Transition Zone 1 stations (Figure 2 Map #'s 7-13)

Annual Peaks (East Central AZ /Transition Zone 2)

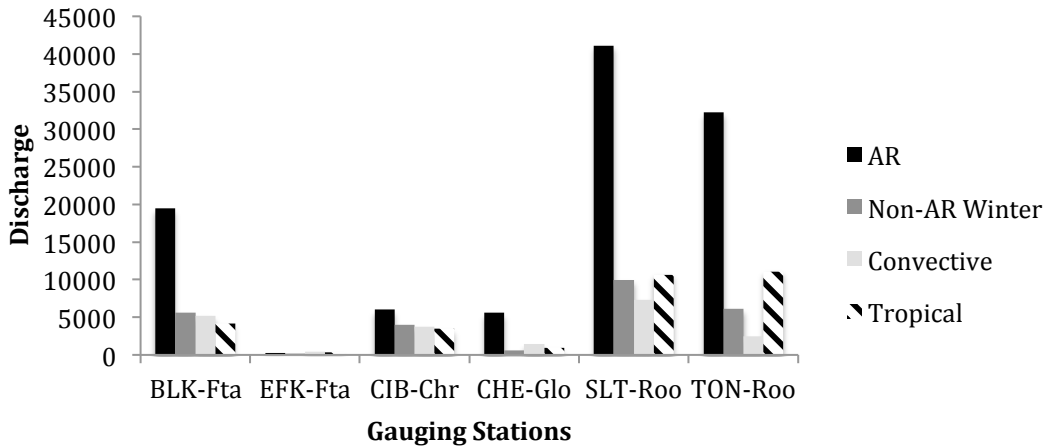


Figure 11. Comparison of annual peaks for East Central AZ Transition Zone 2 stations
(Figure 2 Map #'s 14-19)

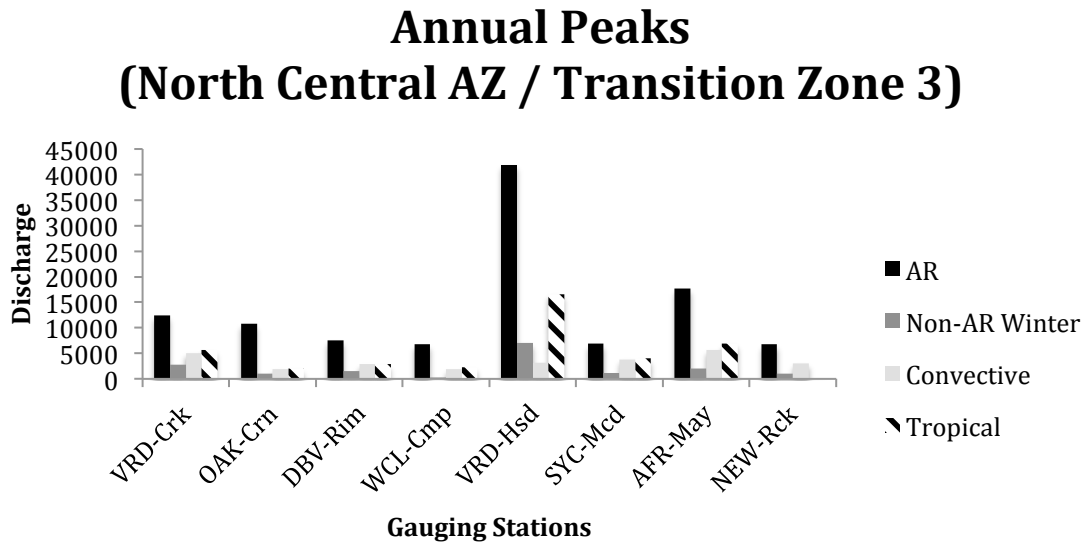


Figure 12. Comparison of annual peaks for North Central Transition Zone 3 stations
(Figure 2 Map #'s 20-27)

Table 10. Mean discharge of annual peaks by mechanism for Mogollon Rim/Transition Zone.

	AR	Non-AR Winter	Convective	Tropical
BSN-Wku	29744.2	2589.4	6561.7	12933.3
GIL-Blu	12868.6	11536.3	3362.8	N/A
SFR-Clf	14788	7029.6	2656.9	653
EAG-Mor	12444.6	1988	1327.6	193.5
BON-Mor	4534.7	1449.3	1455.3	N/A
GIL-Sol	29167.9	9846.7	3776.7	N/A
GIL-Cal	31796.2	6521	2561.3	3250
SCL-Per	20133.6	8626	4720.5	5565
BLK-Fta	19489.8	5586	5158	4175
EFK-Fta	283	179	441.4	378
CIB-Chr	6021.4	3970.8	3713.9	3470
CHE-Glo	5627.8	583.2	1458.7	925
SLT-Roo	41126.2	9940	7324	10676.7
TON-Roo	32277.5	6166.1	2453.7	11071
VRD-Crk	12423.7	2722	5045.8	5656.7
OAK-Crn	10810.9	1054.7	1941.7	2000
DBV-Rim	7554	1466.5	2859.7	2876.7
WCL-Cmp	6805.6	295	1867.3	2265
VRD-Hsd	41870	6987.5	3195	16600
SYC-Mcd	6896.5	1187	3831.7	3990
AFR-May	17701.4	2016.3	5625.6	6895
NEW-Rck	6757.8	1007.6	3044.7	56

4.3.4 AR vs. non-AR Winter Storms

As noted in section 4.1, AR events only affect Arizona during the wintertime because summer ARs occur at a latitude too far north to produce flooding in Arizona. To further study the differences between AR and non-AR flooding events, AR events were compared to non-AR winter peak events only.

For this analysis, all AR and non-AR winter season flooding events were extracted from the database for the gauging stations in this study, and the wintertime peak events were arranged in a contingency table by z-score and based on whether an event ranked in the top third, middle third, or bottom third of winter flooding events. When the chi-square test statistic was calculated from Eq. (3), Eq. (4), and Eq. (5), the 0.010 significance level of the test statistic indicated there was very strong evidence that the ranking of wintertime flooding events was related to whether an AR or a synoptic storm had produced them (Table 11).

Table 11. Contingency table for evaluating the difference between ranking of AR and non-AR winter peak flow events.

	AR	Non-AR Winter	Total
Top Third	306	102	408
Middle Third	197	210	407
Bottom Third	152	256	408
	655	568	1223

These results suggest that throughout the studied gauging stations, ARs as a flood-producing mechanism produce larger flooding events than non-AR winter storms

and that ARs are the overall dominant wintertime flood-producing mechanism in those regions that are most sensitive to ARs.

5. Explorations of Factors that May Influence the Spatial Variability of AR

Flooding

The dominance of AR influence in the Mogollon Rim / Central Highlands Transition Zone watersheds prompted further exploration for this spatial variability.

5.1 Basin Characteristics

The possibility that certain basin-specific variables might have an influence on the watersheds in which AR flooding dominates was investigated using basin characteristics data obtained from the US Geological Survey's StreamStats website.⁴ The variables evaluated for each gauging station were: percentage of slope greater than 30°, mean basin slope, outlet elevation, maximum elevation, drainage basin size, percentage of forest cover, and soil permeability. Basin characteristic values for the area above the study gauging stations were plotted against the corresponding AR fraction for that gauging station to see if there was any correlation between AR fraction and the selected basin characteristic variables. Figures 13 – 19 are plots of AR fraction against basin characteristics for the selected gauging stations and reveal interesting hints as to why some basins are more responsive to flooding by atmospheric rivers than others.

The AR fraction of a given watershed appeared to have little relationship to the watershed's drainage basin area (Figure 13) or the maximum elevation within the

⁴ USGS Arizona StreamStats Basin Characteristics:
http://streamstatsags.cr.usgs.gov/ss_defs/basin_char_defs.aspx

watershed (Figure 14). However, a comparison of AR fraction and outlet elevation showed that the AR fraction decreased as the outlet elevation increased (Figure 15).

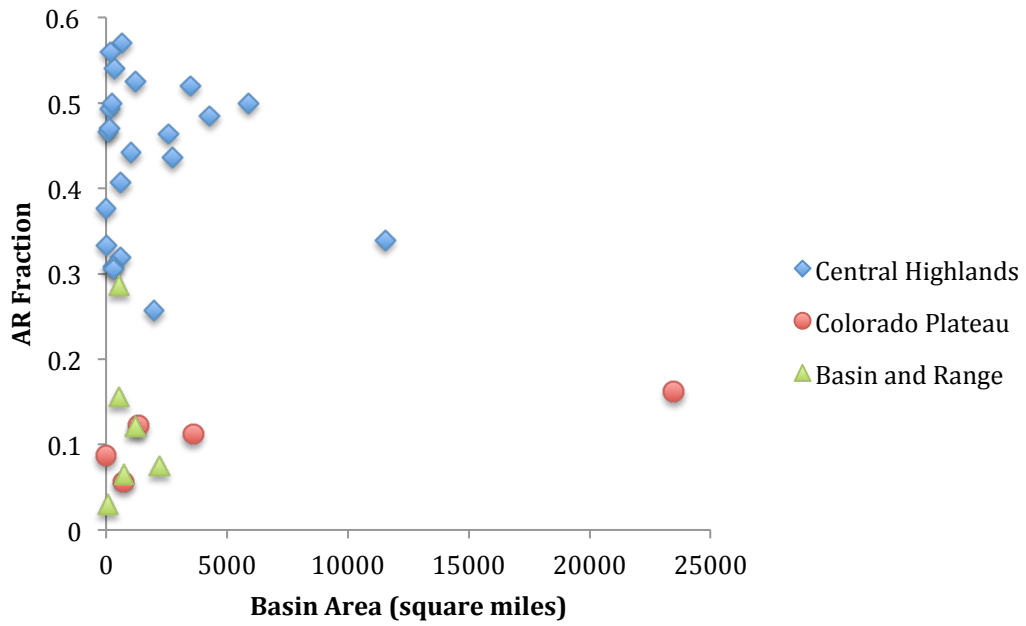


Figure 13. Drainage basin area and AR fraction

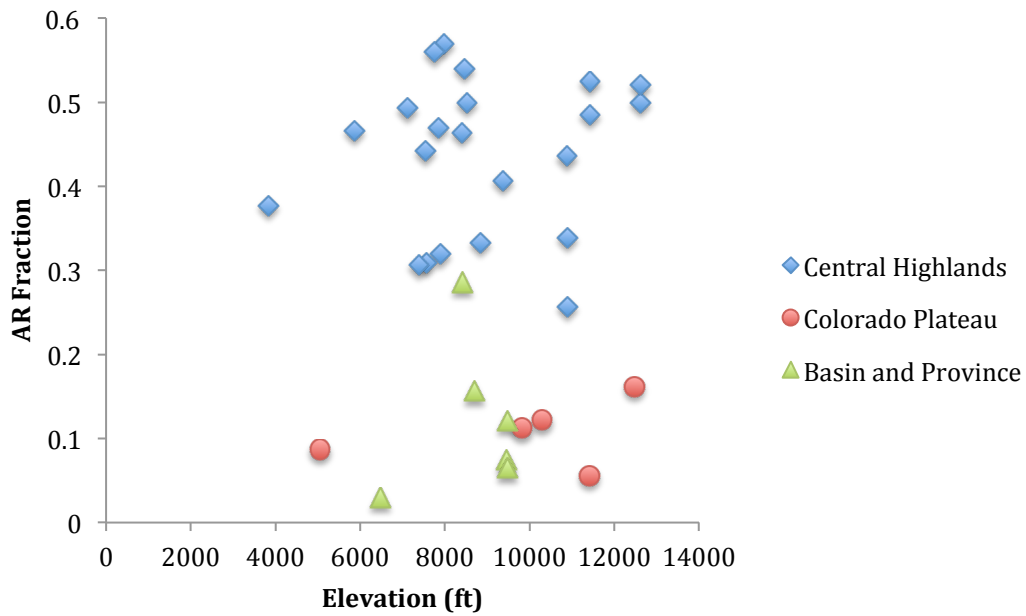


Figure 14. Maximum elevation and AR fraction

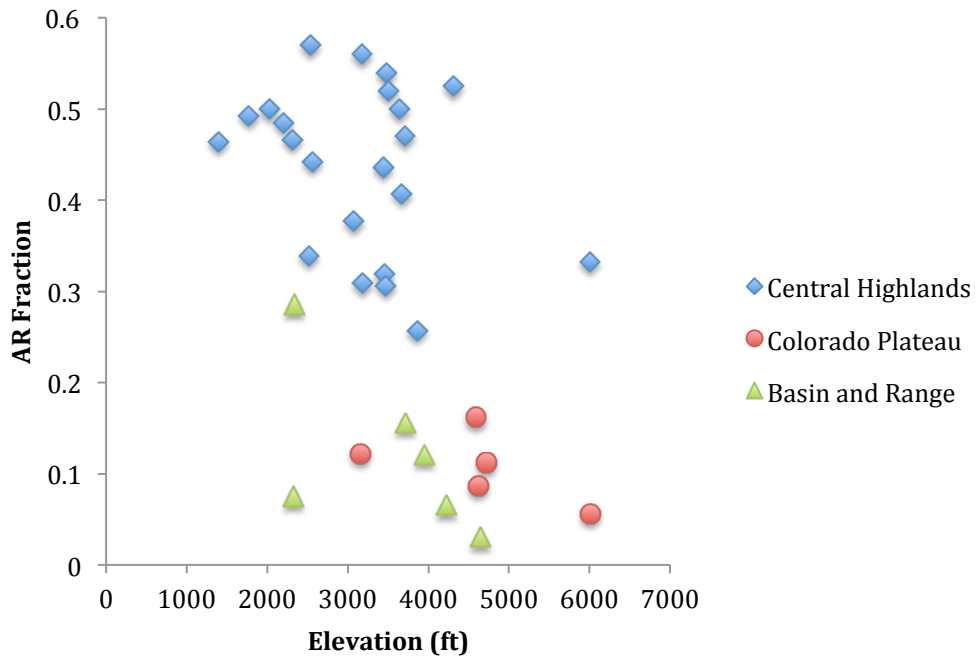


Figure 15. Outlet elevation and AR fraction

Comparing the percentage of slope greater than 30° and the mean basin slope of a drainage basin to AR fraction showed an overall increase in the AR fraction as the slope and the percentage of slope increased (Figure 16, Figure 17).

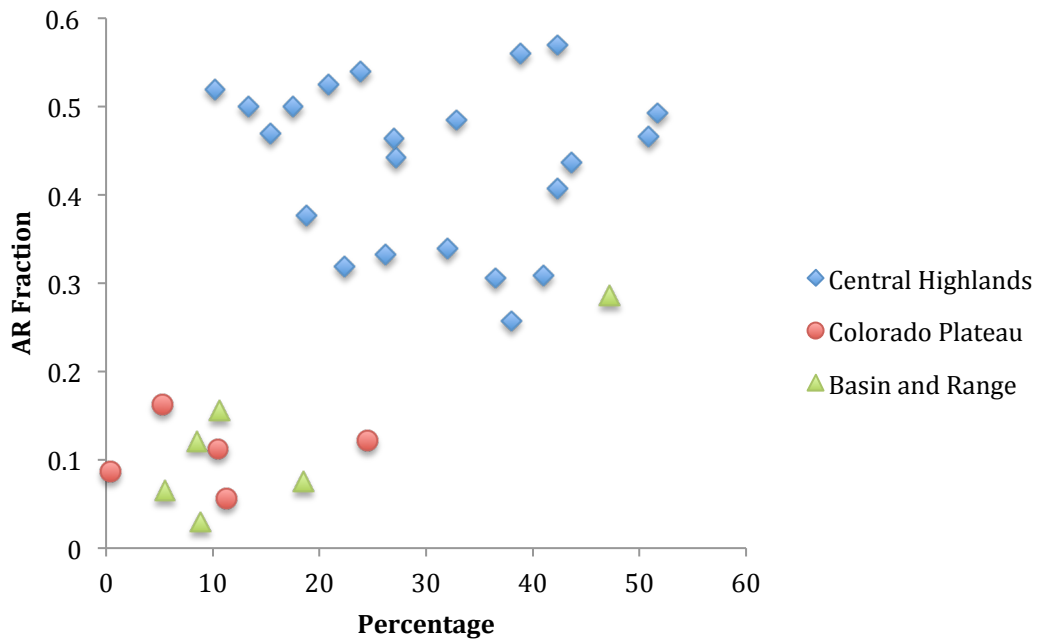


Figure 16. Percentage of slope > 30 and AR fraction

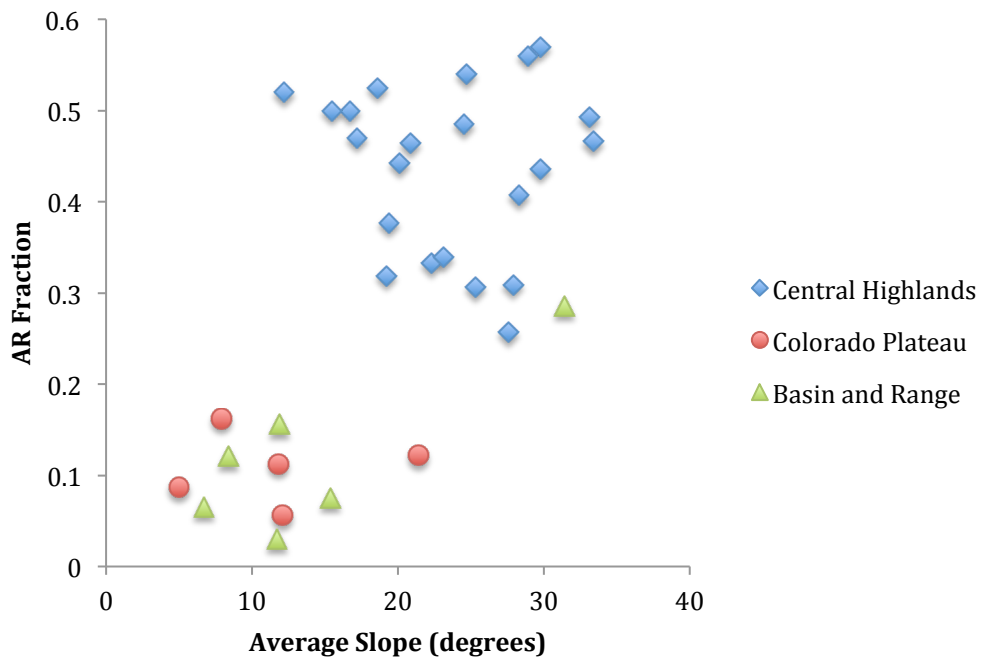


Figure 17. Mean basin slope and AR fraction

There was no noticeable relationship between AR fraction and the percentage of forest cover of a watershed (Figure 18), but as the permeability of the soil increased the AR fraction appeared to decrease (Figure 19).

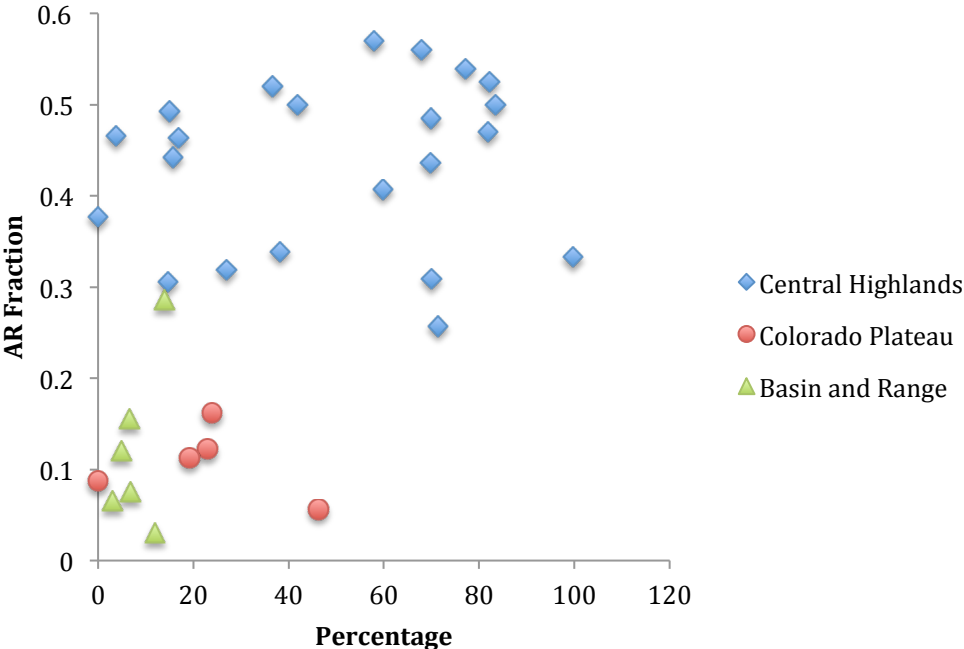


Figure 18. Percentage of forest cover and AR fraction

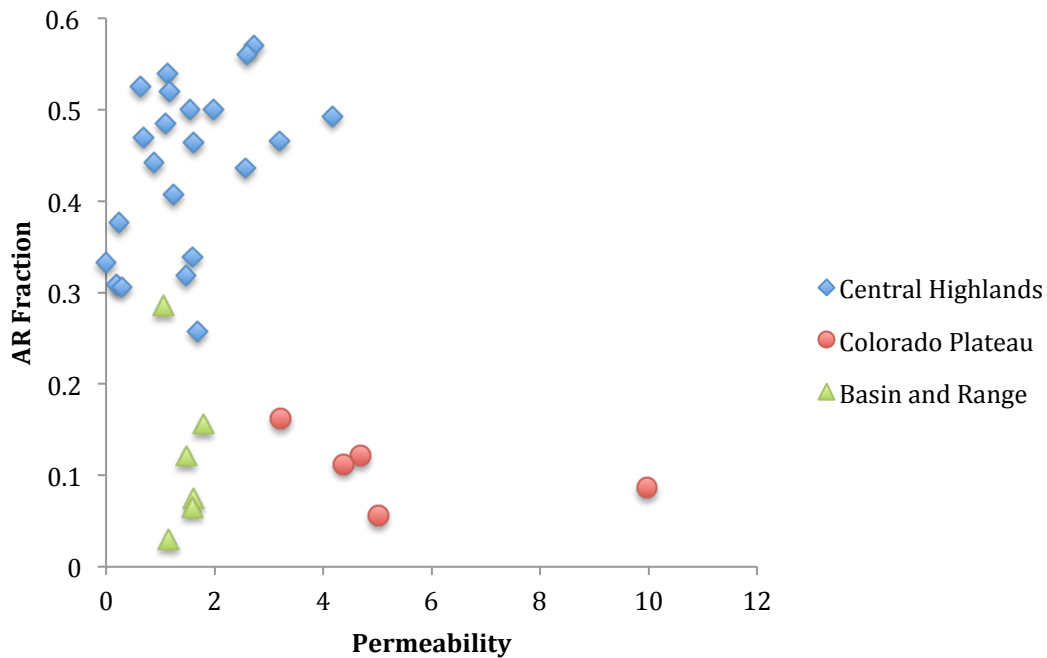


Figure 19. Soil permeability and AR fraction.

These results point to possible basin characteristic variables that may affect the likelihood of AR flooding in Arizona watersheds, especially for the watersheds in the Central Highlands Transition Zone and suggest further exploration.

5.2 AR Trajectories

Finally, the role of AR trajectories was assessed. The different trajectories and points at which the ARs made landfall into North America were determined using the SSM/I composites (Appendix A). The trajectories of the ARs were divided into (1) westerly, (2) southerly and southwestern (3) and northwestern. The points of entry into North America were classified as either (1) Baja Peninsula or (2) California. Using these categories, the number of AR flooding events associated with each trajectory were evaluated (Table 12) and the importance of the point of entry was assessed (Table 13).

Table 12. Contingency table for evaluating the importance of trajectory of entry on the number of peak flow events.

	0-1	2-5	6-10	11+	Total
Westerly	28	6	4	4	42
South / southwesterly	65	21	11	18	115
Northwestern	5	1	1	0	7
	98	28	16	22	164

Table 13. Contingency table for evaluating the importance of point of entry on the number of peak flow events.

	0-1	2-5	6-10	11+	Total
California	48	12	8	3	71
Baja California	51	16	8	18	93
	99	28	16	21	164

To determine whether the trajectory or the point of entry of an AR affected the likelihood of Arizona AR flooding, the AR data were categorized into a contingency table by number of flooding events (0-1, 2-5, 6-10, and >11); for westerly, southerly and southwestern, or northwestern trajectories; and whether the ARs made landfall by crossing the Baja Peninsula or through California. A Pearson's chi-square test of independence was performed using the methods and equations described in section 4.3.1 to determine whether the occurrence or non-occurrence of an AR-related flood was independent of any of the above variables.

Results of the chi-square test showed insufficient evidence that the likelihood of AR flooding was significantly related to either the trajectory or point of entry. Nevertheless, the categorization of AR trajectories and points of entry indicated that ARs with a southerly and southwestern trajectory were more frequently observed in Arizona than those with a westerly trajectory, and that more ARs made landfall through the Baja Peninsula than through California.

Future studies of AR trajectory and points of entry in relation to flooding could look at the magnitude of flooding associated with these variables. Instead of looking at the number of flooding events, a comparison of the average magnitude of flooding events associated with each variable may show whether there are certain trajectories or points of entry that are more favorable to AR-related flooding.

6. Discussion

The objective of this study was to assess the importance of atmospheric rivers as flood producers in Arizona, and the role ARs played in Arizona flood events compared to that of other Arizona flood producing mechanisms. The findings described above raise the following points of discussion related to these objectives:

Certain regions in Arizona are more susceptible to AR-related flooding than others.

There are certain regions and watersheds in Arizona that were more sensitive to AR-related flooding. The AR fractions of stations in the Central Highlands Transition Zone of the state had the highest values for both annual peaks and all peaks-above-base. The AR fractions of this region outranked all but one of the AR fractions observed at

gauging stations in either the Northern Arizona / Colorado Plateau region or the Southeastern Arizona Basin and Range region.

The distribution of AR-related flooding in the Central Highlands Transition Zone, however, was not homogeneous. Variability appeared to be linked to the watersheds of this region, some of which appeared to be more influenced by the abrupt elevation change of the Mogollon Rim than others. The Gila watershed, which has its headwaters in New Mexico, is in the eastern part of the Transition Zone, and the AR fractions of gauging stations in this watershed were on average smaller than those of the Salt and Verde, which are located in the center of the Central Highlands when the Mogollon Rim elevation change is greatest. These results imply that certain watersheds and regions within the Central Highlands have more favorable conditions for experiencing large and frequent AR-related flooding events.

The Northern Arizona / Colorado Plateau watersheds and the Southeastern Arizona Basin and Range regions showed the least sensitivity to ARs. The AR fractions observed at gauging stations in these regions were much smaller than those observed in the Central Highlands (see Table 2). This shows that the majority of Arizona AR activity manifests itself in the Central Arizona Transition Zone Highlands, and that ARs are not a dominant flood-producing mechanism in either the Northern Arizona Colorado Plateau region or in Southeastern Arizona (a region where warm-season flooding has more dominance).

Despite these differences in regional watershed-based AR flood sensitivity, the seasonality of atmospheric river events affecting Arizona and the flooding associated

with them is consistent throughout the state. AR Days and AR-related flooding were observed only in the cool season months of October – May, and were absent entirely in Arizona in the months of June – August. This result is in agreement with the early findings of Neiman et al. (2008a) for ARs affecting the west coast, who stated that most ARs affecting western North America occurred during the cool season in latitudes to the south of 41.0°N).

ARs produce floods of greater magnitude than floods produced by other mechanisms.

A comparison of z-scores for peak flow events throughout the selected watersheds showed that in the Central Highlands, the z-score calculated for AR-related peak flows were overall positive throughout all Central Highlands gauging stations for both annual peaks only and all peaks-above-base. With the exception of Station #15, the AR z-scores outranked the z-scores of the other flood-producing mechanisms for both annual and all-peaks-above-base in the Central Highlands. These results imply that in this region the peak flows produced by AR-related events tend to be greater than those produced by other mechanisms. It also demonstrates a strong consistency in behavior throughout all Central Highlands stations, and suggests that regardless of variability in AR fraction and z-score value there is an overall similarity in flooding behavior within this region.

The Colorado Plateau and Basin and Range z-scores show far less consistency in flooding behavior throughout each region. There was no one flood-producing mechanism in which the z-scores for that mechanism consistently outranked the z-scores of the other flood-producing mechanisms for either of these regions; rather, the mechanism for which the greatest z-score value was calculated varied by gauge. The lack of consistent behavior

in Colorado Plateau and Basin and Range gauging stations implies that neither region has a mechanism that uniformly produces peak flow events larger than those of other flood-producing mechanisms throughout the region. These results may also be affected by a lack of reliable gauging station data, especially in the Colorado Plateau region and the western part of Arizona.

The results of Pearson's chi-square test of independence comparing the ranking of peak flow events within a watershed to the mechanism that produced them, performed for five Arizona watersheds, showed that in some watersheds the ranking of a peak flow was not independent of the mechanism that produced it. However, in some other watersheds the ranking of peak flows were independent of mechanism. The peak flows were ranked in two different ways: by the raw discharge of the event, and by the z-score relative to the station at which it was observed. Ranking of peak flows in the Gila and Verde watersheds were found to be dependent on the mechanism that had produced it, regardless of how the peaks had been ranked – there was some level of dependence on the mechanism that had produced the flood and how large it had been compared to other peak flows in the watershed. In the Santa Cruz watershed, ranking was independent of the mechanism that had produced the peak flow regardless of how the peaks were ranked. For the Salt and the Little Colorado, however, the significance of the results varied with the method of ranking. Peak flows in the Little Colorado watershed appeared to depend on the flood-producing mechanism only when the peaks were ranked by z-score, while in the Salt watershed the ranking was not independent of the flooding mechanism when the peaks were ranked by discharge. These results show that not all watersheds are affected by

flood-producing mechanisms in the same way – that in one watershed a specific flood-producing mechanism may be responsible for most of the largest peak flow events seen in that watershed, but for another watershed the flooding mechanism may have little to no effect on how large a peak flow event may be. But these results do seem consist with the overall observation that the Central Highlands are affected by ARs in ways that the other regions aren't.

While these results indicate that in some regions and watersheds, ARs produce flooding events of greater magnitude than other flood-producing mechanisms it should be noted that ARs are not a universal producer of large flooding events throughout Arizona, and their influence appears mostly limited to specific watersheds in the Central Highlands. This is consistent with what many other AR studies have shown: orography matters.

Some variables that affect the frequency, magnitude, and location of AR-related flooding in Arizona can be identified.

The location of AR-related flooding was determined to be limited primarily to the Central Highlands region, and within this region mostly in the Salt and Verde watersheds. This appears to be related to the orography of the Mogollon Rim / Central Highlands and echoes results observed by other researchers.

An analysis of basin characteristic variables and AR fraction indicated that outlet elevation, percentage of slope greater than 30°, and mean basin slope increased directly with the AR fraction, while permeability of the soil had an inverse relationship.

AR trajectory and the location at which an AR makes landfall during inland penetration were also shown to be important. ARs affecting Arizona were more likely to have a southerly or southwestern trajectory than a westerly trajectory, and more Arizona ARs made landfall through the Baja Peninsula than through California, whether they produced flooding or not. These observations are in agreement with Rutz et al. 2015, who stated that there are certain trajectories and paths of entry (such as the Baja Peninsula coast) that are favorable for inland penetration of ARs.

7. Conclusions

This study investigated the role of atmospheric rivers as Arizona flood producers and how they compare to other Arizona flood-producing mechanisms. The results showed that ARs play an important part in flooding in Arizona watersheds, but that their importance and effects are not widespread, but rather regionalized to specific parts of the state. Previous studies of Arizona ARs have focused primarily on the characteristics of a specific AR event (Neiman et al. 2013), the AR activity within a specific region of Arizona (Rivera et al. 2014), or the general behavior of ARs that may affect Arizona (Rutz et al. 2015). This study provides an insight into the trends seen in the AR activity and behavior throughout the state of Arizona as a whole, and how ARs as a flood producing mechanism compare to the other flooding mechanisms that are present in Arizona.

The main findings of this study are:

- 1) Not all atmospheric river events produce flooding in Arizona, but AR events were observed for every year during the period of study. This suggests that the presence of an AR alone does not produce flooding.
- 2) ARs dominate the flood record of the Central Highlands Transition Zone region, and most AR activity occurs in this region. Different watersheds within the Transition Zone vary in AR sensitivity, with the Verde and the Salt watersheds receiving the most AR-related flooding events – suggesting that watersheds in the Mogollon Rim / Central Highlands have characteristics that make them more favorable to flooding. In contrast, the Northern Arizona Colorado Plateau region and Southeastern Arizona Basin and Range regions experienced little AR activity.
- 3) Although ARs play a role in Arizona flooding, their importance is not universal. Unlike AR events that affect California and the other western Pacific Coast states, Arizona AR events do not necessarily produce the largest floods. Only in certain regions of the Central Highlands were AR events likely to be responsible for the largest flooding events.
- 4) One of the most important variables as to whether an AR will produce flooding or not appears to be the trajectory at which the AR intersects the North American coast. ARs that made landfall at a southwestern or southerly trajectory were more likely to produce flooding than ARs that made landfall at a westerly trajectory. In addition to this, an AR that made landfall across the Baja Peninsula was more likely to produce flooding than an AR with a trajectory across the Southern California coastline.

By studying the flooding behavior of AR events in Arizona and how they compare to other flood-producing mechanisms, this study has provided insights into the flood risks that ARs present in different regions of Arizona and has identified watershed factors that may be influencing the flooding. There is much more that needs to be explored related to atmospheric rivers and Arizona floods, and it is hoped that this study will be a catalyst for future investigations.

8. References

- Bao, J.-W., S. A. Michelson, P.J. Neiman, F. M. Ralph and J. M. Wilczak, 2006: Interpretation of enhanced integrated water vapor bands associated with extratropical cyclones: Their formation and connection to tropical moisture. *Mon. Wea. Rev.*, **134**, 1063-1080.
- Dee D. P., S. M. Uppala, A. J. Simmons, P. Berrisford, P. Poli, S. Kobayashi, U. Andrae, M. A. Balmaseda, G. Balsamo, P. Bauer, P. Bechtold, A. C. M. Beljaars, L. van de Berg, J. Bidlot, N. Bormann, C. Delsol, R. Dragani, M. Fuentes, A. J. Geer, L. Haimberger, S. B. Healy, H. Hersbach, E. V. Hólm, L. Isaksen, P. Kållborg, M. Köhler, M. Matricardi , A. J. McNally, B. M. Monge-Sanz, J.-J. Morcrette, B.-K. Park, C. Peubey, P. de Rosnay , C. Tavalato, J.-N. Thépaut, and F. Vitart F, 2011: The Era-Interim reanalysis: configuration and performance of the data assimilation system. *Quarterly Journal of the Royal Meteorological Society*, **137**, 553–597.
- Dettinger, Michael, 2004: Fifty-Two Years of “Pineapple-Express” Storms across the West Coast of North America. U.S. Geological Survey, Scripps Institution of Oceanography for the California Energy Commission, PIER Energy-Related Environmental Research. CEC-500-2005-004.
- Dettinger, M.D., 2011: Climate change, atmospheric rivers and floods in California—A multimodel analysis of storm frequency and magnitude changes. *J. Am. Water Resources Assoc.*, **47** (3), 514-523.

- Dettinger, M.D., Ralph, F.M., Das, T., Neiman, P.J., and Cayan, D., 2011: Atmospheric rivers, floods, and the water resources of California. *Water*, **3** (Special Issue on Managing Water Resources and Development in a Changing Climate), 455-478.
- Estes, Dr. Gary W., 1998: Weather Patterns and American River Floods, Proceedings of the 1998 California Weather Symposium, Sierra College, Rocklin, CA, June.
- Gimeno, L., Nieto, R., Vázquez, M., & Lavers, D., 2014: Atmospheric rivers: A mini-review. *Frontiers in Earth Science Front. Earth Sci.*, **2**, 1-6.
- Hirschboeck, K.K., 1987: Hydroclimatically-defined mixed distributions in partial duration flood series, in Singh, V.P., ed., *Hydrologic Frequency Modeling*, D. Reidel Publishing Company, 199-212.
- Hirschboeck, K.K., 1988: Flood hydroclimatology, in Baker, V.R., Kochel, R.C. and Patton, P.C., eds., *Flood Geomorphology*, John Wiley & Sons, 27-49.
- Hirschboeck, K.K., Ely, L. and Maddox, R.A., 2000: Hydroclimatology of meteorologic floods, in Wohl, Ellen, ed, *Inland Flood Hazards: Human, Riparian and Aquatic Communities*, Cambridge University Press, p. 39-72.
- House, P.K., and Hirschboeck, K.K., 1997: Hydroclimatological and paleohydrological context of extreme winter flooding in Arizona, 1993: in Larson, R.A., and Slosson, J.E., eds., *Storm Induced Geological Hazards: Case Histories from the 1992-1993 Winter Storm in Southern California and Arizona: Boulder, Colorado*, Geological Society of America Reviews in Engineering Geology, v. XI, p. 1-24.
- Hughes, Mimi, Kelly M. Mahoney, Paul J. Neiman, Benjamin J. Moore, Michael Alexander, and F. Martin Ralph, 2014: The Landfall and Inland Penetration of a

- Flood-Producing Atmospheric River in Arizona. Part II: Sensitivity of Modeled Precipitation to Terrain Height and Atmospheric River Orientation. *J. Hydrometeor Journal of Hydrometeorology*, **15**, 1954-1974.
- Lavers, D. A., R. P. Allan, E. F. Wood, G. Villarini, D. J. Brayshaw, and A. J. Wade. Winter floods in Britain are connected to atmospheric rivers. *Geophys. Res. Lett.*, **38**, L23803.
- Monteverdi, Dr. John P., 1995: Overview of the Meteorology of Rain Events in California, Proceedings of the 1995 California Weather Symposium, Sierra College, Rocklin, CA, June.
- Moore, B.J., P.J. Neiman, F.M. Ralph, F. Barthold, 2012: Physical processes associated with heavy flooding rainfall in Nashville, Tennessee and vicinity during 1-2 May 2010: The role of an atmospheric river and mesoscale convective systems. *Mon. Wea. Rev.*, **140**, 358-378.
- Neiman, P. J., F.M. Ralph, G.A. Wick, J. Lundquist, and M.D. Dettinger, 2008a: Meteorological characteristics and overland precipitation impacts of atmospheric rivers affecting the West Coast of North America based on eight years of SSM/I satellite observations. *J. Hydrometeor.*, **9**, 22-47.
- Neiman, P. J., L. J. Schick, F. M. Ralph, M. Hughes, G. A. Wick, 2011: Flooding in Western Washington: The Connection to Atmospheric Rivers. *J. Hydrometeor.*, **12**, 1337-1358.
- Neiman, P.J., F. Martin Ralph, Benjamin J. Moore, Mimi Hughes, Kelly M. Mahoney, Jason M. Cordeira, and Michael D. Dettinger, 2013: The Landfall and Inland

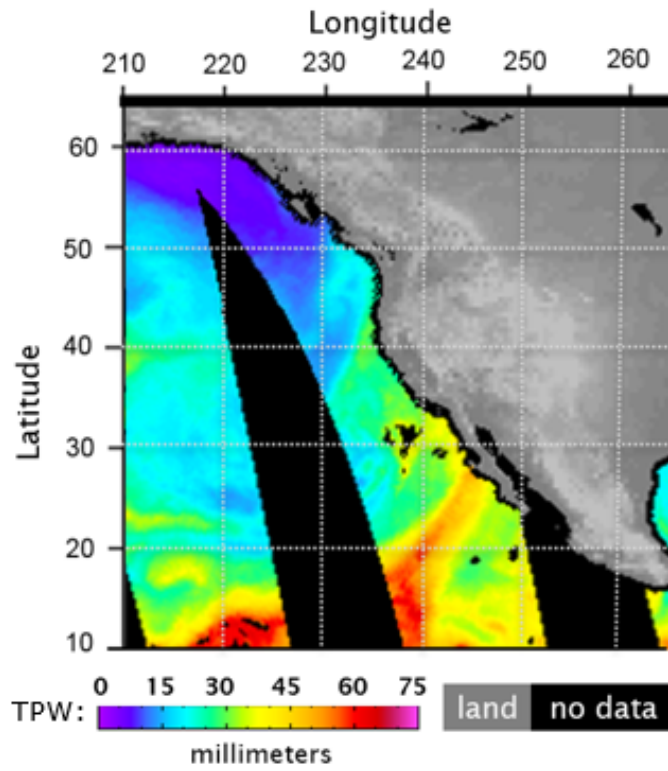
- Penetration of a Flood-Producing Atmospheric River in Arizona. Part I: Observed Synoptic-Scale, Orographic, and Hydrometeorological Characteristics. *J. Hydrometeor.*, **14**, 460–484.
- Newell, Reginald E.; Nicholas E. Newell; Yong Zhu; Courtney Scott, 1992: Tropospheric rivers? – A pilot study. *Geophys. Res. Lett.* **19** (24): 2401–2404.
- Ralph, F. M., P. J. Neiman, G. N. Kiladis, K. Weickman, and D. W. Reynolds, 2011: A multi-scale observational case study of a Pacific atmospheric river exhibiting tropical-extratropical connections and a mesoscale frontal wave. *Mon. Wea. Rev.*, **139**, 1169-1189.
- Ralph, F. M., and M. D. Dettinger, 2012: Historical and national perspectives on extreme West Coast precipitation associated with atmospheric rivers during December 2010. *Bull. Amer. Meteor. Soc.*, **93**, 783-790.
- Ralph, F. M., P. J. Neiman, and R. Rotunno, 2005: Dropsonde Observations in Low-Level Jets Over the Northeastern Pacific Ocean from CALJET-1998 and PACJET-2001: Mean Vertical-Profile and Atmospheric-River Characteristics. *Mon. Wea. Rev.*, **133**, 889-910.
- Ralph, F. M., P. J. Neiman, and G.A. Wick, 2004: Satellite and CALJET aircraft observations of atmospheric rivers over the eastern North-Pacific Ocean during the winter of 1997/98. *Mon. Wea. Rev.*, **132**, 1721-1745.
- Ralph, F. M., P. J. Neiman, G. A. Wick, S. I. Gutman, M. D. Dettinger, D. R. Cayan, and A. B. White, 2006: Flooding on California's Russian River: Role of atmospheric rivers. *Geophys. Res. Lett.*, **33**, L13801.

- Rivera, Erick R., Francina Dominguez, and Christopher L. Castro, 2014: Atmospheric Rivers and Cool Season Extreme Precipitation Events in the Verde River Basin of Arizona. *J. Hydrometeor.*, **15**, 813–829.
- Rutz, J. J. and Steenburgh, W. J. 2012: Quantifying the role of atmospheric rivers in the interior western United States. *Atmosph. Sci. Lett.*, **13**, 257–261.
- Rutz J.J., W. James Steenburgh, and F. Martin Ralph, 2014: Climatological Characteristics of Atmospheric Rivers and Their Inland Penetration over the Western United States. *Mon. Wea. Rev.*, **142**, 905–921.
- Rutz, Jonathan J., W. James Steenburgh, and F. Martin Ralph. 2015: The Inland Penetration of Atmospheric Rivers over Western North America: A Lagrangian Analysis. *Mon. Wea. Rev.*, **143.5**, 1924-1944.
- Smith, B.L., S.E. Yuter, P.J. Neiman, and D.E. Kingsmill, 2010: Water vapor fluxes and orographic precipitation over northern California associated with a land-falling atmospheric river. *Mon. Wea. Rev.*, **138**, 74-100.
- Stohl, A., C. Forster, and H. Sodemann, 2008: Remote sources of water vapor forming precipitation on the Norwegian west coast at 60° N - a tale of hurricanes and an atmospheric river. *J. Geophys. Res.*, **113**, D05102.
- Viale, M., and M. N. Nuñez, 2011: Climatology of Winter Orographic Precipitation over the Subtropical Central Andes and Associated Synoptic and Regional Characteristics. *J. Hydrometeor.*, **12**, 481-507.
- Weaver, R. L. 1962: Meteorology of hydrologically critical storms in California. *Hydrol. Rep. 37*, 207 pp., Hydrol. Serv. Div., U.S. Weather Bur., Washington, D. C.

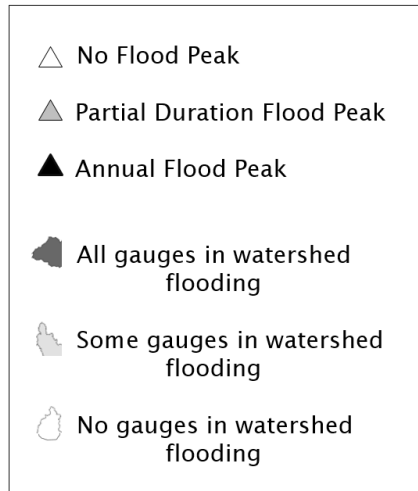
Zhu, Y., and R. E. Newell 1998: A proposed algorithm for moisture fluxes from atmospheric rivers, *Mon. Weather Rev.*, **126**, 725–735.

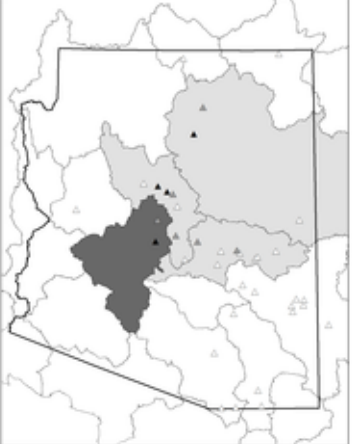


APPENDIX A

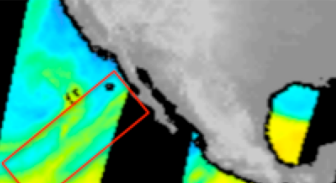

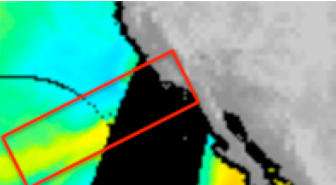

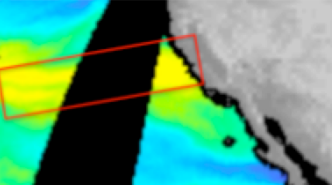
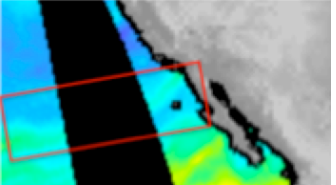
KEY TO AR FLOOD EVENT MAPS

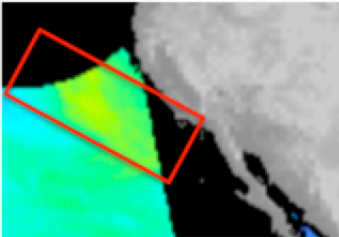
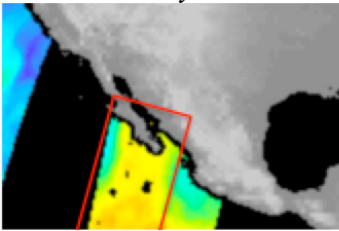

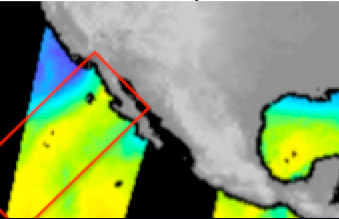
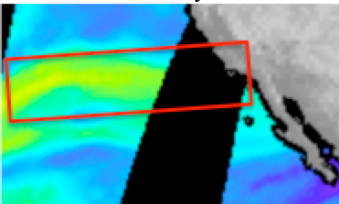
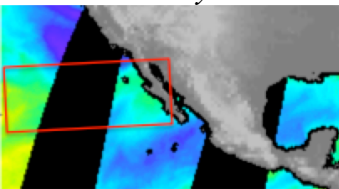


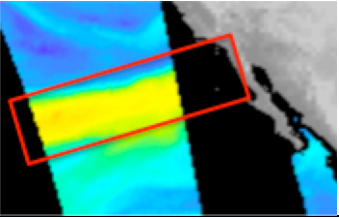
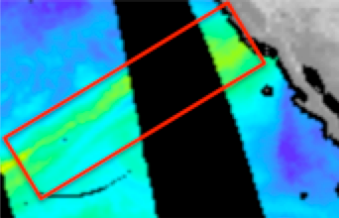

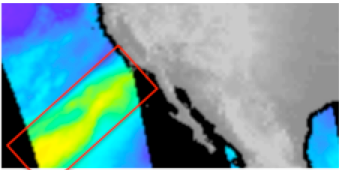

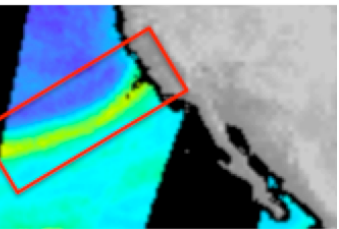
TPW = Satellite-derived Total Precipitable Water in mm

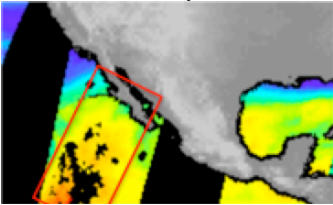
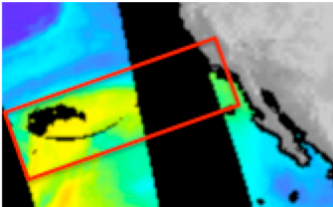
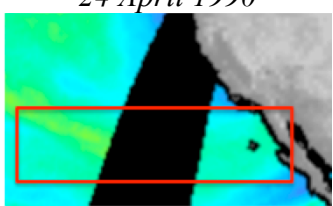
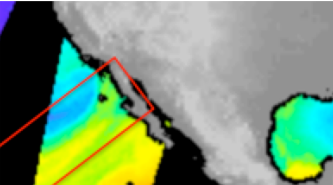
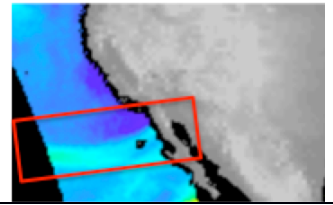
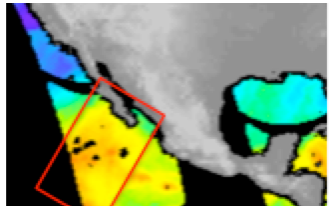


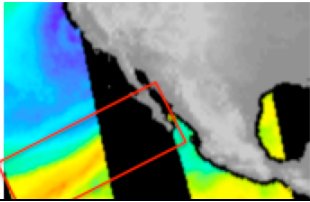
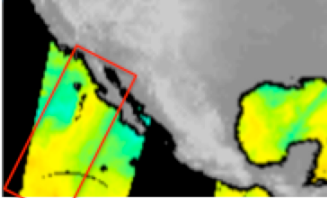
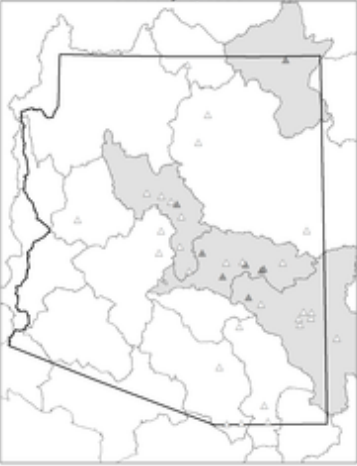
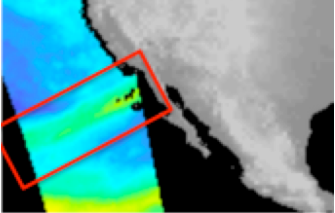
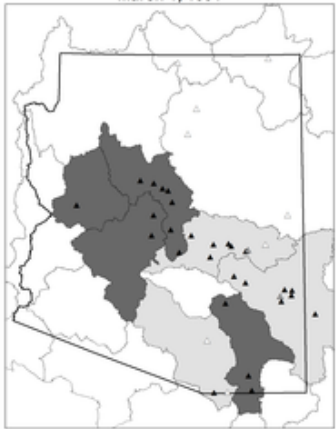
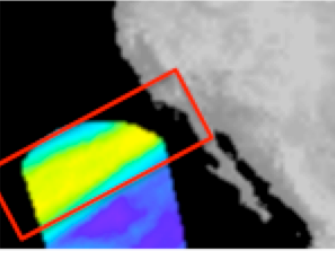

WY 1988		
<i>31 October 1987</i>	 <p style="text-align: center;">October 31, 1987</p>	<p>10 peaks (4 annual)</p> <p>Flooding in: Moenkopi, Little Colorado, Cibecue, Tonto, Verde, Oak, Dry Beaver Rim, Agua Fria, and New</p> <p>Mean z-score: 0.609 Strong AR water vapor content Has a southwestern trajectory Crosses Baja Peninsula coast</p>
<i>17 January 1988</i>	 <p style="text-align: center;">January 17, 1988</p>	<p>3 peaks (1 annual)</p> <p>Flooding in: Tonto, Sycamore, and New</p> <p>Mean z-score: 0.3 Low AR water vapor content Has a westerly trajectory Crosses northern Baja Peninsula coast</p>
<i>20 April 1988</i>	 <p style="text-align: center;">April 20, 1988</p>	<p>3 peaks (no annual)</p> <p>Flooding in: Tonto, Agua Fria, and New</p> <p>Mean z-score: -0.605 Low AR water vapor content Has a southwestern trajectory Crosses northern Baja Peninsula coast</p>

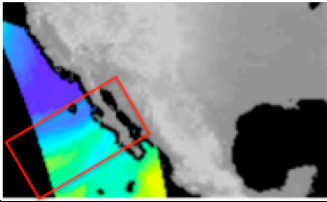
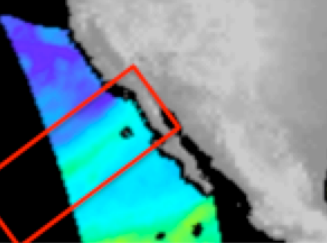

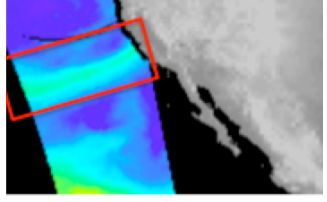

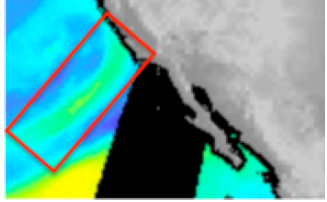

<p>28 April 1988</p> 	<p>April 28, 1988</p> 	<p>3 peaks (1 annual)</p> <p>Flooding in: East Fork, Black, and Salt Mean z-score: -0.321 Moderate AR water vapor content Has a southwestern trajectory Crosses Baja Peninsula coast</p>
<p>WY 1989</p>		
<p>14 October 1988</p> 	<p>October 14, 1988</p> 	<p>4 peaks (4 annual)</p> <p>Flooding in: Verde, San Francisco, and Gila Mean z-score: -1.787 Moderate AR water vapor content Has a southwestern trajectory Crosses Southern California coast</p>
<p>4 November 1988</p> 	<p>No gauging stations flooded during this event.</p>	<p>Moderate AR water vapor content Has a westerly trajectory Crosses Southern California coast</p>
<p>14 November 1988</p> 	<p>No gauging stations flooded during this event.</p>	<p>Low AR water vapor content Has a westerly trajectory Crosses Southern California coast</p>

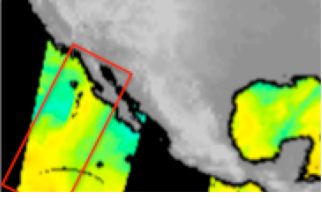

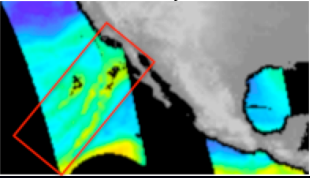
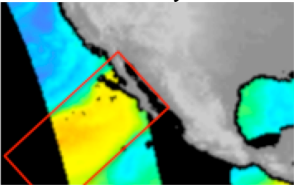
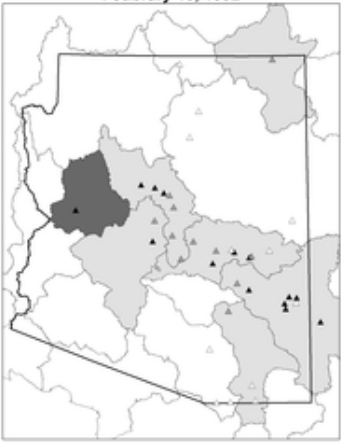
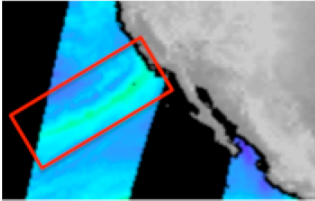

<p><i>25 November 1988</i></p> 	<p>No gauging stations flooded during this event.</p>	<p>Low AR water vapor content Has a northwestern trajectory Crosses northern Baja Peninsula coast</p>
<p><i>4 January 1989</i></p> 	<p>January 4, 1989</p> 	<p>2 peaks (2 annual)</p> <p>Flooding in: New and Big Sandy Mean z-score: -1.281 Strong AR water vapor content Has a southerly trajectory Crosses Baja Peninsula coast</p>
<p><i>10 February 1989</i></p> 	<p>No gauging stations flooded during this event.</p>	<p>Moderate AR water vapor content Has a southwestern trajectory Crosses Baja Peninsula coast</p>
<p><i>20 February 1989</i></p> 	<p>No gauging stations flooded during this event.</p>	<p>Low AR water vapor content Has a westerly trajectory Crosses Southern California coast</p>
<p><i>28 February 1989</i></p> 	<p>No gauging stations flooded during this event.</p>	<p>Low AR water vapor content Has a westerly trajectory Crosses Baja Peninsula coast</p>

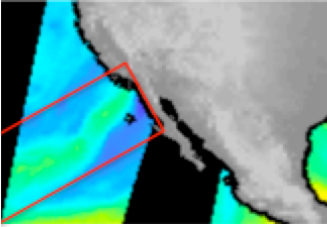

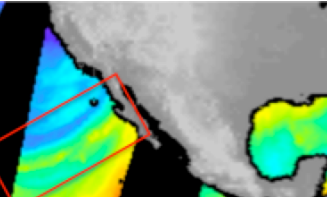
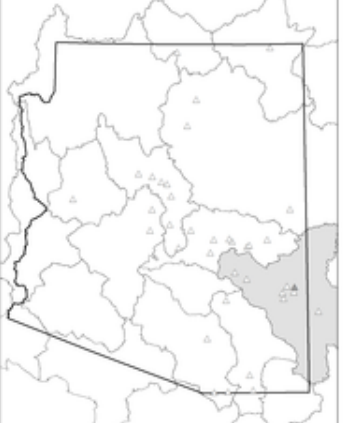
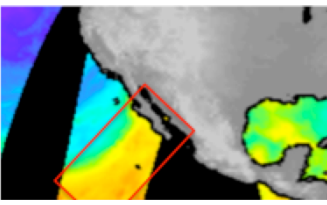

<p>3 March 1989</p> 	<p>No gauging stations flooded during this event.</p>	<p>Strong AR water vapor content Has a westerly trajectory Crosses northern Baja Peninsula coast</p>
<p>7 March 1989</p> 	<p>March 7, 1989</p> 	<p>1 peak (1 annual)</p> <p>Flooding in: West Clear Creek Mean z-score: -1.331 Low water vapor content Has a southwestern trajectory Crosses Southern California coast</p>
<p>11 March 1989</p> 	<p>March 11, 1989</p> 	<p>3 peaks (3 annual)</p> <p>Flooding in: Black, Salt, and East Fork Mean z-score: -1.518 Moderate water vapor content Has a southwestern trajectory Crosses Southern California coast</p>
<p>WY 1990</p>		
<p>26 November 1989</p> 	<p>No gauging stations flooded during this event.</p>	<p>Low AR water vapor content Has a southwestern trajectory Crosses central California coast</p>

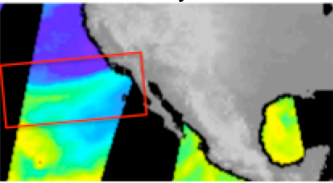
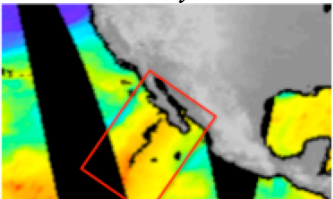
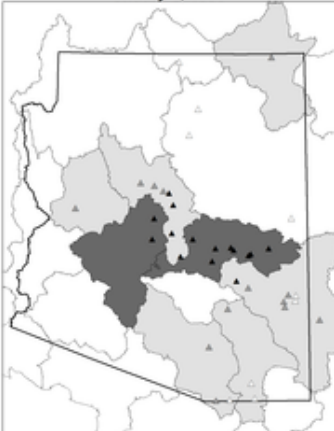
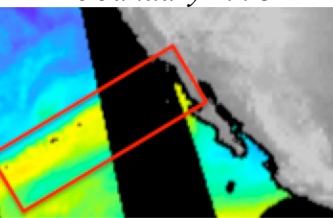
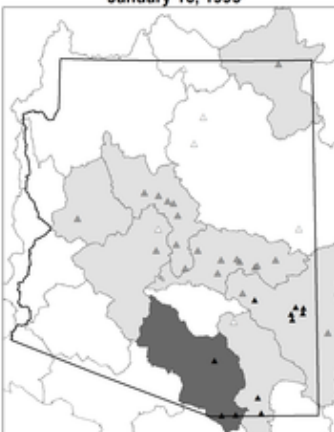
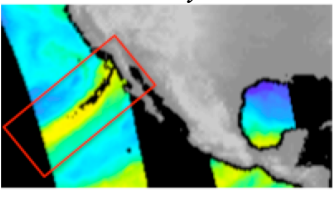

<p><i>23 January 1990</i></p> 	<p>No gauging stations flooded during this event.</p>	<p>Strong AR water vapor content Has a southerly trajectory Crosses Baja Peninsula coast</p>
<p><i>3 March 1990</i></p> 	<p>No gauging stations flooded during this event.</p>	<p>Moderate AR water vapor content Has a southwestern-westerly trajectory Crosses Southern California coast</p>
<p><i>24 April 1990</i></p> 	<p>No gauging stations flooded during this event.</p>	<p>Low AR water vapor content Has a westerly trajectory Crosses northern Baja Peninsula coast</p>
WY 1991		
<p><i>20 November 1990</i></p> 	<p>No gauging stations flooded during this event.</p>	<p>Moderate AR water vapor content Has a southwestern trajectory Crosses Baja Peninsula coast</p>
<p><i>26 November 1990</i></p> 	<p>No gauging stations flooded during this event.</p>	<p>Low AR water vapor content Has a westerly trajectory Crosses northern Baja Peninsula coast</p>
<p><i>13 December 1990</i></p> 	<p>No gauging stations flooded during this event.</p>	<p>Strong AR water vapor content Has a southerly trajectory Crosses Baja Peninsula coast</p>

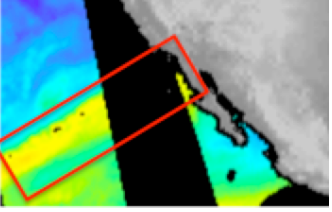
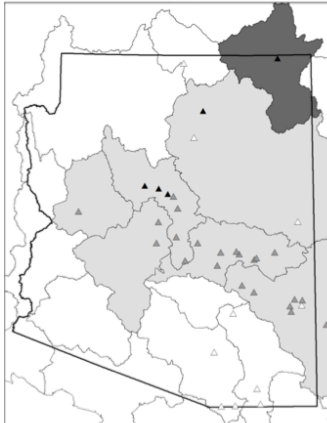
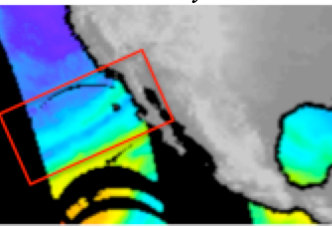

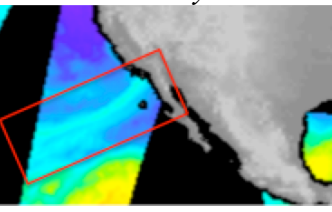

<p>16 December 1990</p> 	<p>No gauging stations flooded during this event.</p>	<p>Strong AR water vapor content Has a southwesterly trajectory Crosses Baja Peninsula coast</p>
<p>4 January 1991</p> 	<p>January 4, 1991</p> 	<p>6 peaks (no annual)</p> <p>Flooding in: Dry Beaver, Chinle, Black, Salt, San Carlos, and Tonto Mean z-score: 0.026 Strong AR water vapor content Has a southerly trajectory Crosses Baja Peninsula coast</p>
<p>1 March 1991</p> 	<p>March 1, 1991</p> 	<p>25 peaks (24 annual)</p> <p>Widespread flooding throughout AZ Mean z-score: 1.007 Low AR water vapor content Has a southwestern trajectory Crosses northern Baja Peninsula coast</p>
<p>5 March 1991</p> 	<p>March 5, 1991</p> 	<p>5 peaks (no annual)</p> <p>Flooding in: Black, East Fork, Verde, Gila, and San Francisco Mean z-score: -0.387 Strong water vapor content Has a southwestern trajectory Crosses northern Baja Peninsula coast</p>

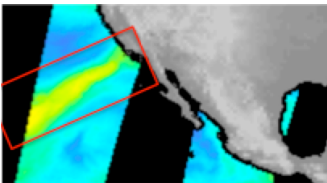

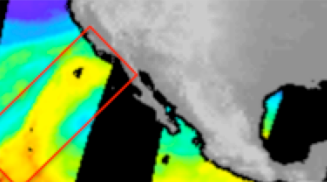

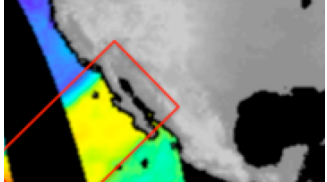
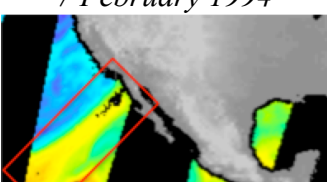

<p><i>11 March 1991</i></p> 	<p>No gauging stations flooded during this event.</p>	<p>Low AR water vapor content Has a southwestern trajectory Crosses Baja Peninsula coast</p>
<p><i>26 March 1991</i></p> 	<p>March 26, 1991</p> 	<p>7 peaks (no annual)</p> <p>Flooding in: Big Sandy, Cherry, Tonto, Sycamore, Agua Fria, New, and Salt</p> <p>Mean z-score: Low AR water vapor content Has southwestern trajectory Crosses northern Baja Peninsula coast</p>
<p><i>6 April 1991</i></p> 	<p>April 06, 1991</p> 	<p>2 peaks (no annual)</p> <p>Flooding in: Black and East Fork</p> <p>Mean z-score: Low AR water vapor content Has westerly trajectory Crosses Southern California coast</p>
<p><i>20 April 1991</i></p> 	<p>April 20, 1991</p> 	<p>1 peak (no annual)</p> <p>Flooding in: East Fork</p> <p>Mean z-score: -0.156</p> <p>Low AR water vapor content Has southwestern trajectory Crosses Southern California coast</p>

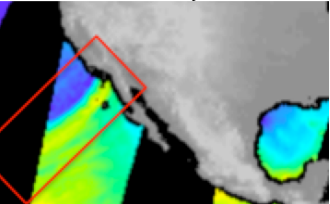
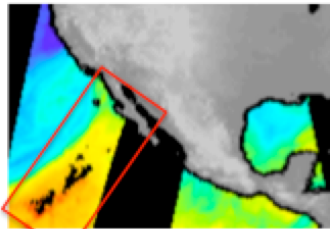
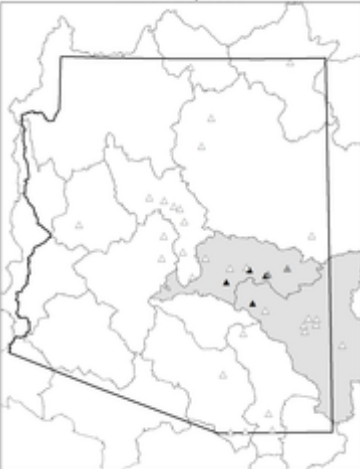
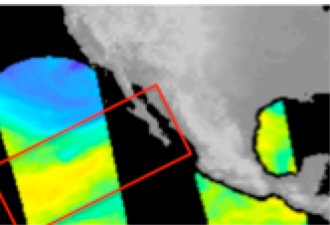
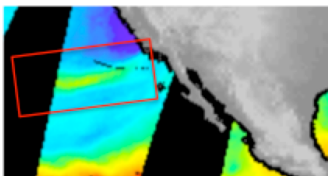
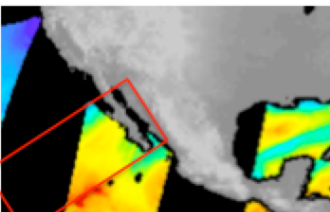
WY 1992		
<p><i>5 January 1992</i></p> 	<p>January 5, 1992</p> 	<p>9 peaks (no annual)</p> <p>Flooding in: Tonto, Dry Beaver, West Clear Creek, Sycamore, New, Gila, San Francisco, and Verde</p> <p>Mean z-score: -0.54</p> <p>Strong AR water vapor content</p> <p>Has a southerly trajectory</p> <p>Crosses Baja Peninsula coast</p>
<p><i>7 February 1992</i></p> 	<p>No gauging stations flooded during this event.</p>	<p>Low AR water vapor content</p> <p>Has a southerly trajectory</p> <p>Crosses northern Baja Peninsula coast</p>
<p><i>12 February 1992</i></p> 	<p>February 13, 1992</p> 	<p>23 peaks (13 annual)</p> <p>Widespread flooding throughout AZ</p> <p>Mean z-score: 0.503</p> <p>Strong AR water vapor content</p> <p>Has a southwestern trajectory</p> <p>Crosses Baja Peninsula coast</p>
<p><i>5 March 1992</i></p> 	<p>March 05, 1992</p> 	<p>5 peaks (no annual)</p> <p>Flooding in: Gila, Tonto, Verde, and West Clear Creek</p> <p>Mean z-score: -0.257</p> <p>Low AR water vapor content</p> <p>Has a southwestern trajectory</p> <p>Crosses Southern California coast</p>

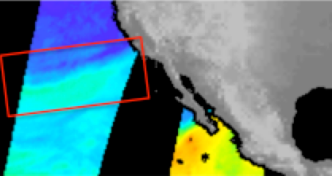
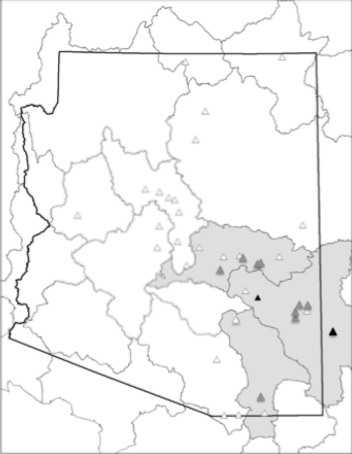
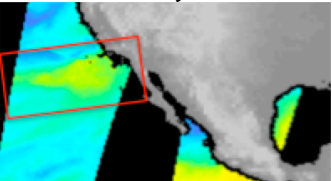

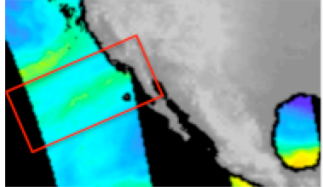
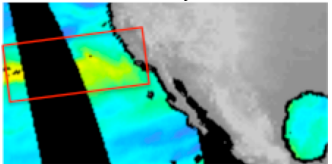

<p><i>13 April 1992</i></p> 	<p>April 13, 1992</p> 	<p>1 peak (no annual)</p> <p>Flooding in: Little Colorado Mean z-score: 0.034 Low AR water vapor content Has a southwestern trajectory Crosses Southern California coast</p>
<p>WY 1993</p>		
<p><i>5 December 1992</i></p> 	<p>December 5, 1992</p> 	<p>1 peak (no annual)</p> <p>Flooding in: San Francisco Mean z-score: -0.496 Moderate AR water vapor content Has a southwestern trajectory Crosses Baja Peninsula coast</p>
<p><i>28 December 1992</i></p> 	<p>December 28, 1992</p> 	<p>19 peaks (no annual)</p> <p>Widespread flooding throughout AZ Mean z-score: 0.458 Strong AR water vapor content Has a southwestern trajectory Crosses Baja Peninsula coast</p>

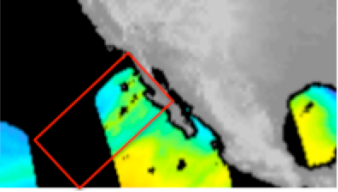

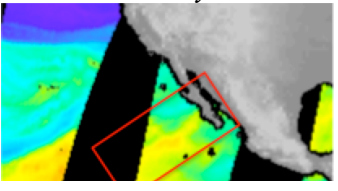
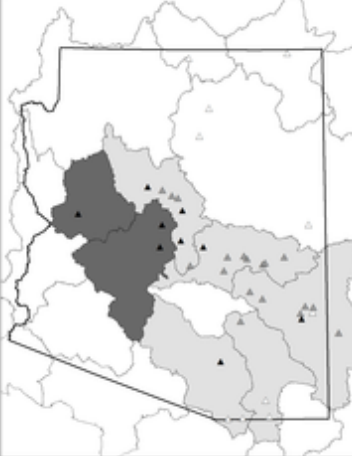
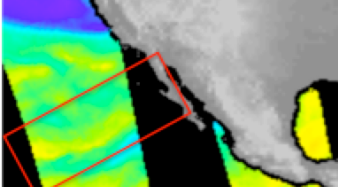

<p>3 January 1993</p> 	<p>No gauging stations flooded during this event.</p>	<p>Low AR water vapor content Has a westerly trajectory Crosses Southern California coast</p>
<p>6 January 1993</p> 	<p>January 6, 1993</p> 	<p>25 peaks (13 annual) Widespread flooding throughout AZ Mean z-score: 1.678 Strong AR water vapor content Has a southwestern trajectory Crosses Baja Peninsula coast See: House and Hirschboeck (1997)</p>
<p>16 January 1993</p> 	<p>January 16, 1993</p> 	<p>28 peaks (10 annual) Widespread flooding throughout AZ Mean z-score: 1.445 Moderate AR water vapor content Has a southwestern trajectory Crosses northern Baja Peninsula coast See: House and Hirschboeck (1997)</p>
<p>7 February 1993</p> 	<p>February 7, 1993</p> 	<p>17 peaks (1 annual) Widespread flooding throughout AZ Mean z-score: 0.554 Moderate AR water vapor content Has a southwestern trajectory Crosses northern Baja Peninsula coast See: House and Hirschboeck (1997)</p>

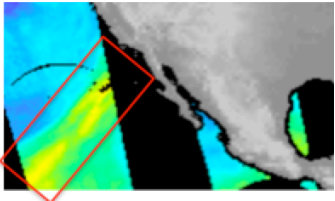

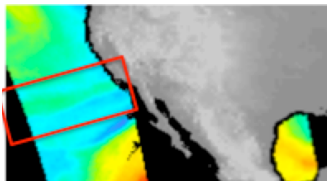
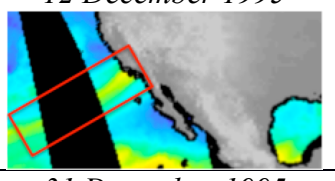
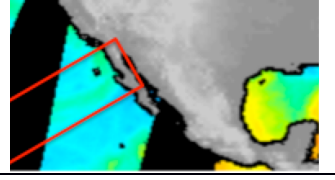
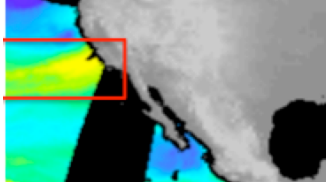
<p><i>19 February 1993</i></p> 	<p>February 19, 1993</p> 	<p>24 peaks (4 annual)</p> <p>Widespread flooding throughout AZ</p> <p>Mean z-score: 1.235</p> <p>Moderate AR water vapor content</p> <p>Has a southwestern trajectory</p> <p>Crosses northern Baja Peninsula coast</p> <p>See: House and Hirschboeck (1997)</p>
<p><i>24 February 1993</i></p> 	<p>February 24, 1993</p> 	<p>1 peak (no annual)</p> <p>Flooding in: Little Colorado</p> <p>Mean z-score: 2.26</p> <p>Low AR water vapor content</p> <p>Has a southwestern trajectory</p> <p>Crosses northern Baja Peninsula coast</p>
<p><i>26 February 1993</i></p> 	<p>February 26, 1993</p> 	<p>1 peak (no annual)</p> <p>Flooding in: New</p> <p>Mean z-score: -1.115</p> <p>Low AR water vapor content</p> <p>Has a southwestern trajectory</p> <p>Crosses northern Baja Peninsula coast</p>

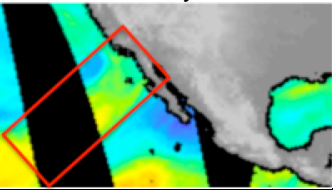
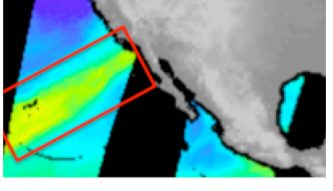
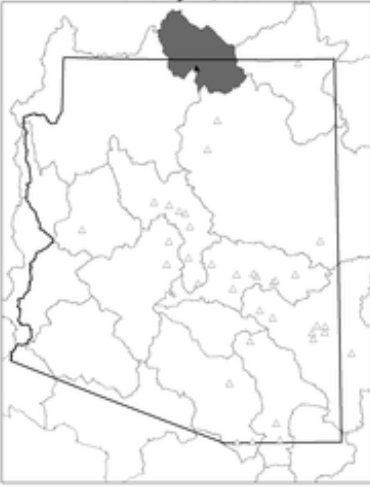
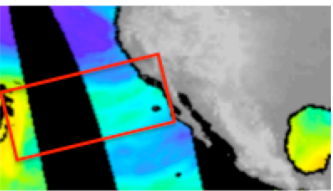
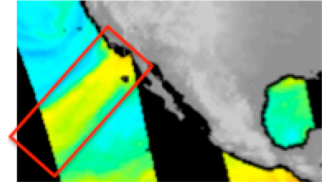
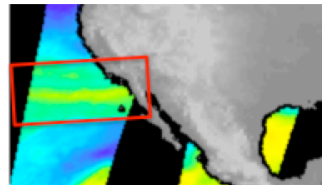
<p>17 March 1993</p> 	<p>March 17, 1993</p> 	<p>1 peak (no annual)</p> <p>Flooding in: Dry Beaver Mean z-score: 0.305 Moderate AR water vapor content Has a southwestern trajectory Crosses Southern California coast</p>
<p>WY 1994</p>		
<p>22 November 1993</p> 	<p>November 22, 1993</p> 	<p>3 peaks (1 annual)</p> <p>Flooding in: Cherry, Tonto, and West Clear Creek Mean z-score: -0.704 Strong AR water vapor content Has a southerly trajectory Crosses northern Baja Peninsula coast</p>
<p>12 December 1993</p> 	<p>No gauging stations flooded during this event.</p>	<p>Moderate AR water vapor content Has a southwestern trajectory Crosses Baja Peninsula coast</p>
<p>7 February 1994</p> 	<p>February 7, 1994</p> 	<p>6 peaks (3 annual)</p> <p>Flooding in: Aravaipa, Tonto, Verde, Sycamore, New, and Gila Mean z-score: -0.795 Moderate AR water vapor content Has a southwestern trajectory Crosses northern Baja Peninsula coast</p>

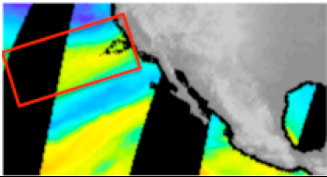
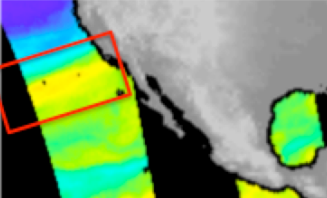

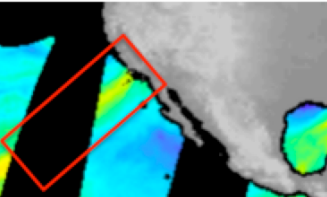

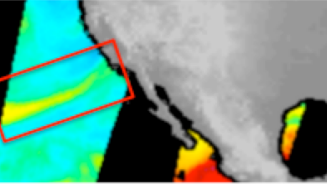
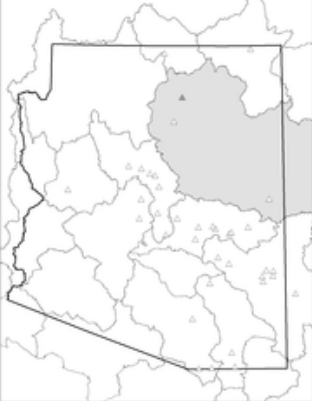
<p><i>18 February 1994</i></p> 	<p>No gauging stations flooded during this event.</p>	<p>Moderate AR water vapor Has a southwestern trajectory Crosses Southern California coast</p>
<p><i>20 March 1994</i></p> 	<p>March 20, 1994</p> 	<p>4 peaks (3 annual)</p> <p>Flooding in: San Carlos, Black, East Fork, and Salt Mean z-score: -0.437 Strong AR water vapor content Has a southwestern trajectory Crosses Baja Peninsula coast</p>
<p><i>26 March 1994</i></p> 	<p>No gauging stations flooded during this event.</p>	<p>Moderate AR water vapor Has a southwestern trajectory Crosses Baja Peninsula coast</p>
WY 1995		
<p><i>3 November 1994</i></p> 	<p>No gauging stations flooded during this event.</p>	<p>Low AR water vapor content Has a westerly trajectory Crosses Southern California coast</p>
<p><i>8 November 1994</i></p> 	<p>No gauging stations flooded during this event.</p>	<p>Strong AR water vapor content Has a southwestern trajectory Crosses Baja Peninsula coast</p>

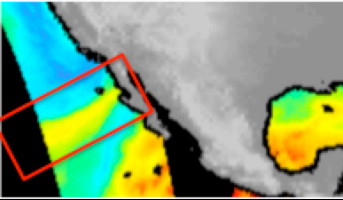
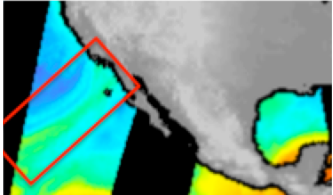
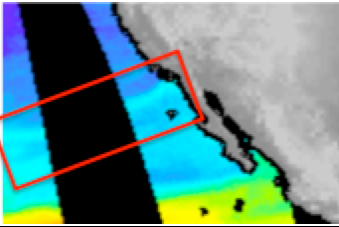
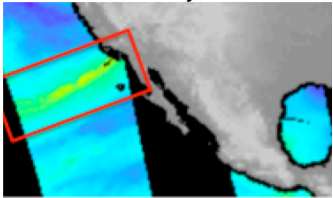

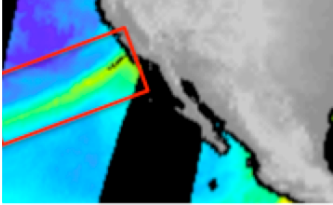

<p>6 December 1994</p> 	<p>December 6, 1994</p> 	<p>9 peaks (1 annual)</p> <p>Flooding in: Gila, San Francisco, Eagle, Bonito, San Pedro, Black, and Salt</p> <p>Mean z-score: 0.724</p> <p>Low AR water vapor content</p> <p>Has westerly trajectory</p> <p>Crosses Southern California coast</p>
<p>4 January 1995</p> 	<p>January 4, 1995</p> 	<p>16 peaks (8 annual)</p> <p>Flooding in: Big Sandy, Gila, San Francisco, Eagle, Bonita, San Carlos, Aravaipa, Black, Cherry, Salt, Tonto, Verde, Sycamore, and New</p> <p>Mean z-score: 1.033</p> <p>Low AR water vapor content</p> <p>Has westerly trajectory</p> <p>Crosses Southern California coast</p>
<p>8 January 1995</p> 	<p>No gauging stations flooded during this event.</p>	<p>Low AR water vapor content</p> <p>Has a southwestern trajectory</p> <p>Crosses Southern California coast</p>
<p>12 January 1995</p> 	<p>January 12, 1995</p> 	<p>6 peaks (no annual)</p> <p>Flooding in: Big Sandy, Dry Beaver, Gila, Eagle, Black, and Salt</p> <p>Mean z-score: -0.389</p> <p>Low AR water vapor content</p> <p>Has westerly trajectory</p> <p>Crosses Southern California coast</p>

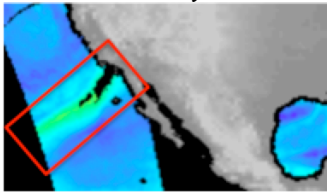

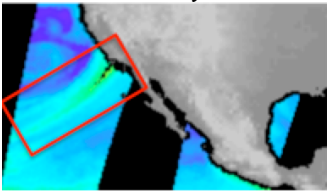

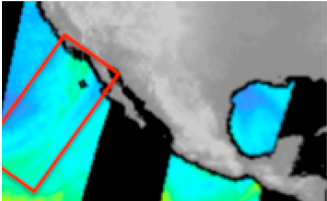
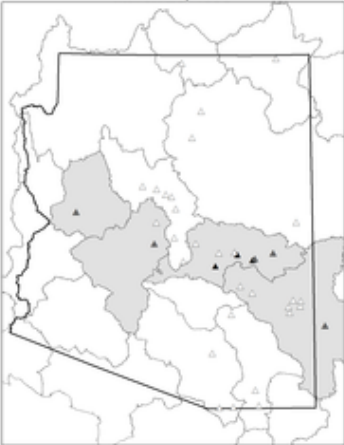
<p><i>25 January 1995</i></p> 	<p>January 25, 1995</p> 	<p>9 peaks (no annual)</p> <p>Flooding in: Big Sandy, Black, Cherry, Tonto, Verde, Sycamore, New, San Carlos, and Salt</p> <p>Mean z-score: 0.09</p> <p>Low AR water vapor content</p> <p>Has southwestern trajectory</p> <p>Crosses northern Baja Peninsula coast</p>
<p><i>14 February 1995</i></p> 	<p>February 14, 1995</p> 	<p>24 peaks (7 annual)</p> <p>Widespread flooding throughout AZ</p> <p>Mean z-score: 0.772</p> <p>Moderate AR water vapor content</p> <p>Has southwestern trajectory</p> <p>Crosses Baja Peninsula coast</p>
<p><i>4 March 1995</i></p> 	<p>March 4, 1995</p> 	<p>20 peaks (9 annual)</p> <p>Widespread flooding throughout AZ</p> <p>Mean z-score: 0.89</p> <p>Moderate AR water vapor content</p> <p>Has southwestern trajectory</p> <p>Crosses Baja Peninsula coast</p>

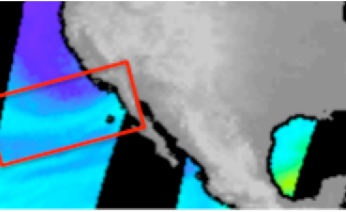
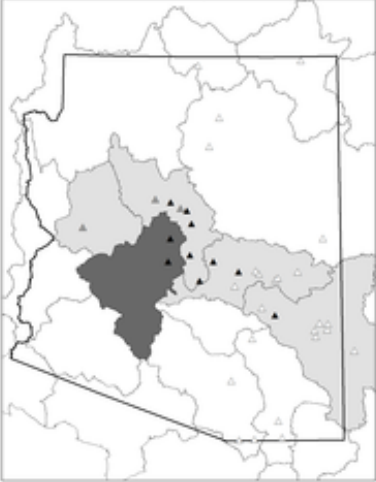
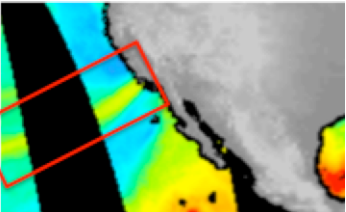

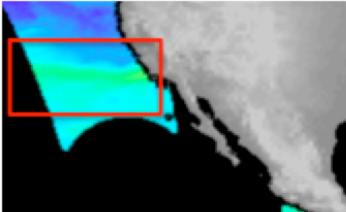
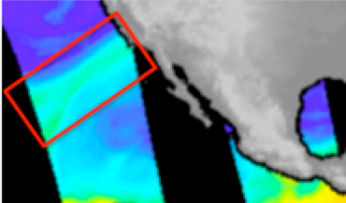
<p><i>10 March 1995</i></p> 	<p>March 10, 1995</p> 	<p>13 peaks (1 annual)</p> <p>Flooding in: Little Colorado, Dry Beaver, Cibecue, West Clear Creek, Big Sandy, Cherry, Salt, Tonto, Verde, Oak, Sycamore, and New Mean z-score: 0.004 Moderate AR water vapor content Has a southwestern trajectory Crosses Southern California coast</p>
WY 1996		
<p><i>10 November 1995</i></p> 	<p>No gauging stations flooded during this event.</p>	<p>Low AR water vapor content Has a westerly trajectory Crosses Southern California coast</p>
<p><i>12 December 1995</i></p> 	<p>No gauging stations flooded during this event.</p>	<p>Moderate AR water vapor content Has a southwestern trajectory Crosses Southern California coast</p>
<p><i>31 December 1995</i></p> 	<p>No gauging stations flooded during this event.</p>	<p>Low AR water vapor content Has a southwestern trajectory Crosses Baja Peninsula coast</p>
<p><i>17 January 1996</i></p> 	<p>No gauging stations flooded during this event.</p>	<p>Moderate AR water vapor content Has a westerly trajectory Crosses Southern California coast</p>

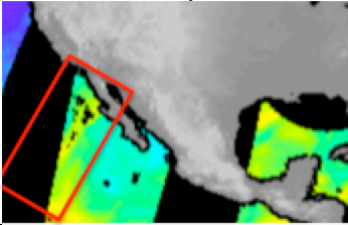
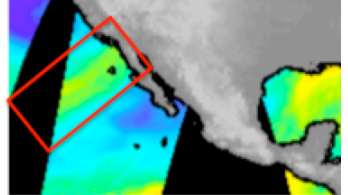
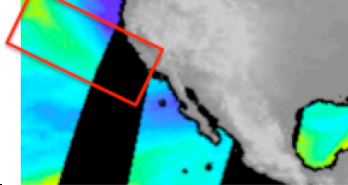
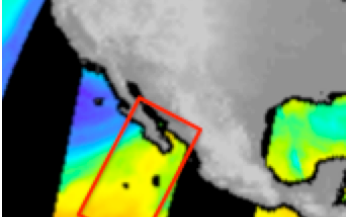
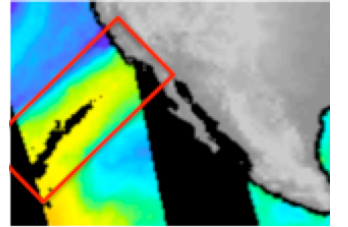
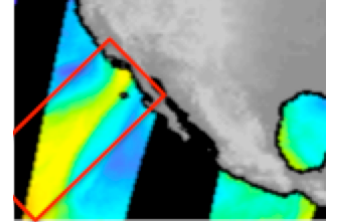
<p>31 January 1996</p> 	<p>No gauging stations flooded during this event.</p>	<p>Low AR water vapor content Has a southwestern trajectory Crosses Southern California coast</p>
<p>21 February 1996</p> 	<p>February 21, 1996</p> 	<p>1 peak (1 annual)</p> <p>Flooding in: Paria Mean z-score: -2.1 Moderate AR water vapor Has a southwestern trajectory Crosses northern Baja Peninsula coast</p>
<p>5 March 1996</p> 	<p>No gauging stations flooded during this event.</p>	<p>Low AR water vapor content Has a westerly trajectory Crosses Southern California coast</p>
<p>WY 1997</p>		
<p>22 November 1996</p> 	<p>No gauging stations flooded during this event.</p>	<p>Moderate AR water vapor content Has a southwestern trajectory Crosses Southern California coast</p>
<p>6 December 1996</p> 	<p>No gauging stations flooded during this event.</p>	<p>Moderate AR water vapor content Has a westerly trajectory Crosses northern Baja Peninsula coast</p>

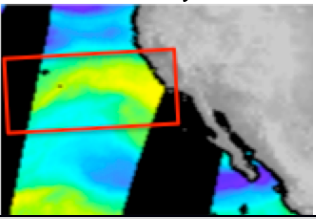
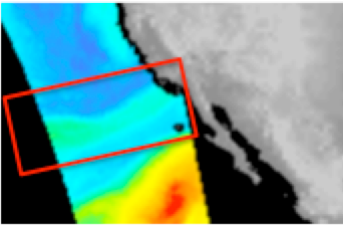

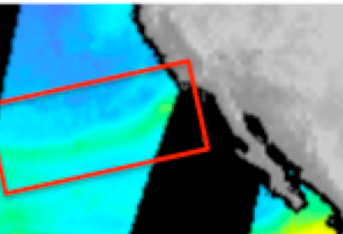

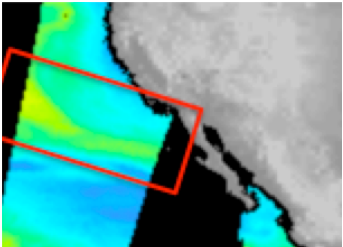

<p>10 December 1996</p> 	<p>No gauging stations flooded during this event.</p>	<p>Moderate AR water vapor content Has a westerly trajectory Crosses Southern California coast</p>
<p>3 January 1997</p> 	<p>January 3, 1997</p> 	<p>1 peak (no annual) Flooding in: PAR-Lee Mean z-score: -0.32 Moderate AR water vapor content Has a westerly trajectory Crosses Southern California coast</p>
<p>25 January 1997</p> 	<p>January 25, 1997</p> 	<p>9 peaks (8 annual) Flooding in: Oak, Dry Beaver, Big Sandy, Eagle, Cherry, Tonto, West Clear Creek, Verde, and Salt Mean z-score: -0.725 Low AR water vapor content Has a southwestern trajectory Crosses Southern California coast</p>
<p>WY 1998</p>		
<p>2 October 1997</p> 	<p>October 2, 1997</p> 	<p>1 peak (no annual) Flooding in: Moenkopi Mean z-score: -0.519 Low AR water vapor content Has a southwestern trajectory Crosses Southern California coast</p>

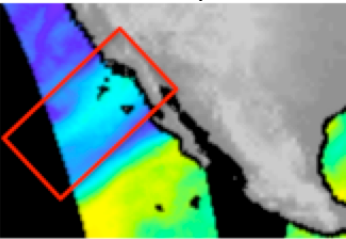
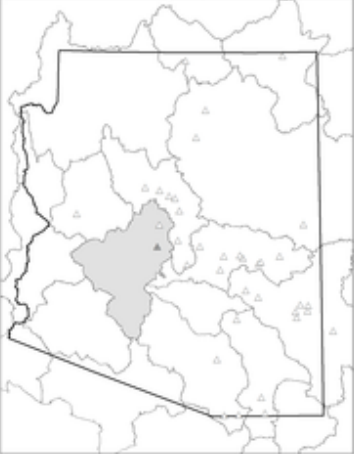
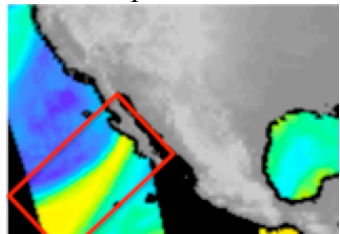
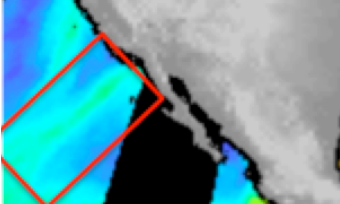
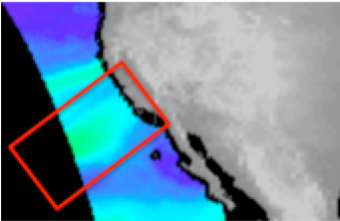

<p>11 November 1997</p> 	<p>No gauging stations flooded during this event.</p>	<p>Moderate AR water vapor content Has a southwestern trajectory Crosses Baja Peninsula coast</p>
<p>27 November 1997</p> 	<p>No gauging stations flooded during this event.</p>	<p>Low AR water vapor content Has a southwestern trajectory Crosses northern Baja Peninsula coast</p>
<p>8 December 1997</p> 	<p>No gauging stations flooded during this event.</p>	<p>Low AR water vapor content Has a southwestern trajectory Crosses Southern California coast</p>
<p>8 February 1998</p> 	<p>February 8, 1998</p> 	<p>6 peaks (1 annual) Flooding in: Big Sandy, Sycamore, Aravaipa, New, San Carlos, and Tonto Mean z-score: -0.331 Low AR water vapor content Has a southwestern trajectory Crosses Southern California coast</p>
<p>14 February 1998</p> 	<p>February 14, 1998</p> 	<p>3 peaks (1 annual) Flooding in: Sycamore, New, and Big Sandy Mean z-score: 0.04 Low AR water vapor content Has a southwestern trajectory Crosses Southern California coast</p>

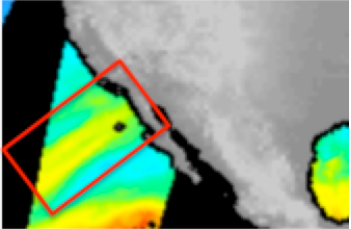
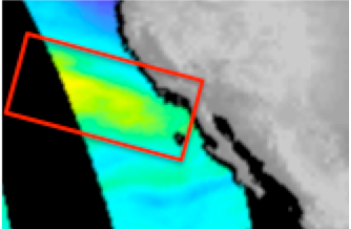
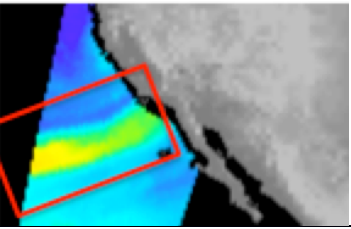
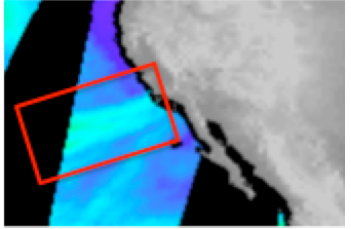

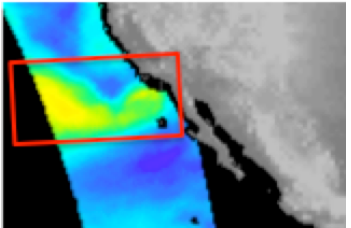
<p><i>17 February 1998</i></p> 	<p>February 17, 1998</p> 	<p>1 peak (no annual)</p> <p>Flooding in: New Mean z-score: -1.194 Low AR water vapor content Has a southwestern trajectory Crosses Southern California coast</p>
<p><i>23 February 1998</i></p> 	<p>February 23, 1998</p> 	<p>3 peaks (no annual)</p> <p>Flooding in: Big Sandy, New, and Sycamore Mean z-score: -0.256 Low AR water vapor content Has a southwestern trajectory Crosses Southern California coast</p>
<p><i>25 March 1998</i></p> 	<p>March 25, 1998</p> 	<p>6 peaks (2 annual)</p> <p>Flooding in: East Fork, Big Sandy, Gila, Black, and Salt Mean z-score: -0.595 Low AR water vapor content Has a southerly trajectory Crosses Southern California coast</p>

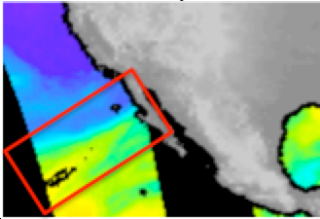
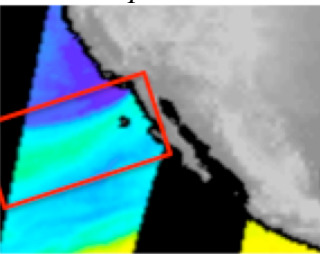
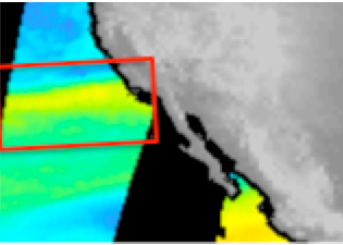

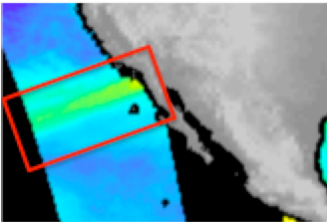
<p>28 March 1998</p> 	<p>March 28, 1998</p> 	<p>12 peaks (10 annual)</p> <p>Flooding in: Verde, Oak, Dry Beaver, West Clear Creek, Sycamore, Agua Fria, New, Big Sandy, Gila, Cherry, and Tonto</p> <p>Mean z-score: 0.2 Low AR water vapor content Has a westerly trajectory Crosses northern Baja Peninsula coast</p>
WY 1999		
<p>25 October 1998</p> 	<p>October 25, 1998</p> 	<p>1 peak (1 annual)</p> <p>Flooding in: East Fork</p> <p>Mean z-score: -0.017 Moderate AR water vapor content Has a southwestern trajectory Crosses Southern California coast</p>
<p>21 January 1999</p> 	<p>No gauging stations flooded during this event.</p>	<p>Low AR water vapor content Has a westerly trajectory Crosses Southern California coast</p>
<p>24 January 1999</p> 	<p>No gauging stations flooded during this event.</p>	<p>Low AR water vapor content Has a southwestern trajectory Crosses Southern California coast</p>

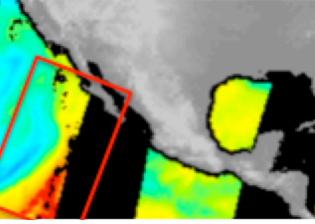

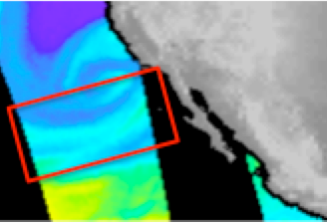

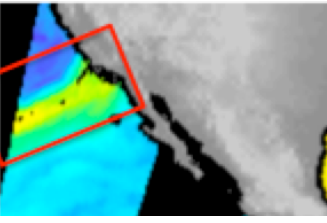
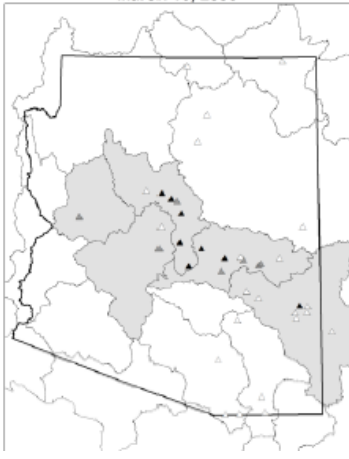
<p><i>5 February 1999</i></p> 	<p>No gauging stations flooded during this event.</p>	<p>Moderate AR water vapor content Has a southerly trajectory Crosses northern Baja Peninsula coast</p>
<p><i>10 February 1999</i></p> 	<p>No gauging stations flooded during this event.</p>	<p>Low AR water vapor content Has a southwestern trajectory Crosses northern Baja Peninsula coast</p>
<p><i>1 April 1999</i></p> 	<p>No gauging stations flooded during this event.</p>	<p>Low AR water vapor content Has a northwestern trajectory Crosses northern Baja Peninsula coast</p>
<p><i>24 April 1999</i></p> 	<p>No gauging stations flooded during this event.</p>	<p>Strong AR water vapor content Has a southerly trajectory Crosses Baja Peninsula coast</p>
WY 2000		
<p><i>17 January 2000</i></p> 	<p>No gauging stations flooded during this event.</p>	<p>Strong AR water vapor content Has a southwestern trajectory Crosses Southern California coast</p>
<p><i>25 January 2000</i></p> 	<p>No gauging stations flooded during this event.</p>	<p>Moderate AR water vapor content Has a southwestern trajectory Crosses Southern California coast</p>

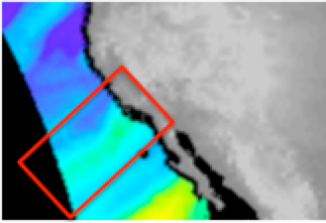

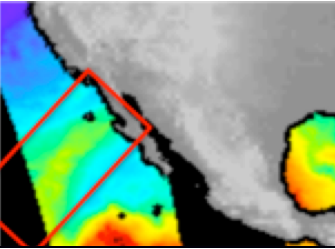
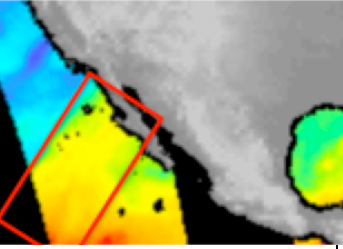

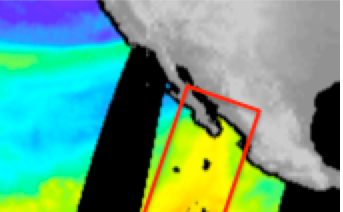
<p><i>13 February 2000</i></p> 	<p>No gauging stations flooded during this event.</p>	<p>Moderate AR water vapor content Has a westerly trajectory Crosses Southern California coast</p>
WY 2001		
<p><i>10 October 2000</i></p> 	<p>October 10, 2000</p> 	<p>8 peaks (2 annual)</p> <p>Flooding in: San Francisco, Eagle, Bonita, San Pedro, Gila, Santa Cruz, and East Fork Mean z-score: 0.322 Low AR water vapor content Has a westerly trajectory Crosses Southern California coast</p>
<p><i>29 October 2000</i></p> 	<p>October 29, 2000</p> 	<p>6 peaks (1 annual)</p> <p>Flooding in: Verde, Gila, New, Big Sandy, Tonto, and Sycamore Mean z-score: -0.633 Low AR water vapor content Has a westerly trajectory Crosses Southern California coast</p>
<p><i>6 November 2000</i></p> 	<p>November 06, 2000</p> 	<p>9 peaks (6 annual)</p> <p>Flooding in: Gila, San Francisco, Eagle, San Carlos, Santa Cruz, Black, and Salt Mean z-score: -0.184 Low AR water vapor content Has a northwestern trajectory Crosses Baja Peninsula coast</p>

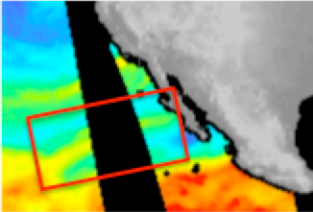
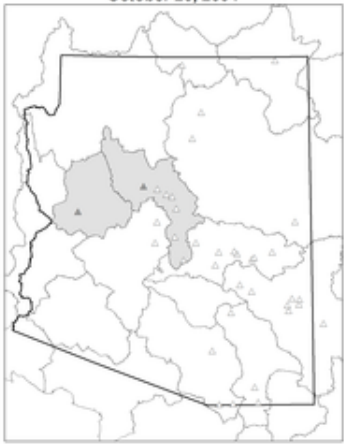
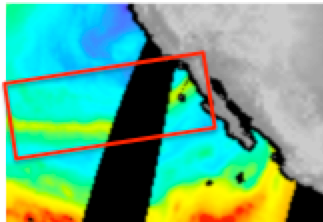
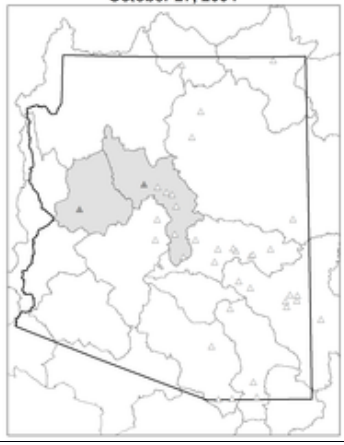
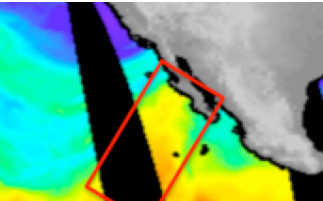
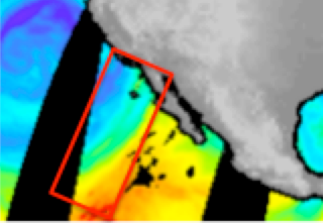
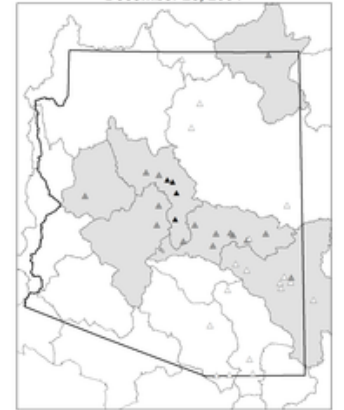
<p><i>13 February 2001</i></p> 	<p>February 13, 2001</p> 	<p>1 peak (no annual)</p> <p>Flooding in: New Mean z-score: -1.262 Low AR water vapor content Has a southwestern trajectory Crosses northern Baja Peninsula coast</p>
<p><i>6 April 2001</i></p> 	<p>No gauging stations flooded during this event.</p>	<p>Strong AR water vapor content Has a southwestern trajectory Crosses Baja Peninsula coast</p>
<p><i>19 April 2001</i></p> 	<p>No gauging stations flooded during this event.</p>	<p>Low AR water vapor content Has a southwestern trajectory Crosses northern Baja Peninsula coast</p>
<p><i>1 May 2001</i></p> 	<p>May 1, 2001</p> 	<p>1 peak (1 annual)</p> <p>Flooding in: East Fork Mean z-score: -0.017 Low AR water vapor content Has a southwestern trajectory Crosses Southern California coast</p>

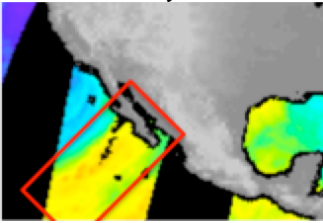

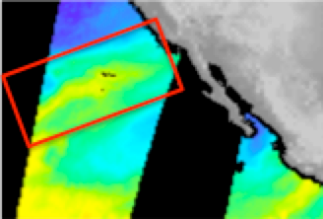
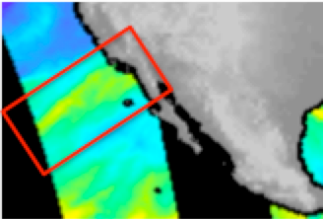
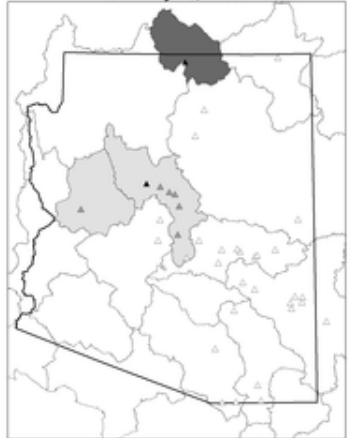
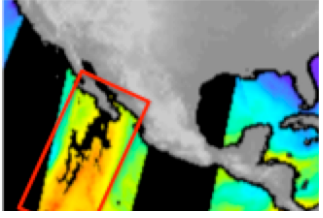
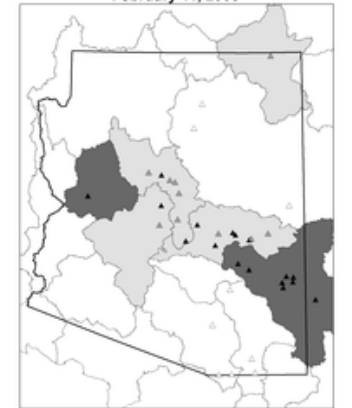
WY 2002		
<p><i>1 November 2001</i></p> 	<p>No gauging stations flooded during this event.</p>	<p>Moderate AR water vapor content Has a southwestern trajectory Crosses northern Baja Peninsula coast</p>
<p><i>23 November 2001</i></p> 	<p>No gauging stations flooded during this event.</p>	<p>Moderate AR water vapor content Has a northwesterly trajectory Crosses northern Baja Peninsula coast</p>
<p><i>30 November 2001</i></p> 	<p>No gauging stations flooded during this event.</p>	<p>Moderate AR water vapor content Has a southwestern trajectory Crosses Southern California coast</p>
<p><i>14 December 2001</i></p> 	<p>December 14, 2001</p> 	<p>1 peak (1 annual)</p> <p>Flooding in: Bonita Mean z-score: -3.062 Low AR water vapor content Has a westerly trajectory Crosses Southern California coast</p>
<p><i>30 December 2001</i></p> 	<p>No gauging stations flooded during this event.</p>	<p>Moderate AR water vapor content Has a westerly trajectory Crosses Southern California coast</p>

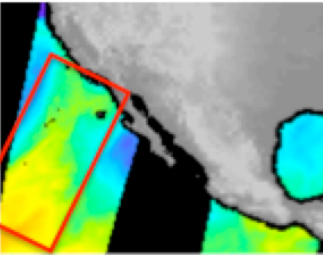
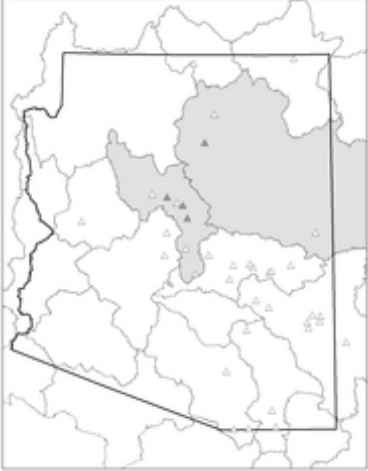
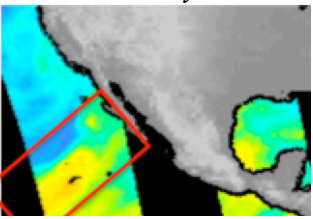

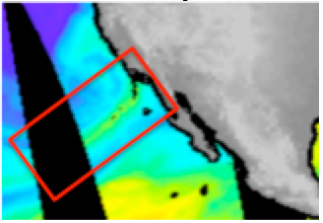

<p>29 January 2002</p> 	<p>No gauging stations flooded during this event.</p>	<p>Moderate AR water vapor content Has a southwestern trajectory Crosses Baja Peninsula coast</p>
<p>16 April 2002</p> 	<p>No gauging stations flooded during this event.</p>	<p>Low AR water vapor content Has a southwestern trajectory Crosses northern Baja Peninsula coast</p>
<p>WY 2003</p>		
<p>9 November 2002</p> 	<p>November 9, 2002</p> 	<p>1 peak (no annual)</p> <p>Flooding in: East Fork Mean z-score: -0.95 Moderate AR water vapor content Has a westerly trajectory Crosses Southern California coast</p>
<p>17 December 2002</p> 	<p>No gauging stations flooded during this event.</p>	<p>Low AR water vapor content Has a southwestern trajectory Crosses northern Baja Peninsula coast</p>

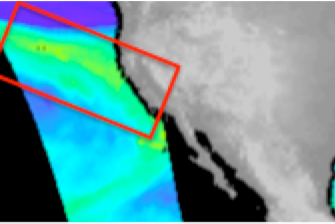

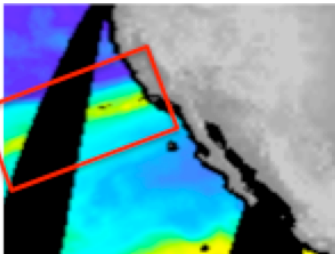
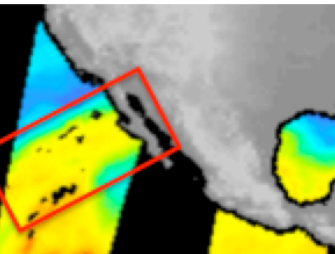
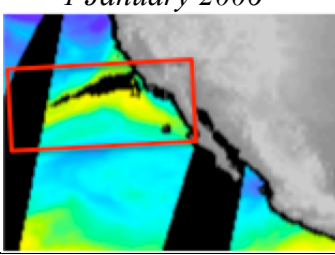
<p><i>13 February 2003</i></p> 	<p>February 13, 2003</p> 	<p>4 peaks (1 annual)</p> <p>Flooding in: Dry Beaver, Oak, New, and Verde</p> <p>Mean z-score: -0.154 Strong AR water vapor content Has a southerly trajectory Crosses northern Baja Peninsula coast</p>
<p><i>25 February 2003</i></p> 	<p>February 25, 2003</p> 	<p>3 peaks (1 annual)</p> <p>Flooding in: New, Tonto, and Sycamore</p> <p>Mean z-score: -0.659 Low AR water vapor content Has a westerly trajectory Crosses northern Baja Peninsula coast</p>
<p><i>15 March 2003</i></p> 	<p>March 15, 2003</p> 	<p>13 peaks (8 annual)</p> <p>Flooding in: Verde, Oak, Dry Beaver, West Clear Creek, Big Sandy, Eagle, Black, Salt, Cherry, Tonto, Sycamore, and New</p> <p>Mean z-score: -0.322 Moderate AR water vapor content Has a southwestern trajectory Crosses Southern California coast</p>

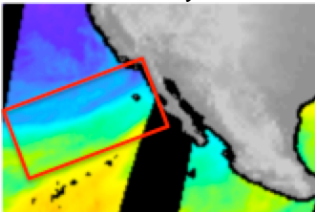
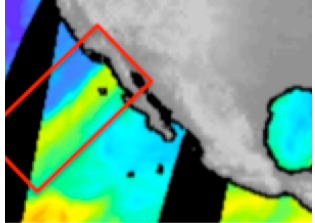
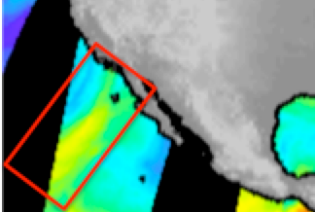
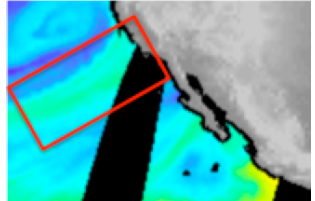
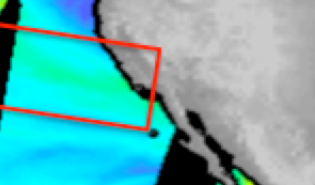
<p><i>14 April 2003</i></p> 	<p>April 14, 2003</p> 	<p>1 peak (no annual)</p> <p>Flooding in: EFW-Fta Mean z-score: -0.381 Low AR water vapor content Has a southwestern trajectory Crosses Southern California coast</p>
WY 2004		
<p><i>1 November 2003</i></p> 	<p>No gauging stations flooded during this event.</p>	<p>Low AR water vapor content Has a southwestern trajectory Crosses Baja Peninsula coast</p>
<p><i>12 November 2003</i></p> 	<p>November 12, 2003</p> 	<p>3 peaks (3 annual)</p> <p>Flooding in: San Francisco, Gila, and East Fork Mean z-score: -0.474 Strong AR water vapor content Has a southwestern trajectory Crosses Baja Peninsula Coast</p>
<p><i>2 January 2004</i></p> 	<p>No gauging stations flooded during this event.</p>	<p>Strong AR water vapor content Has a southerly trajectory Crosses southern Baja Peninsula coast</p>

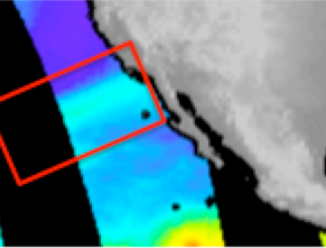
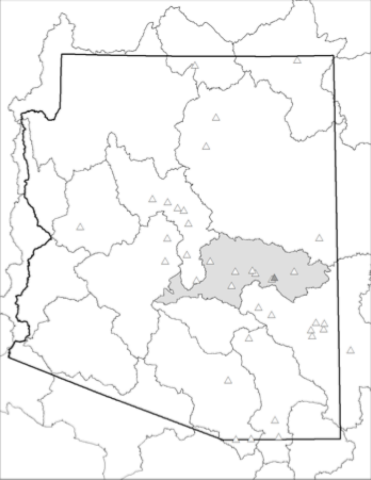
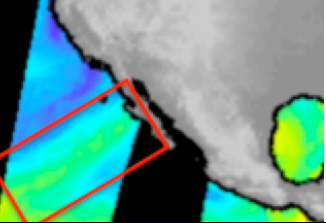
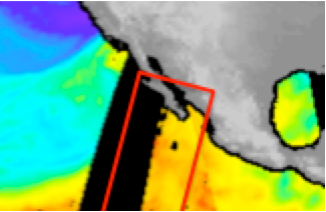

WY 2005		
<p><i>20 October 2004</i></p> 	<p>October 20, 2004</p> 	<p>1 peak (no annual)</p> <p>Flooding in: Big Sandy Mean z-score: 1.083 Moderate AR water vapor content Has a westerly trajectory Crosses Baja Peninsula Coast</p>
<p><i>27 October 2004</i></p> 	<p>October 27, 2004</p> 	<p>1 peak (no annual)</p> <p>Flooding in: Big Sandy Mean z-score: 1.373 Moderate AR water vapor content Has westerly-southwestern trajectory Crosses northern Baja Peninsula coast</p>
<p><i>28 November 2004</i></p> 	<p>No gauging stations flooded during this event.</p>	<p>Strong AR water vapor content Has a southerly trajectory Crosses Baja Peninsula coast</p>
<p><i>28 December 2004</i></p> 	<p>December 28, 2004</p> 	<p>17 peaks (4 annual)</p> <p>Widespread flooding throughout AZ Mean z-score: 0.625 Low AR water vapor content Has a southerly trajectory Crosses northern Baja Peninsula coast</p>

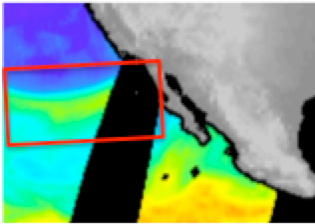

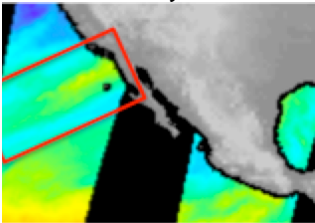
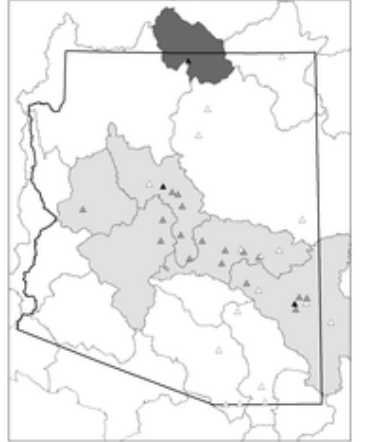
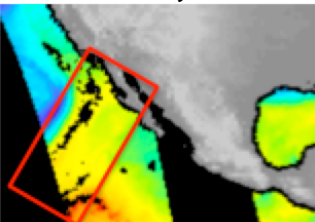
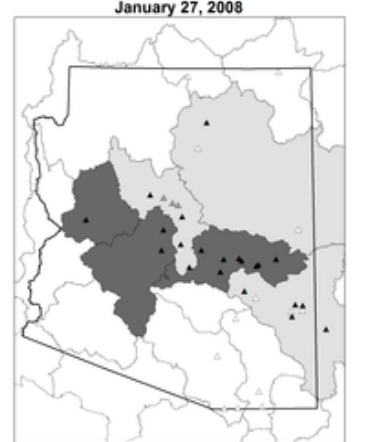
<p><i>4 January 2005</i></p> 	<p>January 4, 2005</p> 	<p>18 peaks (1 annual)</p> <p>Widespread flooding throughout AZ</p> <p>Mean z-score: 0.447</p> <p>Strong AR water vapor content</p> <p>Has a southwestern trajectory</p> <p>Crosses Baja Peninsula coast</p>
<p><i>8 January 2005</i></p> 	<p>No gauging stations flooded during this event.</p>	<p>Low AR water vapor content</p> <p>Has a southwestern trajectory</p> <p>Crosses northern Baja Peninsula coast</p>
<p><i>10 January 2005</i></p> 	<p>January 10, 2005</p> 	<p>7 peaks (1 annual)</p> <p>Flooding in: Paria, Big Sandy, Verde, Oak, Dry Beaver, and West Clear Creek</p> <p>Mean z-score: 0.936</p> <p>Low AR water vapor content</p> <p>Has a southwestern trajectory</p> <p>Crosses Southern California coast</p>
<p><i>11 February 2005</i></p> 	<p>February 11, 2005</p> 	<p>23 peaks (15 annual)</p> <p>Widespread flooding throughout AZ</p> <p>Mean z-score: 1.21</p> <p>Strong AR water vapor content</p> <p>Has a southerly trajectory</p> <p>Crosses Baja Peninsula coast</p>

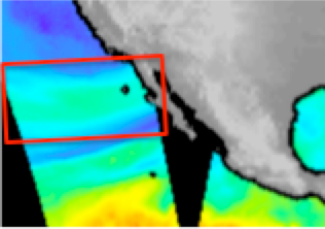

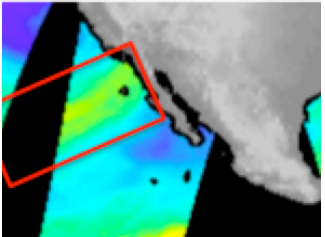

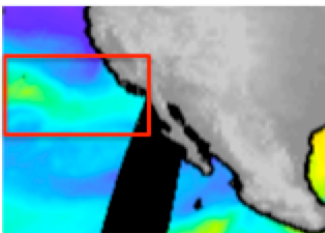

<p><i>15 February 2005</i></p> 	<p>February 15, 2005</p> 	<p>4 peaks (no annual)</p> <p>Flooding in: Verde, Dry Beaver, West Clear Creek, and Little Colorado</p> <p>Mean z-score: -0.072</p> <p>Low AR water vapor content</p> <p>Has a southerly trajectory</p> <p>Crosses Southern California coast</p>
<p><i>19 February 2005</i></p> 	<p>February 19, 2005</p> 	<p>21 peaks (no annual)</p> <p>Widespread flooding throughout AZ</p> <p>Mean z-score: 0.464</p> <p>Moderate AR water vapor content</p> <p>Has a southwestern trajectory</p> <p>Crosses Baja Peninsula coast</p>
<p><i>21 February 2005</i></p> 	<p>February 21, 2005</p> 	<p>3 peaks (no annual)</p> <p>Flooding in: Gila, Salt, and Verde</p> <p>Mean z-score: 0.128</p> <p>Low AR water vapor content</p> <p>Has a southwestern trajectory</p> <p>Crosses Southern California coast</p>

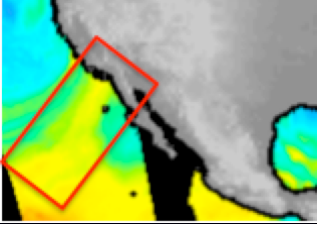
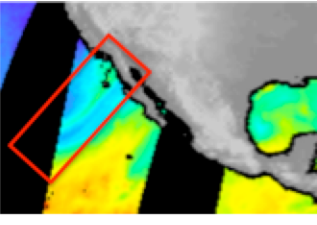

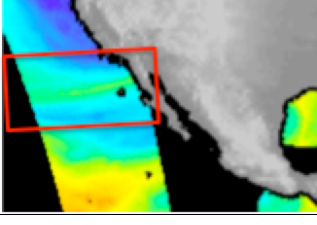
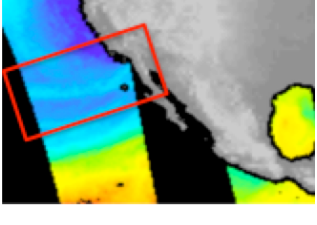
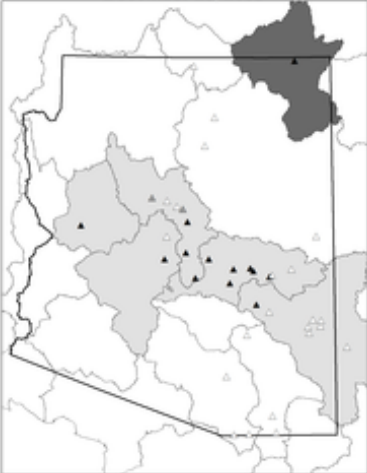
<p><i>19 March 2005</i></p> 	<p>March 19, 2005</p> 	<p>3 peaks (no annual)</p> <p>Flooding in: Oak, Dry Beaver, and West Clear Creek</p> <p>Mean z-score: -0.629</p> <p>Low AR water vapor content</p> <p>Has a northwestern trajectory</p> <p>Crosses California coast</p>
WY 2006		
<p><i>2 December 2005</i></p> 	<p>No gauging stations flooded during this event.</p>	<p>Moderate AR water vapor content</p> <p>Has a southwestern trajectory</p> <p>Crosses Southern California coast</p>
<p><i>13 December 2005</i></p> 	<p>No gauging stations flooded during this event.</p>	<p>Strong AR water vapor content</p> <p>Has a southwestern trajectory</p> <p>Crosses Baja Peninsula coast</p>
<p><i>1 January 2006</i></p> 	<p>No gauging stations flooded during this event.</p>	<p>Moderate AR water vapor content</p> <p>Has a westerly trajectory</p> <p>Crosses northern Baja Peninsula coast</p>

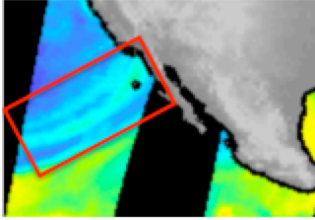

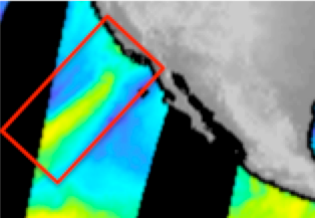
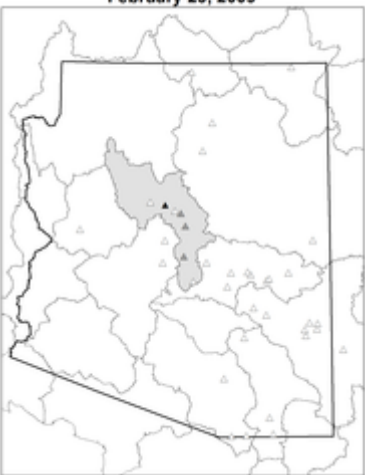
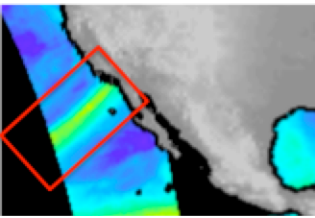

<p><i>18 February 2006</i></p> 	<p>No gauging stations flooded during this event.</p>	<p>Low AR water vapor content Has a southwestern trajectory Crosses Baja Peninsula coast</p>
<p><i>28 February 2006</i></p> 	<p>No gauging stations flooded during this event.</p>	<p>Moderate AR water vapor content Has a southwestern trajectory Crosses northern Baja Peninsula coast</p>
<p><i>4 April 2006</i></p> 	<p>No gauging stations flooded during this event.</p>	<p>Moderate AR water vapor content Has a southwestern trajectory Crosses Southern California coast</p>
<p><i>11 April 2006</i></p> 	<p>No gauging stations flooded during this event.</p>	<p>Low AR water vapor content Has a southwestern trajectory Crosses Southern California coast</p>
WY 2007		
<p><i>14 November 2006</i></p> 	<p>No gauging stations flooded during this event.</p>	<p>Low AR water vapor content Has a northwestern trajectory Crosses Southern California coast</p>

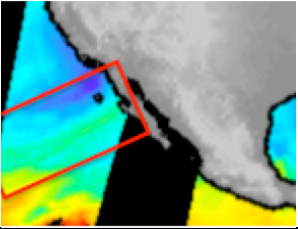
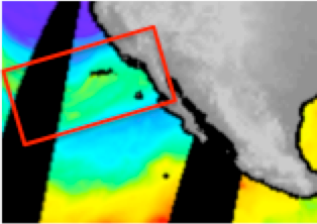
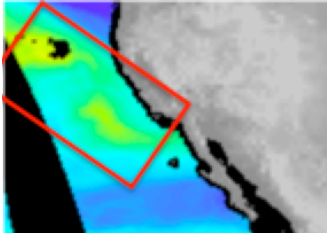
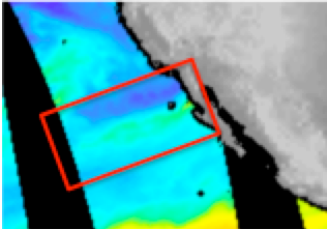
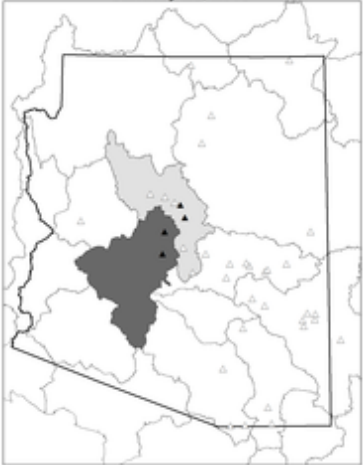
<p>5 January 2007</p> 	<p>January 5, 2007</p> 	<p>1 peak (no annual)</p> <p>Flooding in: White</p> <p>Mean z-score: N/A*</p> <p>Low AR water vapor content</p> <p>Has a southwestern trajectory</p> <p>Crosses Southern California coast</p>
<p>22 March 2007</p> 	<p>No gauging stations flooded during this event.</p>	<p>Low AR water vapor content</p> <p>Has a southwestern trajectory</p> <p>Crosses Baja Peninsula coast</p>
<p>WY 2008</p>		
<p>30 November 2007</p> 	<p>November 30, 2007</p> 	<p>10 peaks (no annual)</p> <p>Flooding in: San Francisco, Tonto, East Fork, Oak, Dry Beaver, Verde, Sycamore, New, Big Sandy, and Gila</p> <p>Mean z-score: 0.188</p> <p>Strong AR water vapor content</p> <p>Has a southerly trajectory</p> <p>Crosses Baja Peninsula coast</p>

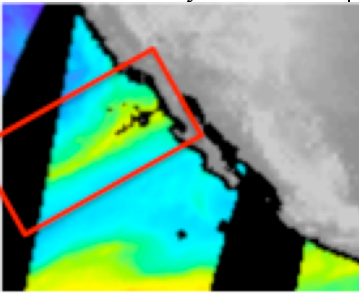
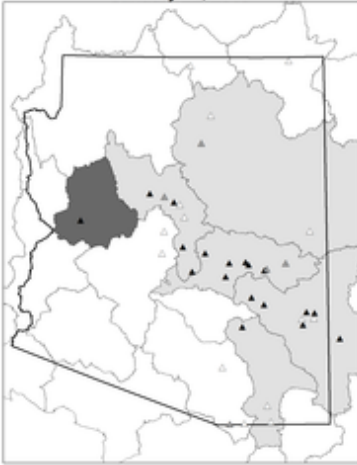
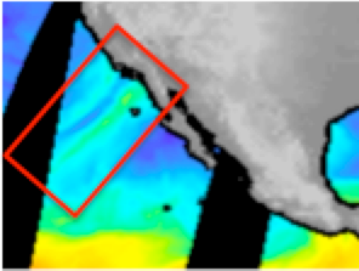

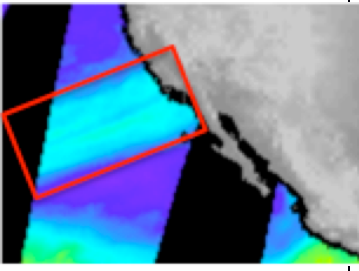

<p>7 December 2007</p> 	<p>December 7, 2007</p> 	<p>12 peaks (2 annual)</p> <p>Flooding in: Oak, Dry Beaver, New, Black, Salt, Cibecue, Cherry, Tonto, West Clear Creek, Verde, Sycamore, and San Carlos Mean z-score: 0.521 Low AR water vapor content Has a westerly trajectory Crosses northern Baja Peninsula coast</p>
<p>5 January 2008</p> 	<p>January 5, 2008</p> 	<p>19 peaks (3 annual)</p> <p>Widespread flooding throughout AZ Mean z-score: 0.122 Low AR water vapor content Has a southwestern trajectory Crosses northern Baja Peninsula coast</p>
<p>27 January 2008</p> 	<p>January 27, 2008</p> 	<p>22 peaks (18 annual)</p> <p>Widespread flooding throughout AZ Mean z-score: 1.181 Strong AR water vapor content Has a southerly trajectory Crosses Baja Peninsula coast</p>

<p><i>4 February 2008</i></p> 	<p>February 4, 2008</p> 	<p>5 peaks (no annual)</p> <p>Flooding in: Big Sandy, Cherry, Salt, Tonto, and Sycamore Mean z-score: -0.313 Low AR water vapor content Has a westerly trajectory Crosses Baja Peninsula coast</p>
<p><i>22 February 2008</i></p> 	<p>February 22, 2008</p> 	<p>1 peak (no annual)</p> <p>Flooding in: Tonto Mean z-score: -0.789 Low AR water vapor content Has a southwestern trajectory Crosses Southern California coast</p>
<p><i>29 March 2008</i></p> 	<p>March 29, 2008</p> 	<p>1 peak (1 annual)</p> <p>Flooding in: Little Colorado Mean z-score: -0.649 Low AR water vapor content Has a westerly trajectory Crosses Southern California coast</p>

WY 2009		
<p>2 November 2008</p> 	<p>No gauging stations flooded during this event.</p>	<p>Strong AR water vapor content Has a southerly trajectory Crosses Southern California coast</p>
<p>17 December 2008</p> 	<p>December 17, 2008</p> 	<p>3 peaks (no annual)</p> <p>Flooding in: Big Sandy, Tonto, and Sycamore Mean z-score: -0.139 Low AR water vapor content Has a southwestern trajectory Crosses northern Baja Peninsula coast</p>
<p>23 December 2008</p> 	<p>No gauging stations flooded during this event.</p>	<p>Low AR water vapor content Has a westerly trajectory Crosses northern Baja Peninsula coast</p>
<p>26 December 2008</p> 	<p>December 28, 2008</p> 	<p>13 peaks (12 annual)</p> <p>Flooding in: Big Sandy, San Carlos, Black, Cibecue, Cherry, Salt, Tonto, Dry Beaver, West Clear Creek, Verde, Sycamore, New, and Chinle Mean z-score: 0.038 Low AR water vapor content Has a westerly trajectory Crosses northern Baja Peninsula coast</p>

<p>16 February 2009</p> 	<p>February 16, 2009</p> 	<p>1 peak (no annual)</p> <p>Flooding in: Big Sandy Mean z-score: -0.684 Low AR water vapor content Has a southwestern trajectory Crosses northern Baja Peninsula coast</p>
<p>23 February 2009</p> 	<p>February 23, 2009</p> 	<p>4 peaks (1 annual)</p> <p>Flooding in: Dry Beaver, Verde, and West Clear Creek Mean z-score: -0.639 Moderate AR water vapor content Has a southwestern trajectory Crosses Southern California coast</p>
<p>3 March 2009</p> 	<p>March 3, 2009</p> 	<p>1 peak (1 annual)</p> <p>Flooding in: White Mean z-score: N/A* Moderate AR water vapor content Has a southwestern trajectory Crosses Southern California coast</p>

WY 2010		
<p><i>13 November 2009</i></p> 	<p>No gauging stations flooded during this event.</p>	<p>Low AR water vapor Has a southwestern trajectory Crosses Baja Peninsula coast</p>
<p><i>8 December 2009</i></p> 	<p>No gauging stations flooded during this event.</p>	<p>Low AR water vapor content Has a southwestern trajectory Crosses northern Baja Peninsula coast</p>
<p><i>31 December 2009</i></p> 	<p>No gauging stations flooded during this event.</p>	<p>Low AR water vapor content Has a northwestern trajectory Crosses northern Baja Peninsula coast</p>
<p><i>20 January 2010</i></p> 	<p>January 20, 2010</p> 	<p>4 peaks (4 annual)</p> <p>Flooding in: Dry Beaver, West Clear Creek, Agua Fria, and New Mean z-score: 1.74 Low AR water vapor content Has a westerly trajectory Crosses Baja Peninsula coast</p> <p>See: Neiman et al. (2013)</p>

<p><i>22 January 2010</i></p> 	<p>January 22, 2010</p> 	<p>20 peaks (16 annual)</p> <p>Widespread flooding throughout AZ Mean z-score: 0.921 Moderate AR water vapor content Has a southwestern trajectory Crosses northern Baja Peninsula coast</p> <p>See: Neiman et al. (2013)</p>
<p><i>6 February 2010</i></p> 	<p>February 6, 2010</p> 	<p>2 peaks (no annual)</p> <p>Flooding in: Dry Beaver and Big Sandy Mean z-score: -0.543 Low AR water vapor content Has a southwestern trajectory Crosses northern Baja Peninsula coast</p>
<p><i>30 March 2010</i></p> 	<p>March 30, 2010</p> 	<p>1 peak (no annual)</p> <p>Flooding in: Dry Beaver Mean z-score: -0.982 Low AR water vapor content Has a westerly trajectory Crosses Southern California coast</p>

APPENDIX B

Z-SCORES

	AR	Non-AR Winter	Convective
AFR-May	0.808	-0.427	-0.44
BLK-Fta	0.269	-0.125	-0.514
BON-Mor	0.26	-0.261	-0.035
CHE-Glo	0.457	-0.589	-0.55
CIB-Chr	0.338	-0.606	0.034
DBV-Rim	0.517	-0.509	-0.443
EAG-Mor	0.606	-0.139	-0.414
EFW-Fta	0.067	-0.126	0.17
GIL-Blu	0.629	0.053	-0.477
Gil-Cal	0.488	-0.092	-0.907
GIL-Sol	0.524	0.012	-0.888
NEW-Rck	0.393	-0.295	-0.248
OAK-Crn	0.61	-0.735	-0.707
SCL-Per	0.523	-0.335	-0.534
SFR-Clf	0.452	-0.083	-0.605
SLT-Roo	0.487	-0.437	-0.643
SYC-Mcd	0.457	-0.624	-0.136
TON-Roo	0.331	-0.502	-0.489
VRD-Crk	0.4	-0.42	-0.634
VRD-Hsd	0.571	-0.546	-1.029
WCL-Cmp	0.404	-0.192	-0.494

Appendix B.1.1: The z-score of the discharge of all peaks-above-base in the Central Highlands Transition Zone for each flood-producing mechanism.

	AR	Non-AR Winter	Convective
AFR-May	1.052	-0.265	-0.937
BLK-Fta	0.522	-0.392	-0.533
BON-Mor	0.224	-0.375	0.062
CHE-Glo	0.654	-0.529	-0.416
CIB-Chr	0.575	-0.792	-0.084
DBV-Rim	0.762	-0.652	-0.423
EAG-Mor	0.796	-0.404	-0.369
EFW-Fta	0.101	-0.426	0.046
GIL-Blu	0.518	0.365	-0.727
GIL-Cal	0.507	-0.095	-0.843
GIL-Sol	0.618	0.048	-0.65
NEW-Rck	0.55	-0.357	-0.48
OAK-Crn	0.83	-0.976	-0.49
SCL-Per	0.459	-0.43	-0.464
SFR-Clf	0.701	-0.197	-0.45
SLT-Roo	0.387	-0.385	-0.612
SYC-Mcd	0.47	-0.893	-0.032
TON-Roo	0.527	-0.446	-0.768
VRD-Crk	0.351	-0.319	-0.425
VRD-Hsd	0.489	-0.69	-1.063
WCL-Cmp	0.456	-1.082	-0.322

Appendix B.1.2: The z-score of the discharge of all annual peaks in the Central Highlands Transition Zone for each flood-producing mechanism.

	AR	Non-AR Winter	Convective
CHN-Nmw	-0.083	0.069	-0.121
LCO-Cam	0.772	-0.24	0.199
LCO-Stj	-0.31	-0.521	0.363
MKW-Mnk	-0.194	-0.304	0.241
PAR-Lee	-0.579	0.096	0.093

Appendix B.2.1: The z-score of the discharge of all peaks-above-base in the Northern Arizona Colorado Plateau for each flood-producing mechanism.

	AR	Non-AR Winter	Convective
CHN-Nmw	-0.266	0.094	-0.072
LCO-Cam	1.164	-0.179	0.519
LCO-Stj	-0.398	-0.36	0.37
MKW-Mnk	-0.55	-0.298	0.36
PAR-Lee	-0.407	0.066	0.172

Appendix B.2.2: The z-score of the discharge of all annual peaks in the Northern Arizona Colorado Plateau for each flood-producing mechanism.

	AR	Non-AR Winter	Convective
ARV-Mth	0.218	0.204	-0.323
BSN-Wku	0.392	-0.432	-0.241
SCR-Loc	0.967	-1.65	0.054
SCR-Nog	0.63	-0.046	-0.241
SCR-Tuc	-0.164	0.389	0.086
SPD-Cha	0.492	0.488	-0.068
SPD-Pal	0.15	0.465	-0.219

Appendix B.3.1: The z-score of the discharge of all peaks-above-base in the Southeastern Arizona Basin and Range for each flood-producing mechanism.

	AR	Non-AR Winter	Convective
ARV-Mth	0.22	0.23	-0.267
BSN-Wku	0.512	-0.842	-0.078
SCR-Loc	1.016	-1.314	0.253
SCR-Nog	1.104	-0.199	-0.195
SCR-Tuc	-0.253	0.189	0.196
SPD-Cha	0.468	0.553	-0.155
SPD-Pal	-0.088	0.589	-0.256

Appendix B.3.2: The z-score of the discharge of all annual peaks in the Southeastern Arizona Basin and Range for each flood-producing mechanism.

APPENDIX C

CONTINGENCY TABLES

	AR-Related	Non-AR Winter	Convective	Tropical	Total
Top Third	17	15	4	0	36
Medium Third	5	18	9	3	35
Bottom Third	6	8	19	2	36
Total	28	42	32	5	107

Appendix C.1.1: Contingency table of direct discharge for the Gila watershed

	AR-Related	Non-AR Winter	Convective	Tropical	Total
Top Third	16	15	5	0	36
Medium Third	6	16	10	3	35
Bottom Third	6	11	17	2	36
Total	28	42	32	5	107

Appendix C.1.2: Contingency table of z-score of discharge for the Gila watershed

	AR-Related	Non-AR Winter	Convective	Tropical	Total
Top Third	23	3	1	2	29
Medium Third	10	15	2	1	28
Bottom Third	5	16	7	1	29
Total	38	34	10	4	86

Appendix C.2.1: Contingency table of direct discharge for the Verde watershed

	AR-Related	Non-AR Winter	Convective	Tropical	Total
Top Third	23	3	1	2	29
Medium Third	9	15	2	2	28
Bottom Third	6	16	7	0	29
Total	38	34	10	4	86

Appendix C.2.2: Contingency table of z-score of discharge for the Verde watershed.

	AR-Related	Non-AR Winter	Convective	Tropical	Total
Top Third	2	5	24	3	34
Medium Third	3	5	21	5	34
Bottom Third	3	3	25	3	34
Total	8	13	70	11	102

Appendix C.3.1: Contingency table of direct discharge for the Santa Cruz watershed.

	AR-Related	Non-AR Winter	Convective	Tropical	Total
Top Third	3	4	24	3	34
Medium Third	3	5	20	6	34
Bottom Third	2	4	26	2	34
Total	8	13	70	11	102

Appendix C.3.2: Contingency table of z-score of discharge for the Santa Cruz watershed.

	AR-Related	Non-AR Winter	Convective	Tropical	Total
Top Third	6	10	5	2	23
Medium Third	0	12	11	1	24
Bottom Third	2	11	9	1	23
Total	8	33	25	4	70

Appendix C.4.1: Contingency table of direct discharge for the Little Colorado watershed.

	AR-Related	Non-AR Winter	Convective	Tropical	Total
Top Third	3	7	13	0	23
Medium Third	4	8	9	3	24
Bottom Third	1	18	3	1	23
Total	8	33	25	4	70

Appendix C.4.2: Contingency table of z-score of discharge for the Little Colorado watershed.

	AR-Related	Non-AR Winter	Convective	Tropical	Total
Top Third	24	4	3	3	34
Medium Third	9	12	8	4	33
Bottom Third	14	14	6	0	34
Total	47	30	17	7	101

Appendix C.5.1: Contingency table of direct discharge for the Salt watershed.

	AR-Related	Non-AR Winter	Convective	Tropical	Total
Top Third	24	4	3	3	34
Medium Third	9	14	7	3	33
Bottom Third	14	12	7	1	34
Total	47	30	17	7	101

Appendix C.5.2: Contingency table of z-score of discharge for the Salt watershed.

	0-1	2-5	6-10	11+	Total
Westerly	28	6	4	4	42
South / southwesterly	65	21	11	18	115
Northwestern	5	1	1	0	7
	98	28	16	22	164

Appendix C.6.1: Contingency table of trajectory and number of AR events.

	0-1	2-5	6-10	11+	Total
California	48	12	8	3	71
Baja California	51	16	8	18	93
	99	28	16	21	164

Appendix C.6.2: Contingency table of point of entry and number of AR events.

APPENDIX D

PARAMETERS FOR DIFFERENCE IN MEANS

	AR	Non-AR Winter	Convective
BSN-Wku			
Mean	3.884	3.276	3.417
Standard Deviation	0.642	0.811	0.431
CHN-Nmw			
Mean	3.1	3.14	3.09
Standard Deviation	0.34	0.26	0.284
GIL-Sol			
Mean	4.145	3.894	3.453
Standard Deviation	0.496	0.378	0.42
LCO-Cam			
Mean	3.881	3.654	3.75
Standard Deviation	0.23	0.228	0.18
NEW-Rck			
Mean	3.235	2.85	2.88
Standard Deviation	0.546	0.36	0.689
OAK-Crn			
Mean	3.773	3.2	3.21
Standard Deviation	0.372	0.273	0.25
SCR-Nog			
Mean	3.574	3.35	3.285
Standard Deviation	0.252	0.225	0.325
SFR-Clf			
Mean	3.795	3.555	3.32
Standard Deviation	0.395	0.479	0.317
SLT-Roo			
Mean	4.21	3.835	3.75
Standard Deviation	0.448	0.251	0.254
VRD-Hsd			
Mean	4.31	3.8	3.579
Standard Deviation	0.451	0.23	0.288

Appendix D.1: The mean and standard deviations of the logarithmic value of discharge for each flood-producing mechanism by station.

	AR vs. Non-AR Winter	AR vs. Convective
BSN-Wku		
Pooled variance (s^2)	0.5184	0.3614
Degrees of freedom	67	49
t-statistic at 0.010	2.158 – 2.39	3.90 – 2.423
GIL-Sol		
Pooled variance (s^2)	0.1958	0.2214
Degrees of freedom	37	29
t-statistic at 0.010	2.423 – 2.457	2.462
NEW-Rck		
Pooled variance (s^2)	0.226	0.339
Degrees of freedom	70	52
t-statistic at 0.010	2.158 – 2.39	2.39 – 2.423
OAK-Crn		
Pooled variance (s^2)	0.1164	0.1243
Degrees of freedom	41	33
t-statistic at 0.010	2.39 – 2.423	2.423 – 2.457
SFR-Clf		
Pooled variance (s^2)	0.1864	0.1383
Degrees of freedom	39	34
t-statistic at 0.010	2.423 – 2.457	2.423 – 2.457
SLT-Roo		
Pooled variance (s^2)	0.1513	0.1685
Degrees of freedom	50	42
t-statistic at 0.010	2.39 – 2.423	2.39 -2.423
VRD-Hsd		
Pooled variance (s^2)	N/A ¹	0.1852
Degrees of freedom	53	40
t-statistic at 0.010	2.39 – 2.423	2.423

Appendix D.2.1: The pooled variances, degrees of freedom, and rejection regions for each pair of comparisons at Central Highlands Transition Zone gauging stations.

CHN-Nmw		
Pooled variance (s^2)	0.08	0.0868
Degrees of freedom	36	51
t-statistic at 0.010	2.423 – 2.457	2.39 – 2.423
LCO-Cam		
Pooled variance (s^2)	0.0523	0.0425
Degrees of freedom	26	10
t-statistic at 0.010	2.479	2.764
SCR-Nog		
Pooled variance (s^2)	0.0557	0.0968
Degrees of freedom	10	19
t-statistic at 0.010	2.764	2.539

Appendix D.2.2: The pooled variances, degrees of freedom, and rejection regions for each pair of comparisons at Northern Arizona / Colorado Plateau and Southeastern Arizona / Basin and Range gauging stations.